

P. Starič, E. Margan

## **Wideband Amplifiers**

Part 3:

### **Wideband Amplifier Stages With Semiconductor Devices**

*The only way to find the limits of what is possible  
is by pushing towards the impossible!*

Arthur C. Clarke

## Back To Basics

This part deals with some elementary amplifier configurations which can serve as building blocks of multi-stage amplifiers described in Part 4 and 5, together with the inductive peaking circuits described in Part 2.

Today two schools of thought prevail amongst amplifier designers: the first one (to which most of the more experienced generation belongs) says that cheap operational amplifiers can never fulfill the conflicting requirements of good wideband design; the other (mostly the fresh forces) says that the analog IC production technology advances so fast that, by the time needed to design a good wideband amplifier, the new opamps on the market will render it obsolete.

Both of them are right, of course!

An important point, however, is that very few amplifier designers have a silicon chip manufacturing facility next door. Those who have, often discover that component size reduction solves half of the problems, whilst packing the components close together produces a nearly equal number of new problems.

Another important point is that computer simulation tells you only a part of what will be going on in the actual circuit. Not because there would be anything wrong with the computer, its program or the circuit modeling method used, but because designers, however experienced they are, can not take everything into account right from the start; and, in order to be able to complete the simulation in the foreseeable future, many things are left out intentionally.

A third important point is that by being satisfied with the performance offered by *LEGO*-tronics (playing with general purpose building blocks, as we call it — and we really do not mean anything bad by that!), one intentionally limits oneself to a performance which, in most cases, is an order of magnitude below of what is achievable by the current ‘state of the art’ technology. Not to speak of there being only a limited amount of experience to be gained by playing just with the outside of those nice little black boxes.

A wise electronics engineer always takes some time to build a discrete model of the circuit (the most critical part, at least) in order to evaluate the influence of strays and parasitics and find a way of improving it. Even if the circuit will eventually be put on a silicon chip those strays will be scaled down, but will not disappear.

That is why we think that it is important to go back to basics.

<a href="#">Contents</a> .....	3.3
<a href="#">List of Figures</a> .....	3.4
<a href="#">List of Tables</a> .....	3.5
<b>Contents:</b>	
<a href="#">3.0 Introduction: <i>A Farewell to Exact Calculations</i></a> .....	3.7
<a href="#">3.1 Common Emitter Amplifier</a> .....	3.9
<a href="#">3.1.1 Calculation of Voltage Amplification (Based on Fig. 3.1.1d)</a> .....	3.14
<a href="#">3.2 Transistor as an Impedance Converter</a> .....	3.17
<a href="#">3.2.1 Common Base Transistor Small Signal HF Model</a> .....	3.17
<a href="#">3.2.2 The Conversion of Impedances</a> .....	3.20
<a href="#">3.2.3 Examples of Impedance Transformations</a> .....	3.21
<a href="#">3.2.4 Transformation of Combined Impedances</a> .....	3.26
<a href="#">3.3 Common Base Amplifier</a> .....	3.33
<a href="#">3.3.1 Input Impedance</a> .....	3.34
<a href="#">3.4 Cascode Amplifier</a> .....	3.37
<a href="#">3.4.1 Basic Analysis</a> .....	3.37
<a href="#">3.4.2 Damping of the Emitter circuit of <math>Q_2</math></a> .....	3.38
<a href="#">3.4.3 Thermal Compensation</a> .....	3.42
<a href="#">3.5 Emitter Peaking in a Cascode Amplifier</a> .....	3.49
<a href="#">3.5.1 Basic Analysis</a> .....	3.49
<a href="#">3.5.2 Input Impedance Compensation</a> .....	3.54
<a href="#">3.6 Transistor Interstage T-coil Peaking</a> .....	3.57
<a href="#">3.6.1 Frequency Response</a> .....	3.61
<a href="#">3.6.2 Phase Response</a> .....	3.62
<a href="#">3.6.3 Envelope Delay</a> .....	3.62
<a href="#">3.6.4 Step Response</a> .....	3.64
<a href="#">3.6.5 Consideration of the Transistor Input Resistance</a> .....	3.65
<a href="#">3.6.6 Consideration of the Base Lead Stray Inductance</a> .....	3.66
<a href="#">3.6.7 Consideration of the Collector to Base Spread Capacitance</a> .....	3.67
<a href="#">3.6.8 The 'Folded' Cascode</a> .....	3.67
<a href="#">3.7 Differential Amplifiers</a> .....	3.69
<a href="#">3.7.1 Differential Cascode Amplifier</a> .....	3.70
<a href="#">3.7.2 Current Source in the Emitter Circuit</a> .....	3.72
<a href="#">3.8 The <math>f_T</math> Doubler</a> .....	3.75
<a href="#">3.9 JFET Source Follower</a> .....	3.79
<a href="#">3.9.1 Frequency Response Magnitude</a> .....	3.82
<a href="#">3.9.2 Phase Response</a> .....	3.84
<a href="#">3.9.3 Envelope Delay</a> .....	3.84
<a href="#">3.9.4 Step Response</a> .....	3.85
<a href="#">3.9.5 Input Impedance</a> .....	3.89
<a href="#">Résumé of Part 3</a> .....	3.95
<a href="#">References</a> .....	3.97
<a href="#">Appendix 3.1: Thermal analysis</a> .....	(disk) A3.1

**List of Figures:**

<a href="#">Fig. 3.1.1: The common emitter amplifier</a>	3.9
<a href="#">Fig. 3.2.1: The common base amplifier</a>	3.17
<a href="#">Fig. 3.2.2: Transistor gain as a function of frequency</a>	3.19
<a href="#">Fig. 3.2.3: Emitter to base impedance conversion</a>	3.20
<a href="#">Fig. 3.2.4: Base to emitter impedance conversion</a>	3.21
<a href="#">Fig. 3.2.5: Capacitive load reflects into the base with negative components</a>	3.23
<a href="#">Fig. 3.2.6: Inductive source reflects into the emitter with negative components</a>	3.24
<a href="#">Fig. 3.2.7: Base to emitter <math>RC</math> network transformation</a>	3.26
<a href="#">Fig. 3.2.8: Emitter to base <math>RC</math> network transformation</a>	3.28
<a href="#">Fig. 3.2.9: <math>R_e C_e</math> network transformation</a>	3.30
<a href="#">Fig. 3.2.10: Common collector amplifier</a>	3.30
<a href="#">Fig. 3.3.1: Common base amplifier</a>	3.33
<a href="#">Fig. 3.3.2: Common base amplifier input impedance</a>	3.35
<a href="#">Fig. 3.4.1: Cascode amplifier circuit schematic</a>	3.37
<a href="#">Fig. 3.4.2: Cascode amplifier small signal model</a>	3.37
<a href="#">Fig. 3.4.3: Cascode amplifier parasitic resonance damping</a>	3.39
<a href="#">Fig. 3.4.4: <math>Q_2</math> emitter input impedance with damping</a>	3.40
<a href="#">Fig. 3.4.5: The step response pre-shoot due to <math>C_{\mu 1}</math> cross-talk</a>	3.40
<a href="#">Fig. 3.4.6: <math>Q_2</math> compensation method with a base <math>RC</math> network</a>	3.41
<a href="#">Fig. 3.4.7: <math>Q_2</math> emitter impedance compensation</a>	3.42
<a href="#">Fig. 3.4.8: Thermally distorted step response</a>	3.43
<a href="#">Fig. 3.4.9: The optimum bias point</a>	3.44
<a href="#">Fig. 3.4.10: The thermal compensation network</a>	3.46
<a href="#">Fig. 3.4.11: The dynamic collector resistance and the Early voltage</a>	3.46
<a href="#">Fig. 3.4.12: The compensated cascode amplifier</a>	3.47
<a href="#">Fig. 3.5.1: Emitter peaking in cascode amplifiers</a>	3.50
<a href="#">Fig. 3.5.2: Emitter peaking pole pattern</a>	3.53
<a href="#">Fig. 3.5.3: Negative input impedance compensation</a>	3.56
<a href="#">Fig. 3.6.1: Cascode amplifier with a T-coil interstage coupling</a>	3.57
<a href="#">Fig. 3.6.2: T-coil loaded with the simplified input impedance</a>	3.58
<a href="#">Fig. 3.6.3: T-coil coupling frequency response</a>	3.62
<a href="#">Fig. 3.6.4: T-coil coupling phase response</a>	3.63
<a href="#">Fig. 3.6.5: T-coil coupling envelope delay response</a>	3.63
<a href="#">Fig. 3.6.6: T-coil coupling step response</a>	3.64
<a href="#">Fig. 3.6.7: Cascode input impedance including the base spread resistance</a>	3.65
<a href="#">Fig. 3.6.8: T-coil compensation for the base spread resistance</a>	3.65
<a href="#">Fig. 3.6.9: T-coil including the base lead inductance</a>	3.66
<a href="#">Fig. 3.6.10: A more accurate model of <math>r_b C_{\mu}</math></a>	3.67
<a href="#">Fig. 3.6.11: The 'folded' cascode</a>	3.68
<a href="#">Fig. 3.7.1: The differential amplifier</a>	3.69
<a href="#">Fig. 3.7.2: The differential cascode amplifier</a>	3.71
<a href="#">Fig. 3.7.3: Basic current mirror</a>	3.72
<a href="#">Fig. 3.7.4: Improved current generator</a>	3.74
<a href="#">Fig. 3.8.1: Current driven cascode amplifier</a>	3.75
<a href="#">Fig. 3.8.2: Basic <math>f_T</math> doubler circuit</a>	3.76
<a href="#">Fig. 3.9.1: JFET source follower</a>	3.79
<a href="#">Fig. 3.9.2: JFET capacitive loading and the input impedance</a>	3.81
<a href="#">Fig. 3.9.3: JFET frequency response</a>	3.83
<a href="#">Fig. 3.9.4: JFET phase response</a>	3.84
<a href="#">Fig. 3.9.5: JFET envelope delay</a>	3.85

<a href="#">Fig. 3.9.6: JFET step response</a> .....	3.86
<a href="#">Fig. 3.9.7: JFET frequency response including the signal source resistance</a> .....	3.88
<a href="#">Fig. 3.9.8: JFET step response including the signal source resistance</a> .....	3.88
<a href="#">Fig. 3.9.9: JFET source follower input impedance model</a> .....	3.90
<a href="#">Fig. 3.9.10: Normalized negative input conductance</a> .....	3.91
<a href="#">Fig. 3.9.11: JFET negative input impedance compensation</a> .....	3.92
<a href="#">Fig. 3.9.12: JFET input impedance Nyquist diagrams</a> .....	3.93
<a href="#">Fig. 3.9.13: Alternative JFET negative input impedance compensation</a> .....	3.94

#### List of Tables:

<a href="#">Table 3.2.1: The Table of impedance conversions</a> .....	3.25
<a href="#">Table 3.4.1: Poles of T-coil interstage coupling for different loadings</a> .....	3.61

(blank page)

### 3.0 Introduction: *A Farewell to Exact Calculations*

The inductive peaking circuits discussed in [Part 2](#) should be applied to some amplifier stages in order to have any sense. Today the amplifiers are made almost exclusively using semiconductor devices (**bipolar junction transistors**—**BJTs** and **field effect transistors**—**FETs**). The number of books describing semiconductor amplifiers is enormous [e.g., [Ref. 3.7](#), [3.12](#), [3.13](#), [3.14](#), [3.15](#)], whilst books discussing wideband amplifiers in necessary depth are quite rare.

Wideband amplifiers with BJTs and FETs are found in a great diversity of electronic products, in measuring instruments and oscilloscopes in particular. They require a different design approach from the ‘classical’ low frequency amplifier circuits, where the inter-electrode and stray capacitances are less important. In order to improve the wideband performance many special circuits were invented [e.g., [Ref. 3.1](#), [Ch.8](#) and [3.34](#), [Ch.7](#)] and to discuss thoroughly all of them in a book like this would not be possible for several reasons. Here we shall analyze only some basic circuits (the common emitter and the common base amplifiers) and some of the most used wideband circuits (e.g., the differential cascode, the common source follower, and the  $f_T$  doubler configurations; later in [Part 5](#) we shall meet several more complex circuits).

In the first section we analyze the common emitter amplifier. Since the base pole  $\omega_h$  (set by the base spread resistance  $r_b$  and the total input capacitance  $C_\pi + C_M$ ), represents the most prevalent bandwidth limit in the transconductance equation, we discuss how to reduce the input capacitance. In this type of amplifier, as well as in all other types that we intend to discuss, the analysis becomes extremely complicated if all the parameters are considered. Since it is our intention to acquire a clear picture of the basic facts, an analysis with all the minute details would needlessly fog the view. The market is still waiting (probably in vain) for a transistor with  $\pm 1\%$  tolerances in electrical parameters. Also, it is very difficult to specify the stray inductances and capacitances of the wiring with comparable precision. Therefore we shall simplify our expressions and neglect all the parameters which have either little influence or which must be solved numerically for a specific case. After the basic picture is acquired, the reader who wants to make a more precise analysis, can use a computer with a suitable program such as SPICE [[Ref. 3.28](#)], PSpice [[Ref. 3.29](#)], or MicroCAP [[Ref. 3.30](#)], to name a few. Be warned, however, that the result will be as good as allowed by the models of semiconductor devices and, of course, it will be influenced by the user’s ability to correctly model the stray components which depend on layout and which are not explicitly shown either in the initial circuit schematic diagram or included in any semiconductor device model.

The nature of the HF impedance in the emitter circuit changes drastically if we look at it from the base, and vice versa. Since it is useful to know the possible transformations from base to emitter circuit and back, we discuss all the transformations of resistive, capacitive, and inductive impedances. Next we analyze the common base circuit. The cascode circuit, which is effectively a combination of a common emitter and a common base configuration, is often used in wideband amplifiers, so it deserves a thorough analysis, too. The same is valid for the differential cascode amplifier. We also discuss the emitter peaking in a cascode amplifier. The invention of the  $f_T$  doubler has made possible a bandwidth extension of almost twofold within a single stage and we

discuss it next. This is followed by an analysis of the JFET source follower, which is commonly used as the input stage of oscilloscopes and other measuring instruments. Such a stage can have the input impedance **negative** at high frequencies when the JFET source is loaded by a capacitor (which is always the case), and we show how to compensate this very undesirable property.

In [Part 2](#) we have analyzed the T-coil peaking circuit with a purely capacitive tap to ground impedance. However, if the T-coil circuit is used for a transistor interstage coupling, the tap to ground impedance ceases to be purely capacitive. This fact requires a new analysis, which we deal with in the last section.

Probably, the reader will ask how accurately we need to model the active devices in our circuits to obtain a satisfying approximation. In 1954, *Ebers* and *Moll* [[Ref. 3.9](#)] had already described a relatively simple nonlinear model, which, over the years, was improved by the same authors, and by *Gummel* and *Poon* [[Ref. 3.10](#)] in 1970. Modern computer programs for circuit simulation allow the user to trade simulation speed for accuracy by selecting models with different levels of complexity (e.g., an older version of MicroCAP [[Ref. 3.30](#)] had 3 EM and 2 GP models for the BJT, the most complex GP2 using a total of 51 parameters). To simplify the circuit analysis we shall use the linearized high frequency EM2 model, explained in [Sec. 3.1](#).

All these models look so simple and perform so well, that it seems as if anyone could have created them. Nothing could be farther from the truth. It takes lots of classical physics (*Boltzmann's* transport theory, *Gauss's* theorem, *Poisson's* equation, the charge current mean density integral calculus, the complicated p–n junction boundary conditions, *Maxwell's* equations, ...), as well as quantum physics (*Fermi* levels, *Schrödinger's* equation, the *Pauli* principle, charge generation, injection, recombination and photon–electron and phonon–electron scattering phenomena, to name just a few important topics) to be judiciously applied in order to find well defined special cases and clever approximations that would, within limits, provide a model simple enough for everyday use. Of course, if pushed too far the model fails, and there is no other way to the solution but to rework the physics neglected. In our analysis we shall try not to go that far.

It cannot be overstressed that in our analysis we are dealing with **models** of semiconductor devices! As *Philip Darrington*, former Wireless World editor, put it in one of his editorials, “*the map is not the territory*”, just as the schematic diagram is not the circuit. As in any branch of science, we build a (theoretical) model, analyze it, and then compare with the real thing; if it fits, we have had a good nose there, or perhaps we have simply been lucky; if it does not fit we go back to the drawing board.

In the macroscopic world, from which all our experience arises, most models are quite simple, since the size ratio of objects, which can still be perceived directly with our senses, to the atomic size, where some odd phenomena begin to show up, is some 6 orders of magnitude; thus the world appears to us to be smooth and continuous. However, in the world of ever shrinking semiconductor devices we are getting ever closer to the quantum phenomena (e.g., the dynamic range of our amplifiers is limited by thermal noise, which is ultimately a quantum effect). But long before we approach the quantum level we should stay alert: even if we forget that the oscilloscope probe loads our circuit with a shunt capacitance of some 10–20 pF and a serial inductance of about 70–150 nH of the ground lead, the circuit will not forget, and sometimes not forgive, either!



### 3.1 Common Emitter Amplifier

[Fig. 3.1.1a](#) shows a common emitter amplifier (the name reflects that the emitter is the common reference for both input and output signals), whilst [Fig. 3.1.1b](#) represents its small signal equivalent circuit (the EM2 model, see [\[Ref. 3.4 and 3.9\]](#)). If a signal source amplitude is much smaller than the base bias voltage, resulting in an output signal small enough compared to the supply voltage, we can assume that all the equivalent circuit components are linear (not changing with the signal). However, when the transistor has to handle large signals, the equivalent model becomes rather complicated and the analysis is usually carried out by a suitable computer program.

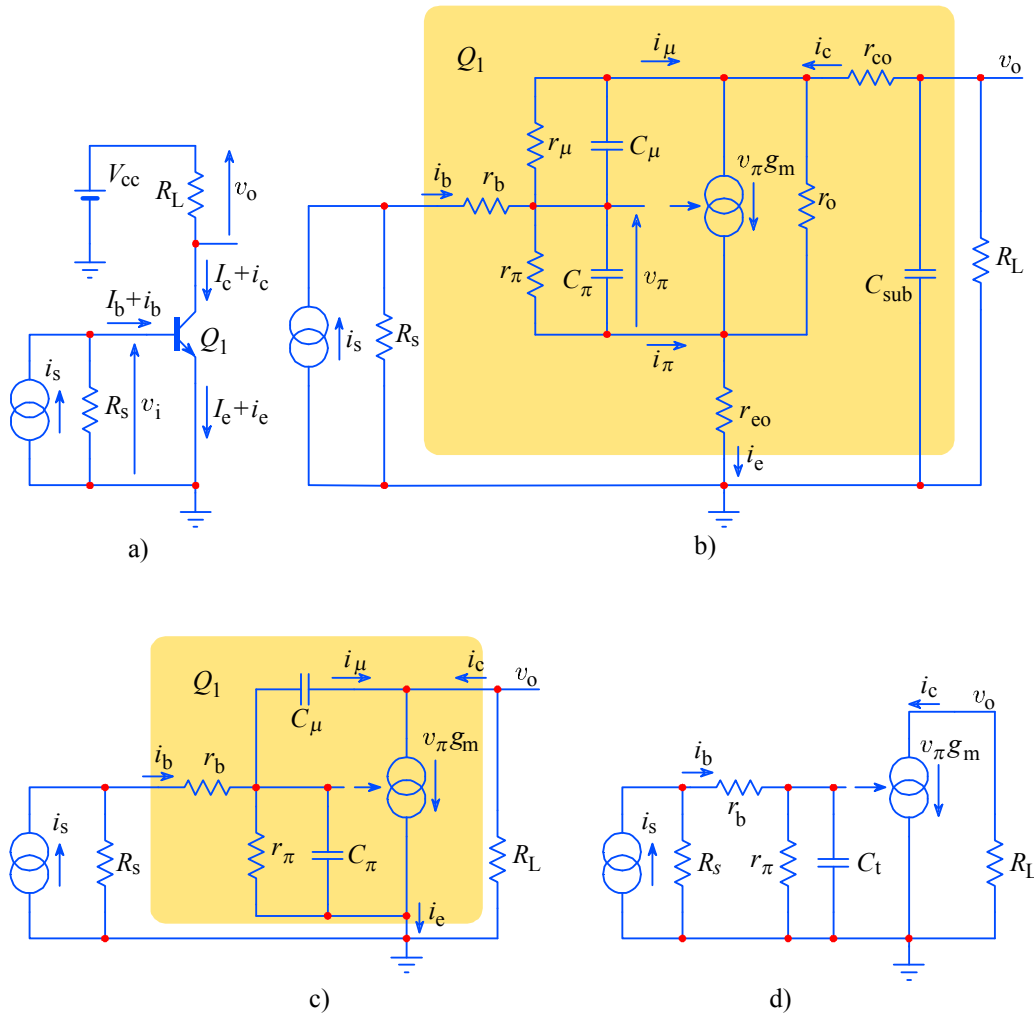


**Fig. 3.1.1:** The common emitter amplifier: a) circuit schematic diagram – the current and voltage vectors are drawn for the NPN type of transistor; b) high frequency small signal equivalent circuit; the components included in the  $Q_1$  model are explained in the text; c) simplified equivalent circuit; d) an oversimplified circuit where  $C_t = C_\pi + AC_\mu = \text{constant}$ .

During the first steps of circuit design we can usually neglect the nonlinear effects and obtain a satisfactory performance description by using a first order approximation of the transistor model, [Fig. 3.1.1c](#). Some of the circuit parameters can even be estimated by an oversimplified model of [Fig. 3.1.1d](#). By assuming a certain

operating point OP, set by the DC bias conditions, we can explain the meaning of the model components. On the basis of these explanations it will become clear why and when we may neglect some of them, thus simplifying the model and its analysis.

$g_m$  transistor mutual conductance in *siemens* [ $S = 1/\Omega$ ]:  $g_m = \frac{i_c}{v_\pi} \approx 1/r_e$

where  $i_c$  is the instantaneous collector current;

$v_\pi$  is the voltage across  $r_\pi$  (see below);

and  $r_e$  is the dynamic emitter resistance:  $r_e = \frac{V_T}{I_e}$  [ $\Omega$ ] (*ohm*);

$I_e$  is the d.c. emitter current [A] (*ampere*);

$V_T$  is the p-n junction ‘thermal’ voltage =  $\frac{k_B T}{q}$  [V] (*volt*);

where  $q$  is the electron charge =  $1.602 \cdot 10^{-19}$  [C] (*coulomb* = [As]);

$T$  is the absolute temperature [K] (*kelvin*);

$k_B$  is the Boltzmann constant =  $1.38 \cdot 10^{-23}$  [J/K] (*joule/kelvin*)  
( = [VAs/K] ).

$r_o$  equivalent collector–emitter output resistance, representing the variation of the collector–emitter potential due to collector signal current at a specified operating point (its value is nearly always much greater than the load):

$$r_o = \frac{v_{ce}}{i_c} = \left. \frac{d V_{ce}}{d I_c} \right|_{OP} = \frac{V_A + V_{ce}}{I_c}$$

where  $V_A$  is the *Early* voltage (see [Fig. 3.4.11](#));

In wideband amplifiers:  $r_o \gg R_L$

$r_\mu$  collector to base resistance, representing the variation of the collector to base potential due to base signal current at some specified DC operating point condition OP( $V_{cc}$ ,  $I_b$ ); in wideband amplifiers its value is always much larger than the source resistance or the base spread resistance:

$$r_\mu = \frac{v_{cb}}{i_b} = \left. \frac{d V_{cb}}{d I_b} \right|_{OP} = \frac{V_A + V_{ce}}{I_b}$$

$$r_\mu \gg R_s + r_b$$

$r_\pi$  base to emitter input resistance (forward biased BE junction), representing the variation of the base to emitter potential owed to the base signal current at a specified operating point:

$$r_\pi = \frac{v_\pi}{i_b} = \left. \frac{d V_{be}}{d I_b} \right|_{OP} = \beta \frac{V_T}{I_c} = \frac{\beta}{g_m} \approx \beta r_e$$

$r_b$  base spread resistance (resistance between the base terminal and the base–emitter junction); value range:  $10 \Omega < r_b < 200 \Omega$ .

$r_{co}$  presumably constant collector resistance of internal bonding and external lead; approximate value  $< 1 \Omega$ .

- $r_{eo}$  presumably constant emitter resistance of internal bonding and external lead; approximate value  $< 1 \Omega$ .
- $C_\mu$  collector–base (reverse biased) junction capacitance; usually the value is small ( $< 10 \text{ pF}$ ); however, in the common emitter circuit it is effectively amplified by the voltage gain (the *Miller* effect, see [Eq. 3.1.9](#)).
- $C_\pi$  base–emitter junction effective capacitance; depends on DC bias:

$$C_\pi = g_m \tau_T - C_\mu$$

where  $\tau_T$  is the characteristic time constant, derived from the ‘transition’ frequency,  $f_T$ , the frequency at which  $\beta(f_T) = 1$  (see below):

$$\tau_T = \frac{1}{\omega_T} = \frac{1}{2\pi f_T}$$

- $C_{\text{sub}}$  collector to substrate capacitance; must be accounted for only in integrated circuits; in discrete devices it can be neglected.
- $\beta$  the transistor current gain, the collector to base current ratio; the gain frequency dependence is modeled by the characteristic time constant  $\tau_T$ :

$$\beta = \frac{i_c}{i_b} = \beta_0 \frac{1}{1 + \beta_0 s \tau_T} \quad \text{where:} \quad \beta_0 = \frac{I_c}{I_b}$$

It is important to realize that some of those resistances are only ‘equivalent resistances’, or ‘incremental resistances’, which can be represented by a tangent to the voltage–current relation curvature at a particular bias point, and as such they are highly nonlinear for large signals. Also, the capacitances are only in part a consequence of the actual p–n junction geometry; they are dominantly volumes in the semiconductor material in which there are energy gaps capable of charge trapping, storing and releasing. In turn the gap energy is voltage dependent, so the effective capacitances are also voltage dependent and therefore also nonlinear.

With bias conditions encountered in wideband amplifier applications, the collector to base resistance  $r_\mu$  and the collector to emitter resistance  $r_o$  are several orders of magnitude larger than the source resistance  $R_s$  and the load resistance  $R_L$ . In order to simplify the analysis we shall neglect  $r_\mu$  and  $r_o$ ; that is why they have not been drawn in [Fig. 3.1.1c](#).

Likewise the DC power supply voltages are also not drawn, because their sources (should!) represent a short circuit for the signal, so we have simply tied the loading resistor and the bias voltages to the ground. Remember that it is the duty of the circuit designer — that is you, yourself! — to provide good power supply bypassing by both adding appropriate capacitors and using wide and short, low resistance, low inductance PCB traces.

The resistors  $r_{co}$  and  $r_{eo}$  represent the external leads and internal wires, and since their value is usually less than  $1 \Omega$ , they are also neglected.

In general we can assume that small signal transistors work at an internal junction temperature of 300 K ( $27^\circ\text{C}$  or  $80^\circ\text{F}$ , roughly the ‘room temperature’ increased by a few degrees owing to some small power dissipation caused by DC bias). Output

transistors work at higher temperatures, depending on the output signal amplitude, the load and the power efficiency of the amplifying stage.

It is interesting to note that  $k_B T/q$  has the dimension of voltage ( $J=VAs$ ,  $C=As$  and  $K$  cancels) and it has been named the junction ‘thermal’ voltage, its value  $V_T = k_B T/q = 26 \text{ mV}$  at  $T = 300 \text{ K}$ . By assuming that the collector current  $I_c$  is almost equal to the emitter current  $I_e$  (actually  $\times \beta/(\beta + 1)$ ), we obtain a well known relation for the effective emitter resistance:

$$r_e = \frac{V_T}{I_e} = \frac{26 \text{ mV}}{I_e} \approx \frac{26 \text{ mV}}{I_c} \quad (3.1.1)$$

The collector to base capacitance  $C_\mu$  depends on the collector to base voltage  $V_{cb}$ . In normal operating conditions (CB junction reverse biased), the corresponding relation [Ref. 3.4, 3.20] is:

$$C_\mu(V_{cb}) = \frac{C_{\mu 0}}{\left[1 + \frac{V_{cb}}{V_{jc}}\right]^{m_c}} \quad (3.1.2)$$

This equation is valid under the assumption that there is no charge in the collector to base depletion layer. The meaning of the symbols are:

$C_{\mu 0}$  = junction capacitance [F] (*farad*) (when  $V_{cb} = 0 \text{ V}$ )

$V_{cb}$  = collector to base voltage [V] (*volts*)

$V_{jc}$  = collector to base barrier potential  $\simeq 0.6\text{--}0.8 \text{ V}$  for silicon transistors

$m_c$  = collector voltage potential gradient factor  
(0.5 for abrupt junctions and 0.33 for graded junctions)

Obviously,  $C_\mu$  decreases inversely with collector voltage. For small signals (amplifier input stage)  $V_{cb}$  does not change very much, so we can assume  $C_\mu$  to be constant, or, in other words, ‘linear’. However, in middle stage and output transistors,  $V_{cb}$  changes considerably. As already mentioned, in such cases the computer aided circuit simulation is mandatory (after the initial linearized approximation has been found acceptable). Fortunately most transistor manufacturers provide the diagrams showing the dependence of  $C_\mu$  from  $V_{cb}$ . The reader can find a very good review for 25 of the most commonly used transistors in [Ref. 3.21, p. 556].

The input base emitter capacitance  $C_\pi$  strongly depends on the emitter current, respectively, on the transconductance  $g_m$ . Since we can not directly access the internal base junction to measure  $C_\pi$  and  $C_\mu$  separately, we calculate  $C_\pi$  from the total equivalent input capacitance  $C_t$  (see Fig. 3.1.1d), from which we first subtract  $C_\mu$ :

$$C_\pi = C_t - C_\mu = g_m \tau_T - C_\mu = \frac{1}{2\pi f_T r_e} - C_\mu \quad (3.1.3)$$

where  $f_T$  is the frequency at which the (frequency dependent) current amplification factor  $\beta = i_c/i_b$  is reduced to 1. Because  $C_\mu$  is usually small compared to  $C_\pi$  we can simplify [Eq. 3.1.3](#) to obtain:

$$C_\pi \approx \frac{1}{2\pi f_T r_e} \quad (3.1.4)$$

The product  $r_e C_\pi$  is called the *transistor time constant*  $\tau_T = 1/\omega_T$ , where  $\omega_T = 2\pi f_T$ . The value  $s_1 = -\omega_T = -1/(r_e C_\pi)$  represents the dominant pole of the amplifier and thus it is the main bandwidth limiting factor. In our further discussions we shall find the way to drastically reduce the influence of  $C_\pi$ , at the expense of the amplification factor.

The next problem is to calculate the input impedance. Here we must consider the *Miller effect* [[Ref. 3.7](#), [3.12](#)] owed to capacitance  $C_\mu$  (in practice, there is also a CB leads stray capacitance, parallel to the junction capacitance, that has to be taken into account). Therefore we first calculate the input admittance looking right into the internal  $r_b C_\mu$  junction in [Fig. 3.1.1c](#). The current  $i_\mu$  flowing through  $C_\mu$  is:

$$i_\mu = (v_\pi - v_o) C_\mu s \quad (3.1.5)$$

where  $v_\pi$  is the voltage across  $r_\pi$ . The output voltage is<sup>1</sup>:

$$v_o = -i_c R_L = -g_m v_\pi R_L \quad (3.1.6)$$

By inserting [Eq. 3.1.6](#) into [Eq. 3.1.5](#), we obtain:

$$i_\mu = (1 + g_m R_L) s C_\mu v_\pi \quad (3.1.7)$$

and from this the junction input admittance:

$$\frac{i_\mu}{v_\pi} = (1 + g_m R_L) C_\mu s \quad (3.1.8)$$

From this equation it follows that the junction input impedance, owed to capacitance  $C_\mu$ , is a capacitance with the value:

$$C_M = (1 + g_m R_L) C_\mu = (1 + A_v) C_\mu \quad (3.1.9)$$

where  $g_m R_L = A_v = v_o/v_i$ , the voltage gain.

The capacitance  $C_M$  is called the *Miller capacitance*, after the *Miller effect* — bandwidth reduction with increasing voltage gain (the Miller effect is probably named after *John Milton Miller*, [[Ref. 3.36](#)]).

<sup>1</sup> Note the negative sign in [Eq. 3.1.6](#): actually, the output voltage is  $v_o = V_{cc} - i_c R_L$ . However, since we have agreed to replace the supply voltage with a short circuit, we are left with the negative part only.

When the voltage gain is large the effect of  $C_\mu$  (and, respectively,  $C_M$ ) becomes prevalent. However, there are ways of reducing the effect of  $A_v C_\mu$  (by lowering the voltage gain or by using other circuit configurations); we discuss it in later sections.

The complete input impedance that the signal source would see at the base is:

$$Z_b = r_b + \frac{1}{\frac{1}{r_\pi} + sC_\pi + sC_M} = r_b + \frac{r_\pi}{1 + s(C_\pi + C_M)r_\pi} \quad (3.1.10)$$

### 3.1.1 Calculation of voltage amplification (based on [Fig. 3.1.1d](#))

On the basis of the analysis made so far, we come to the conclusion that the two capacitances  $C_\pi$  and  $C_\mu$  (effectively  $C_M$ ) are connected in parallel in the base circuit. We can simply add them together and consider their sum to be  $C_t$ . This has been drawn in [Fig. 3.1.1d](#). This equivalent circuit is appropriate for the calculation of both input impedance and the transimpedance. But since we have removed any connection between the output and input (where  $C_\mu$  is effective), this circuit **is not suitable** for the calculation of output impedance. Therefore when calculating the voltage gain we must also consider the pole  $s_2 \simeq -1/R_L C_\mu$  on the collector side, according to [Fig. 3.1.1c](#) (in general, some collector to ground stray capacitance must be added to  $C_\mu$ , but for the time being, we shall write only  $C_\mu$ ).

According to [Fig. 3.1.1d](#), thus neglecting the pole  $s_2$ , but including the source impedance  $R_s$ , we have:

$$\frac{v_i - v_\pi}{R_s + r_b} = v_\pi \left( \frac{1}{r_\pi} + sC_t \right) \quad (3.1.11)$$

From this we can express  $v_\pi$  as:

$$v_\pi = v_i \frac{r_\pi}{r_\pi + R_s + r_b + sC_t r_\pi (R_s + r_b)} \quad (3.1.12)$$

The output voltage is:

$$v_o = -g_m v_\pi R_L = -g_m R_L \frac{r_\pi}{r_\pi + R_s + r_b + sC_t r_\pi (R_s + r_b)} v_i \quad (3.1.13)$$

and the voltage amplification is:

$$A_v = \frac{v_o}{v_i} = -g_m R_L \frac{r_\pi}{r_\pi + R_s + r_b + sC_t r_\pi (R_s + r_b)} \quad (3.1.14)$$

We would like to separate the frequency dependent part of  $A_v$  from the frequency independent part, in a normalized form, as:

$$A_v(s) = A_0 \frac{-s_1}{s - s_1} \quad (3.1.15)$$

where  $A_0$  is the DC gain and  $s_1$  is the system's pole.

To achieve this separation we first divide both the numerator and the denominator of [Eq. 3.1.14](#) by  $C_t r_\pi (R_s + r_b)$ :

$$A_v = -g_m R_L \frac{-\frac{r_\pi}{C_t r_\pi (R_s + r_b)}}{s - \left( -\frac{r_\pi + R_s + r_b}{C_t r_\pi (R_s + r_b)} \right)} \quad (3.1.16)$$

To make the two ratios equal we must multiply the numerator by  $(r_\pi + R_s + r_b)/r_\pi$  and then multiply the whole by the reciprocal:

$$A_v = -g_m R_L \frac{-\frac{r_\pi}{C_t r_\pi (R_s + r_b)} \cdot \frac{r_\pi + R_s + r_b}{r_\pi}}{s - \left( -\frac{r_\pi + R_s + r_b}{C_t r_\pi (R_s + r_b)} \right)} \cdot \frac{r_\pi}{r_\pi + R_s + r_b} \quad (3.1.17)$$

We rearrange this to obtain:

$$A_v = -\frac{g_m R_L r_\pi}{r_\pi + R_s + r_b} \cdot \frac{-\frac{r_\pi + R_s + r_b}{C_t r_\pi (R_s + r_b)}}{s - \left( -\frac{r_\pi + R_s + r_b}{C_t r_\pi (R_s + r_b)} \right)} \quad (3.1.18)$$

and by comparing this with [Eq. 3.1.15](#) the DC gain is:

$$A_0 = -\frac{g_m R_L r_\pi}{r_\pi + R_s + r_b} \quad (3.1.19)$$

and the pole  $s_1$  is:

$$s_1 = -\frac{R_s + r_b + r_\pi}{(R_s + r_b) r_\pi C_t} \quad (3.1.20)$$

Since  $s_1$  is a simple real pole it is equal to the system's upper half power frequency:

$$\begin{aligned} \omega_h = |s_1| &= \frac{R_s + r_b + r_\pi}{(R_s + r_b) r_\pi} \cdot \frac{1}{C_t} \\ &= \left( \frac{1}{R_s + r_b} + \frac{1}{r_\pi} \right) \cdot \frac{1}{C_\pi + (1 + g_m R_L) C_\mu} \end{aligned} \quad (3.1.21)$$

and it can be seen that it is **inversely proportional to all the components**:  $R_s$ ,  $r_b$ ,  $r_\pi$ ,  $C_\pi$ ,  $C_\mu$ ,  $g_m$ , and  $R_L$ .

If  $R_s + r_b \ll r_\pi$  and if  $R_L$  is very small the approximate value of the pole is:

$$|s_1| \approx \frac{1}{r_\pi C_\pi} = \frac{1}{\beta_0} \cdot \frac{g_m}{C_\pi} = \frac{\omega_T}{\beta_0} \quad (3.1.22)$$

where  $\beta_0 = I_c/I_b$ , the DC current amplification factor.

Before more sophisticated circuits were invented, the common emitter amplifier was used extensively (with many amplifier designers having hard times and probably cursing both  $C_\pi$  and  $C_\mu$ ). In 1956 *G. Bruun* [[Ref. 3.22](#)] thoroughly analyzed this type of amplifier with the added shunt–series inductive peaking circuit. In view of modern wideband amplifier circuits, this reference is only of historical value today. Nevertheless, the common emitter stage represents a good starting point for the discussion of more efficient wideband amplifier circuits.



### 3.2 Transistor as an Impedance Converter

In the previous section we have realized that the amplification factor is frequency dependent, decreasing with frequency above some upper frequency limit (asymptotically to  $-20 \text{ dB}/10f$ , just like a first-order low pass system). This can help us to derive different impedance transformations from the emitter to the base circuit and back [Ref. 3.1, 3.2]. Knowing the possible transformations is extremely useful in the wideband amplifier design. We are going to show how the nature of the impedance changes with these transformations. A capacitive impedance may become inductive and positive impedances may occasionally become negative!

#### 3.2.1 Common base small signal transistor model

As we explained in Sec. 3.1, if the voltage gain is not too high the base emitter capacitance  $C_\pi$  is the dominant cause of the frequency response rolling off at high frequencies. By considering this we can make a simplified small signal high frequency transistor model, as shown in Fig. 3.2.1, for the common base configuration, where  $i_c$ ,  $i_e$  and  $i_b$  are the collector-, emitter-, and base-current respectively. For this figure the DC current amplification factor is:

$$\alpha_0 = \frac{I_c}{I_e} \quad (3.2.1)$$

Initially we have written  $g_m \approx 1/r_e$ . A better expression for mutual conductance is:

$$g_m = \frac{\alpha_0}{r_e} = \frac{\beta_0}{(1 + \beta_0) r_e} \quad (3.2.2)$$

where  $\beta_0$  is the common emitter DC current amplification factor. If  $\beta_0 \gg 1$  then  $\alpha_0 \simeq 1$ , so the collector current  $I_c$  is almost equal to the emitter current  $I_e$ , and  $g_m \simeq 1/r_e$ . This simplification is often used in practice.

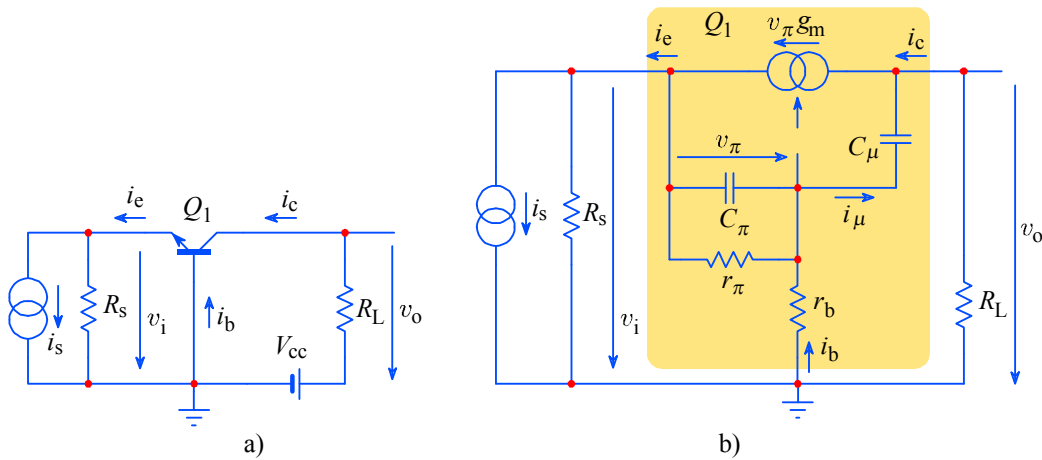


**Fig. 3.2.1:** The common base amplifier: a) circuit schematic diagram; b) high frequency small signal equivalent circuit.

For the moment let us assume that the base resistance  $r_b = 0$  and consider the low frequency relations. The input resistance is:

$$r_\pi = \frac{v_\pi}{i_b} \quad (3.2.3)$$

where  $v_\pi$  is the base to emitter voltage. Since the emitter current is:

$$i_e = i_b + i_c = i_b + \beta_0 i_b = i_b (1 + \beta_0) \quad (3.2.4)$$

then the base current is:

$$i_b = \frac{i_e}{1 + \beta_0} \quad (3.2.5)$$

and consequently:

$$r_\pi = \frac{v_\pi (1 + \beta_0)}{i_e} = r_e (1 + \beta_0) \approx \beta_0 r_e \quad (3.2.6)$$

The last simplification is valid if  $\beta_0 \gg 1$ . To obtain the input impedance at high frequencies the parallel connection of  $C_\pi$  must be taken into account:

$$Z_b = \frac{(1 + \beta_0) r_e}{1 + (1 + \beta_0) s C_\pi r_e} \quad (3.2.7)$$

The base current is:

$$i_b = \frac{v_\pi}{Z_b} = v_\pi \frac{1 + (1 + \beta_0) s C_\pi r_e}{(1 + \beta_0) r_e} \quad (3.2.8)$$

Therefore  $v_\pi$  is:

$$v_\pi = i_b \frac{(1 + \beta_0) r_e}{1 + (1 + \beta_0) s C_\pi r_e} \quad (3.2.9)$$

Consequently, the collector current is:

$$i_c = g_m v_\pi = \frac{\beta_0}{1 + \beta_0} \cdot \frac{1}{r_e} v_\pi = \frac{\alpha_0}{r_e} v_\pi \quad (3.2.10)$$

If we put [Eq. 3.2.9](#) into [Eq. 3.2.10](#) we obtain:

$$\begin{aligned} i_c &= i_b \frac{\beta_0}{1 + \beta_0} \cdot \frac{1}{r_e} \cdot \frac{(1 + \beta_0) r_e}{1 + s (1 + \beta_0) r_e C_\pi} \\ &= i_b \frac{1}{\frac{1}{\beta_0} + s \left( \frac{\beta_0 + 1}{\beta_0} \right) r_e C_\pi} \\ &\approx i_b \frac{1}{\frac{1}{\beta_0} + s \tau_T} = i_b \beta(s) \end{aligned} \quad (3.2.11)$$

In the very last expression we assumed that  $\beta_0 \gg 1$  and  $\tau_T = r_e C_\pi = 1/\omega_T$ , where  $\omega_T = 2\pi f_T$  is the angular frequency at which the current amplification factor  $\beta$  decreases to unity. The parameter  $\tau_T$ , and consequently  $\omega_T$ , depend on the internal configuration and structure of the transistor. [Fig. 3.2.2](#) shows the frequency dependence of  $\beta$  and the equivalent current generator.

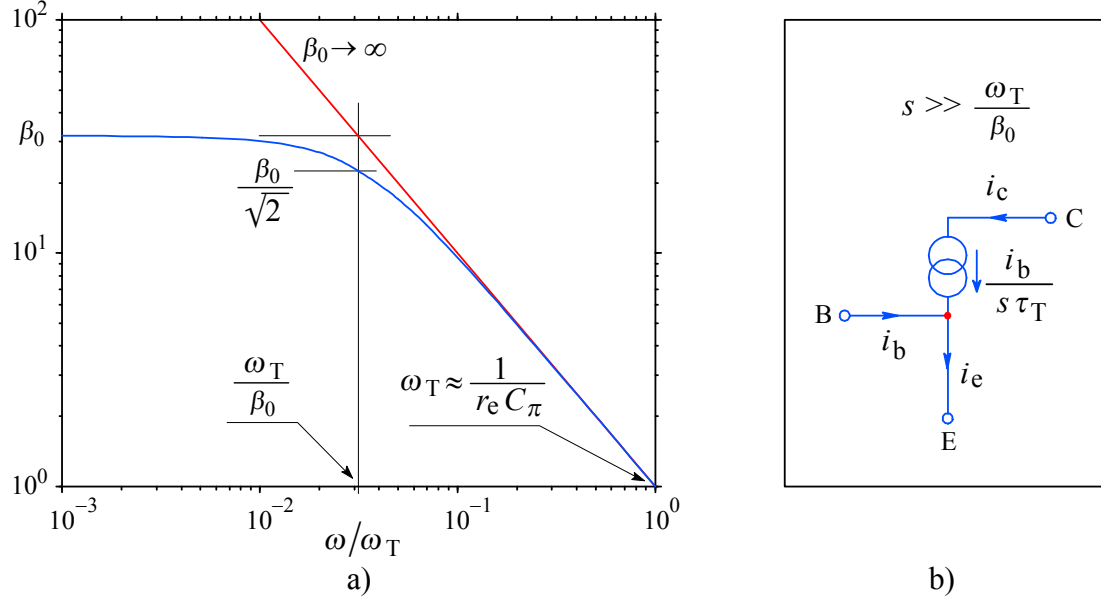


**Fig. 3.2.2:** a) The transistor gain as a function of frequency, modeled by the [Eq. 3.2.11](#); b) the equivalent HF current generator.

In order to correlate [Fig. 3.2.2](#) with [Eq. 3.2.11](#) we rewrite it as:

$$\frac{i_c}{i_b} \approx \beta_0 \frac{-\frac{\omega_T}{\beta_0}}{s - \left(-\frac{\omega_T}{\beta_0}\right)} = \beta_0 \frac{-s_1}{s - s_1} \quad (3.2.12)$$

where  $s_1$  is the pole at  $-\omega_T/\beta_0$ . This relation will become useful later, when we shall apply one of the peaking circuits (from [Part 2](#)) to the amplifier. At very high frequencies, or if  $\beta_0 \gg 1$ , the term  $s \tau_T$  prevails. In this case, from [Eq. 3.2.11](#):

$$\frac{i_c}{i_b} = \beta(s) \approx \frac{1}{s \tau_T} = \frac{1}{j\omega r_e C_\pi} \quad (3.2.13)$$

Obviously  $\beta$  is decreasing with frequency. By definition, at  $\omega = \omega_T$  the current ratio  $i_c/i_b = 1$ ; then the capacitance  $C_\pi$  can be found as:

$$C_\pi \approx \frac{1}{\omega_T r_e} \quad (3.2.14)$$

This simplified relation represents the  $-20 \text{ dB}/10f$  asymptote in [Fig. 3.2.2a](#).

### 3.2.2 The conversion of impedances

We can use the result of [Eq. 3.2.11](#) to transform the transistor internal (and the added external) impedances from the emitter to the base circuitry, and vice versa. Suppose we have the impedance  $Z_e$  in the emitter circuit, as displayed in [Fig. 3.2.3a](#), and we are interested in the corresponding base impedance  $Z_b$ :

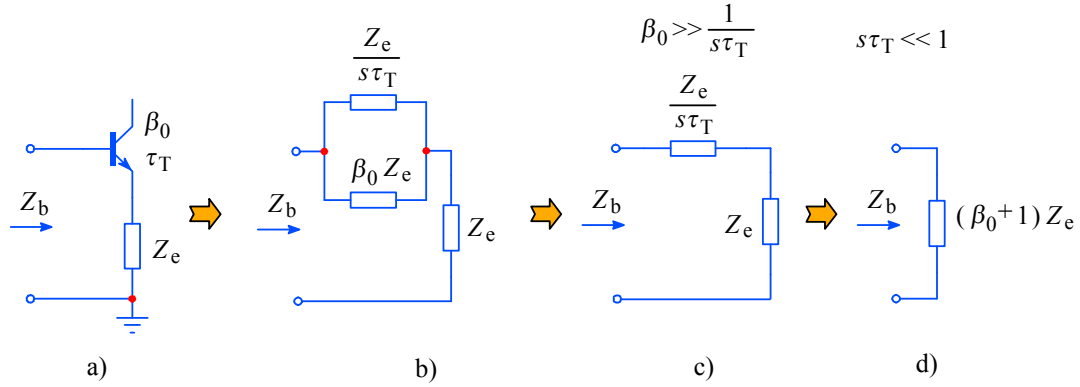


**Fig. 3.2.3:** Emitter to base impedance conversion: a) schematic; b) equivalent circuit; c) simplified for high  $\beta_0$ ; d) simplified for low frequencies.

We know that:

$$Z_b = \beta(s) Z_e + Z_e = [\beta(s) + 1] Z_e \quad (3.2.15)$$

If we insert  $\beta(s)$  according to [Eq. 3.2.11](#), we obtain:

$$Z_b = \frac{Z_e}{\frac{1}{\beta_0} + s\tau_T} + Z_e \quad (3.2.16)$$

The admittance of the first part of this equation is:

$$Y = \frac{\frac{1}{\beta_0} + s\tau_T}{Z_e} = \frac{1}{\beta_0 Z_e} + \frac{s\tau_T}{Z_e} \quad (3.2.17)$$

and this represents a parallel connection of impedances  $\beta_0 Z_e$  and  $Z_e/s\tau_T$ . By adding the series impedance  $Z_e$ , as in [Eq. 3.2.16](#), we obtain the equivalent circuit of [Fig. 3.2.3b](#). At medium frequencies and with a high value of  $\beta_0$  we can assume that  $1/\beta_0 \ll s\tau_T$ , so we can delete the impedance  $\beta_0 Z_e$  and simplify the circuit, as in [Fig. 3.2.3c](#). On the other hand, at low frequencies, where  $s\tau_T \ll 1$ , we can neglect the  $Z_e/s\tau_T$  component and get a very basic equivalent circuit, displayed in [Fig. 3.2.3d](#).

[Eq. 3.2.11](#) is equally useful when we want to transform the impedance from the base into the emitter circuit as shown in [Fig. 3.2.4a](#). In this case we have:

$$Z_e = \frac{Z_b}{\beta(s) + 1} \quad (3.2.18)$$

Again we calculate the admittance, which is:

$$Y_e = \frac{\beta(s) + 1}{Z_b} = [\beta(s) + 1] Y_b = \beta(s) Y_b + Y_b \quad (3.2.19)$$

The first part of this admittance is:

$$Y = \frac{\beta(s)}{Z_b} = \frac{Y_b}{\frac{1}{\beta_0} + s \tau_T} = \frac{1}{Z_b} \cdot \frac{1}{\frac{1}{\beta_0} + s \tau_T} \quad (3.2.20)$$

and the impedance is:

$$Z = \frac{Z_b}{\beta_0} + s \tau_T Z_b \quad (3.2.21)$$

Thus the transformed impedance  $Z_e$  is composed of three elements: the series connection of  $Z_b/\beta_0$  and  $s \tau_T Z_b$ , in parallel with the impedance  $Z_b$ .

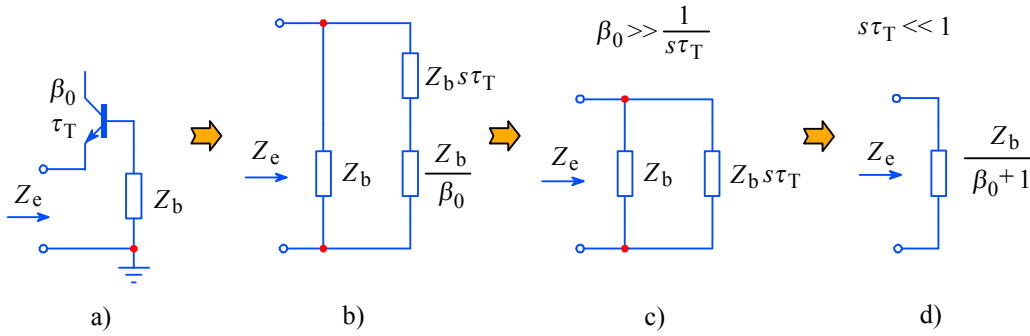


**Fig. 3.2.4:** Base to emitter impedance conversion: a) schematic; b) equivalent circuit; c) simplified for high  $\beta_0$  or for  $f \simeq f_T$ ; d) simplified for low frequencies.

The equivalent emitter impedance is shown in [Fig. 3.2.4b](#).

As in the previous example, for some specific conditions the circuit can be simplified. At medium frequencies and a high  $\beta_0$ , we can assume  $\beta_0 \gg 1/s \tau_T$  and therefore neglect the impedance  $Z_b/\beta_0$ , as in [Fig. 3.2.4c](#). At low frequencies, where  $s \tau_T \ll 1$ , the impedance  $Z_b/(\beta_0 + 1)$  prevails and we can neglect the parallel impedance  $Z_b$ , as in [Fig. 3.2.4d](#).

### 3.2.3 Examples of impedance transformations

The most interesting examples of impedance transformations are the emitter to base transformation of a capacitive emitter impedance and the base to emitter transformation of an inductive base impedance.

In the first case we have  $Z_e = 1/sC$ , where  $C$  is the emitter to ground capacitance.

To obtain the base impedance we apply [Eq. 3.2.5](#):

$$\begin{aligned}
Z_b &= \frac{\beta(s) + 1}{sC} = \left[ \frac{1}{\frac{1}{\beta_0} + s\tau_T} + 1 \right] \frac{1}{sC} = \frac{\frac{1}{\beta_0} + s\tau_T + 1}{\left( \frac{1}{\beta_0} + s\tau_T \right) sC} \\
&= \frac{s\tau_T + \left( 1 + \frac{1}{\beta_0} \right)}{s^2\tau_T C + \frac{sC}{\beta_0}}
\end{aligned} \tag{3.2.22}$$

The inverse of  $Z_b$  is the admittance:

$$Y_b = \frac{s^2\tau_T C + \frac{sC}{\beta_0}}{s\tau_T + \left( 1 + \frac{1}{\beta_0} \right)} \tag{3.2.23}$$

Let us synthesize this expression by a simple continued fraction expansion [[Ref. 3.27](#)]:

$$\frac{s^2\tau_T C + \frac{sC}{\beta_0}}{s\tau_T + \left( 1 + \frac{1}{\beta_0} \right)} = sC - \frac{sC}{s\tau_T + \left( 1 + \frac{1}{\beta_0} \right)} \tag{3.2.24}$$

The fraction on the right is a negative admittance with the corresponding impedance:

$$Z'_b = - \frac{s\tau_T + \left( 1 + \frac{1}{\beta_0} \right)}{sC} = - \frac{\tau_T}{C} - \frac{1 + \frac{1}{\beta_0}}{sC} \tag{3.2.25}$$

It is evident that this impedance is a series connection of a negative resistance:

$$R_n = - \frac{\tau_T}{C} = - r_e \frac{C_\pi}{C} \tag{3.2.26}$$

and a negative capacitance:

$$C_n = - \frac{C}{1 + \frac{1}{\beta_0}} = - \frac{\beta_0}{1 + \beta_0} C = - \alpha_0 C \tag{3.2.27}$$

By adding the positive parallel capacitance  $C$ , as required by [Eq. 3.2.24](#), we obtain the equivalent circuit which is shown in [Fig. 3.2.5](#). Since we deal with an active circuit (transistor) it is quite normal to encounter negative impedances. The complete base admittance is then:

$$Y_b = sC - \frac{1}{\frac{\tau_T}{C} + \frac{1}{s\alpha_0 C}} \tag{3.2.28}$$

By rearranging this expression and substituting  $s = j\omega$  we can separate the real and imaginary parts, obtaining:

$$Y_b = \Re\{Y_b\} + j\Im\{Y_b\} = G_b + j\omega C_b$$

$$= -\frac{\frac{\tau_T}{C}}{\tau_T^2 + \frac{1}{\omega^2 \alpha_0^2}} - j\omega C \frac{\tau_T^2 - \frac{\alpha_0 - 1}{\omega^2 \alpha_0^2}}{\tau_T^2 + \frac{1}{\omega^2 \alpha_0^2}} \quad (3.2.29)$$

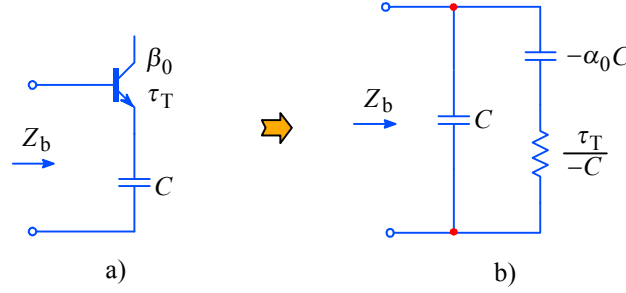


**Fig. 3.2.5:** A capacitive emitter load is reflected into the base (junction) with **negative** components.

The negative input (base) conductance  $G_b$  can cause ringing on steep signals or even continuous oscillations if the signal source impedance has an emphasized inductive component. We shall thoroughly discuss this effect and its compensation later, when we shall analyze the emitter-follower (i.e., common collector) and the JFET source-follower amplifiers.

Now let us derive the emitter impedance  $Z_e$  in the case in which the base impedance is inductive ( $sL$ ). Here we apply [Eq. 3.2.18](#):

$$Z_e = \frac{sL}{\beta(s) + 1} = \frac{sL}{\frac{1}{\frac{1}{\beta_0} + s\tau_T} + 1} \quad (3.2.30)$$

$$= \frac{sL \left( \frac{1}{\beta_0} + s\tau_T \right)}{1 + \frac{1}{\beta_0} + s\tau_T} = \frac{s^2 L \tau_T + \frac{sL}{\beta_0}}{s\tau_T + \left( 1 + \frac{1}{\beta_0} \right)} \quad (3.2.31)$$

By continued fraction expansion we obtain:

$$\frac{s^2 L \tau_T + \frac{sL}{\beta_0}}{s\tau_T + \left( 1 + \frac{1}{\beta_0} \right)} = sL - \frac{sL}{s\tau_T + \left( 1 + \frac{1}{\beta_0} \right)} \quad (3.2.32)$$

The negative part of the result can be inverted to obtain the admittance:

$$Y'_e = -\frac{s\tau_T + \left( 1 + \frac{1}{\beta_0} \right)}{sL} = -\frac{\tau_T}{L} - \frac{1 + \frac{1}{\beta_0}}{sL} \quad (3.2.33)$$

This means we have two parallel impedances. The first one is a **negative** resistance:

$$R_x = -\frac{L}{\tau_T} \quad (3.2.34)$$

and the second one is a **negative** inductance:

$$L_x = -\frac{L}{1 + \frac{1}{\beta_0}} = -\frac{\beta_0}{1 + \beta_0} L = -\alpha_0 L \quad (3.2.35)$$

As required by [Eq. 3.2.32](#), we must add the inductance  $L$  in series, thus arriving at the equivalent emitter impedance shown in the figure below:

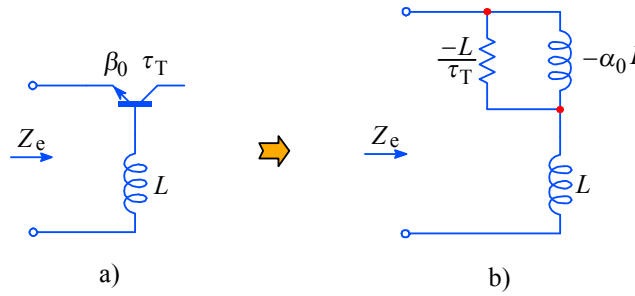


**Fig. 3.2.6:** The inductive source is reflected into the emitter with **negative** components.

We have just analyzed an important aspect of a common base amplifier, with an inductance (i.e., long lead) between the base and ground. The negative resistance, as given by [Eq. 3.2.34](#), may become the reason for ringing or oscillations if the driving circuit seen by the emitter has a capacitive character. We shall discuss this problem more thoroughly when we shall analyze the cascode circuit.

In a way similar to those used for deriving the previous two results, we can transform other impedance types from emitter to base, and vice versa. The [Table 3.2.1](#) displays the six possible variations and the reader is encouraged to derive the remaining four, which we have not discussed.

Note that all the three transformations for the common base circuit in the table apply to the base–emitter **junction** to ground only. In order to obtain the correct base **terminal** to ground impedance the transistor base spread resistance  $r_b$  must be added in series to the circuits shown in the table.



$Z$		
$R$		
$L$		
$C$		

**Table 3.2.1:** The Table of impedance conversions [Ref. 3.8].

### 3.2.4 Transformation of combined impedances

The [Table 3.2.1](#) can also help us in transforming impedances consisting of two or more components.

#### Example 1:

Suppose we have a parallel  $R_b C_b$  combination in the base circuit, as shown in [Fig. 3.2.7a](#). What is the emitter impedance  $Z_e$  if the common base transistor has a current amplification factor  $\beta_0$  and the time constant  $\tau_T$  ( $= 1/\omega_T$ )?

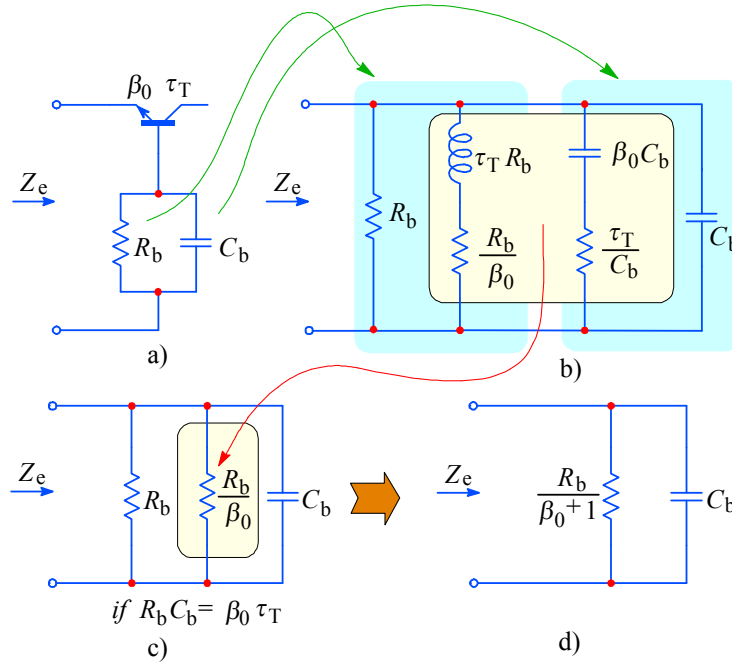


**Fig. 3.2.7:** Base to emitter  $RC$  network transformation: a) schematic; b) equivalent circuit; c) if  $R_b C_b = \beta_0 \tau_T$  the middle components form a resistance; d) final equivalent circuit.

From the [Table 3.2.1](#) we first transform the resistance  $R_b$  from base to emitter and obtain what is shown on the left half of [Fig. 3.2.7b](#). Then we transform the capacitance  $C_b$  and obtain the right half of [Fig. 3.2.7b](#). If we want the transformed network to have the smallest possible influence in the emitter circuit, we can apply the principle of constant resistance network ( $L$  and  $C$  cancel each other when  $RC = L/R$ , [[Ref. 3.27](#)]). To do so let us focus on both middle branches of the transformed network, where we select such values of  $R_b$  and  $C_b$  that:

$$\sqrt{\frac{R_b \tau_T}{C_b \beta_0}} = \frac{R_b}{\beta_0} \quad (3.2.36)$$

which is resolved as:

$$R_b C_b = \tau_T \beta_0 \quad (3.2.37)$$

With such values of  $R_b$  and  $C_b$  the middle two branches obtain the form of a resistor with the value  $R_b/\beta_0$ , as shown in [Fig. 3.2.7c](#), which allows us to further simplify the complete circuit to that in [Fig. 3.2.7d](#).

To acquire a feeling for practical values, let us make a numerical example. Our transistor has:

$$\beta_0 = 80 \quad f_T = 600 \text{ MHz} \quad R_b = 47 \Omega$$

where  $R_b$  is the external base resistance, as in [Fig. 3.2.7](#).

What should be the value of the capacitance  $C_b$ , connected in parallel with  $R_b$ , which would fulfill the requirement expressed by [Eq. 3.2.36](#)?

We start by calculating the transistor time constant:

$$\tau_T = \frac{1}{\omega_T} = \frac{1}{2\pi f_T} = \frac{1}{2\pi \cdot 600 \cdot 10^6} = 265 \text{ ps} \quad (3.2.38)$$

Then we calculate the capacitance by using [Eq. 3.2.37](#):

$$C_b = \frac{\tau_T \beta_0}{R_b} = \frac{265 \cdot 10^{-12} \cdot 80}{47} = 451 \text{ pF} \quad (3.2.39)$$

The equivalent parallel resistance,  $R_q$ , according to [Fig. 3.2.7d](#), is:

$$R_q = \frac{R_b}{1 + \beta_0} = \frac{47}{1 + 80} = 0.58 \Omega \quad (3.2.40)$$

The time constant of the equivalent circuit,  $\tau_q$ , is:

$$\tau_q = R_q C_b = 0.56 \cdot 451 \cdot 10^{-12} = 261.58 \text{ ps} \quad (3.2.41)$$

whilst the base time constant is:

$$\tau_b = R_b C_b = 47 \cdot 451 \cdot 10^{-12} = 21.197 \text{ ns} \quad (3.2.42)$$

and the ratio of time constants is:

$$\frac{\tau_b}{\tau_q} = \beta_0 + 1 \quad (3.2.43)$$

We shall consider these results in the design of the common base amplifier and of the cascode amplifier.

### Example 2:

By using the same principles as we have used above, we shall take another example, which is also very important for the wideband amplifier design. We shall transform a parallel combination  $R_e C_e$ , as shown in [Fig. 3.2.8a](#), from emitter to base. With the data from [Table 3.2.1](#), we can draw the transformed base network separately for  $R_e$  and  $C_e$  and then connect them in parallel. This is shown in [Fig. 3.2.8b](#). Now we

focus only on the middle part of the circuit, which is drawn in [Fig. 3.2.8c](#). If we select such values of  $R_e C_e$  that:

$$R_e C_e = \tau_T \quad (3.2.44)$$

and if we consider that  $\alpha_0 \approx 1$ , then the admittance  $Y$  of the middle part of the circuit becomes zero, because in this case:

$$R_e = -\frac{\tau_T}{C_e} \quad (3.2.45)$$

and:

$$\frac{\tau_T}{R_e} = -\alpha_0 C_e \approx -C_e \quad (3.2.46)$$

and the parallel connection of a positive and an equal negative admittance gives zero admittance:

$$Y = \frac{1}{R_e + \frac{1}{s \frac{\tau_T}{R_e}}} + \frac{1}{-\frac{\tau_T}{C_e} - \frac{1}{s C_e}} = 0 \quad \Big|_{R_e C_e = \tau_T} \quad (3.2.47)$$

A zero admittance is an infinite impedance. So in this case the only components that remain are the parallel connection of  $C_e$  and  $(\beta_0 + 1)R_e$ , as in [Fig. 3.2.9d](#).

Note that this transformation was carried out by taking the **internal base junction** as the viewing point. The actual input impedance at the external base terminal will be equal to the parallel  $RC$  combination of [Fig. 3.2.8d](#) to which the series connected base spread resistance  $r_b$  must be added.

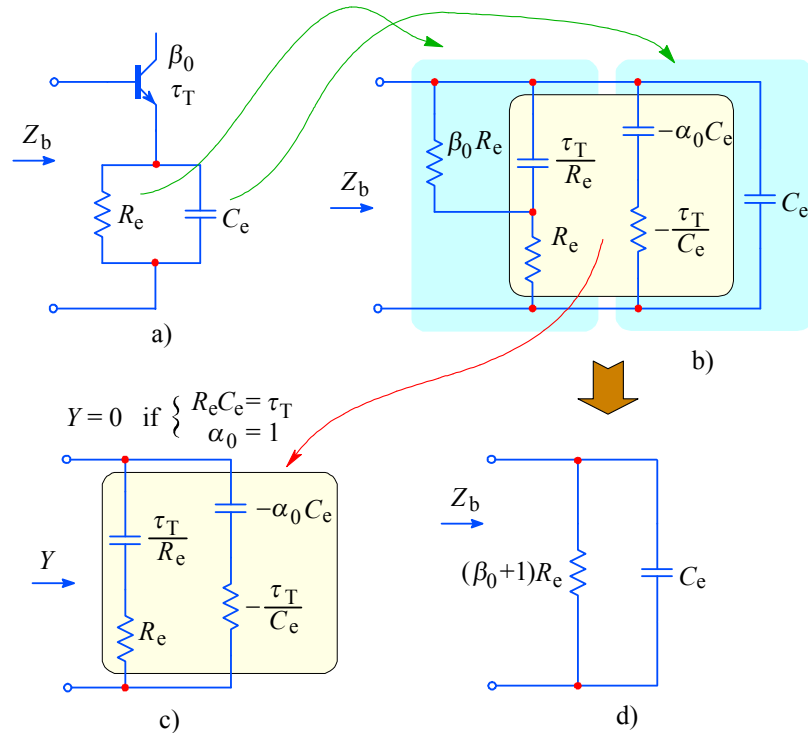


**Fig. 3.2.8:** Transformation of the emitter  $RC$  network as seen from the base: a) schematic; b) equivalent circuit; c) if  $RC = \tau_T$  and  $\alpha_0 = 1$ , the sum of the middle frame component's admittances is zero; d) final equivalent circuit.

The transformation in [Fig. 3.2.8](#) allows us to trade the gain of a common emitter circuit for the reduced input capacitance. Instead of  $C_\pi$  (large) with the emitter grounded, the input capacitance is now equal to the capacitance  $C_e$  (small) which we have inserted in the emitter circuit. Of course, we still have to add the base to collector capacitance  $C_\mu$  or Miller capacitance  $C_M$ . As we shall see in the [Sec. 3.4](#), where we shall discuss the cascode amplifier, the gain is reduced in proportion to  $R_L/R_e$ . Since in a wideband amplifier stage we almost never exceed the voltage gain of ten, we can always apply the above transformation.

For a numerical example let us use the same transistor as before ( $\beta_0 = 80$ ,  $f_T = 600$  MHz). According to [Eq. 3.2.38](#) the corresponding  $\tau_T$  is 265 ps. Let us say that on the basis of the desired current gain of the common-emitter stage we select an emitter resistor  $R_e = 100 \Omega$ . What is the value of the parallel emitter capacitance  $C_e$  which would give the input impedance according to [Fig. 3.2.8d](#)?

Since  $R_e C_e = \tau_T = 265$  ps, it follows that:

$$C_e = \frac{\tau_T}{R_e} = \frac{256 \cdot 10^{-12}}{100} = 2.65 \text{ pF only!} \quad (3.2.48)$$

If the stage has an emitter current  $I_e = 10$  mA, then:

$$r_e = \frac{26 \text{ mV}}{10 \text{ mA}} = 2.6 \Omega \quad (3.2.49)$$

Without the  $R_e C_e$  network in the emitter, the base to emitter capacitance  $C_\pi$  would define the bandwidth and its estimated value would be ([Eq. 3.1.4](#)):

$$C_\pi = \frac{1}{2 \pi r_e f_T} = \frac{1}{2 \pi \cdot 2.6 \cdot 600 \cdot 10^6} = 102 \text{ pF} \quad (3.2.50)$$

By introducing the  $R_e C_e$  network in the emitter circuit, we have reduced the base to emitter capacitance, seen by the input current, by  $102/2.65 = 38.5$  times! Of course, to our 2.65 pF we must add in parallel the capacitance  $C_M = C_\mu (1 + A_v)$  and the base spread resistance  $r_b$  in series with this network to obtain a more accurate input impedance. Since now the collector to base capacitance  $C_\mu$  has become significant, especially because it is ‘magnified’  $(1 + A_v)$  times, we must look for some methods to reduce its effect as much as possible. We shall discuss this in the following sections.

Owing to  $R_e$  the input resistance is increased to:

$$R_i \simeq (1 + \beta_0) R_e = (1 + 80) 100 = 8100 \Omega \quad (3.2.51)$$

Here, too, we have neglected the base resistance  $r_b$ ; it must be added to the value above to obtain a more accurate figure.

In [Fig. 3.2.9a](#) the transistor stage with  $R_e C_e$  is shown again and in [Fig. 3.2.9b](#) is its small signal equivalent input circuit.

In wideband amplifiers we usually make the emitter network with  $C_e \leq 20$  pF. In order to match  $R_e C_e = \tau_T$  the capacitor  $C_e$  is often made adjustable, because  $\tau_T$  in commercially available transistors have rather large tolerances.

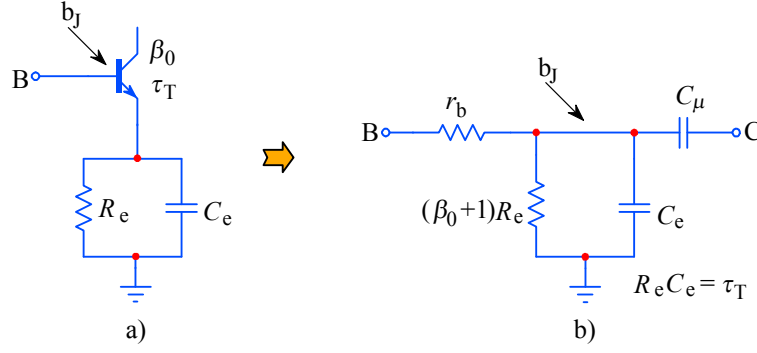


**Fig. 3.2.9:**  $R_e C_e$  network transformation: a) schematic; b) equivalent circuit. The symbol  $b_J$  represents the internal base junction.

With an appropriate  $R_L$  in the collector (not shown in Fig. 3.2.9) we might now calculate the (decreased) voltage amplification  $A_v$  owed to the  $R_e C_e$  network in the emitter circuit of the common emitter stage and consider the decreased value of the Miller capacitance  $C_M$ . Since we shall not use exactly such amplifier configuration we leave this as an exercise to the reader.

But for the application in the cascode amplifier, which we are going to discuss in [Sec. 3.4](#), it is important to know the transconductance  $i_o/v_i$  of the amplifier with the  $R_e C_e$  network. The corresponding circuit is drawn again in [Fig. 3.2.10a](#) and [Fig. 3.2.10b](#) shows the equivalent small signal circuit.

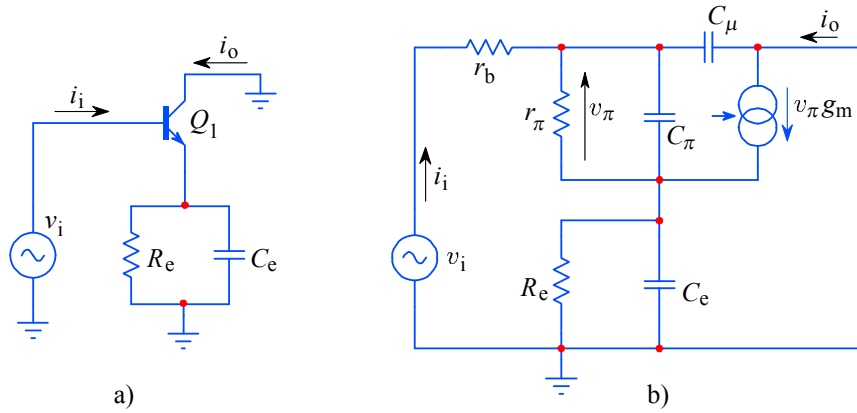


**Fig. 3.2.10:** Common collector amplifier: a) schematic; b) equivalent small signal circuit.

If we neglect the resistance  $r_b$  and the capacitance  $C_\mu$  the following relation is valid for the remaining circuit:

$$v_i = i_i (z_\pi + Z_e) + i_o Z_e \quad (3.2.52)$$

where:

$$i_o = g_m v_\pi \quad \text{and} \quad v_\pi = i_i z_\pi$$

therefore:

$$i_o = g_m i_i z_\pi \quad (3.2.53)$$

The impedances  $z_\pi$  and  $Z_e$  are:

$$z_\pi = \frac{r_\pi}{1 + s C_\pi r_\pi} \quad \text{and} \quad Z_e = \frac{R_e}{1 + s C_e R_e} \quad (3.2.54)$$

We can rewrite [Eq. 3.2.52](#) as:

$$v_i = i_i (z_\pi + Z_e + g_m z_\pi Z_e) \quad (3.2.55)$$

and the input current is:

$$i_i = \frac{v_i}{z_\pi + Z_e + g_m z_\pi Z_e} \quad (3.2.56)$$

The output current can be obtained by inserting [Eq. 3.2.56](#) back into [Eq. 3.2.53](#):

$$i_o = \frac{g_m z_\pi v_i}{z_\pi + Z_e + g_m z_\pi Z_e} \quad (3.2.57)$$

The transadmittance is:

$$\frac{i_o}{v_i} = \frac{g_m z_\pi}{z_\pi + Z_e + g_m z_\pi Z_e} \quad (3.2.58)$$

We can divide the numerator and denominator by  $g_m z_\pi Z_e$ :

$$\frac{i_o}{v_i} = \frac{1}{Z_e} \cdot \frac{1}{\frac{1}{g_m Z_e} + \frac{1}{g_m z_\pi} + 1} \quad (3.2.59)$$

Now we insert the expressions for  $z_\pi$  and  $Z_e$  from [Eq. 3.2.54](#) and replace  $g_m$  by  $1/r_e$ :

$$\frac{i_o}{v_i} = \frac{1}{R_e} \cdot \frac{1 + s C_e R_e}{\frac{r_e}{R_e} (1 + s C_e R_e) + \frac{r_e}{r_\pi} (1 + s C_\pi r_\pi) + 1} \quad (3.2.60)$$

and with a slight rearrangement we obtain:

$$\frac{i_o}{v_i} = \frac{1}{R_e} \cdot \frac{1 + s C_e R_e}{\frac{r_e}{R_e} + \frac{r_e}{r_\pi} + 1 + s (C_e + C_\pi) r_e} \quad (3.2.61)$$

Because  $(r_e/R_e) \ll 1$  and  $(r_e/r_\pi) \ll 1$  we can neglect them, so:

$$\frac{i_o}{v_i} = \frac{1}{R_e} \cdot \frac{1 + s C_e R_e}{1 + s (C_e + C_\pi) r_e} \quad (3.2.62)$$

This equation can be simplified if we ‘tune’ the emitter network so that:

$$\begin{aligned} C_e R_e &= (C_e + C_\pi) r_e \\ \Rightarrow C_e (R_e - r_e) &= C_\pi r_e \\ \Rightarrow C_e R_e &\approx C_\pi r_e \end{aligned} \quad (3.2.63)$$

The transadmittance can thus be expressed simply as:

$$\boxed{\frac{i_o}{v_i} = \frac{1}{R_e}} \quad (3.2.64)$$

Here we must not forget that at the beginning of our analysis we have neglected the resistance  $r_b$ , which, together with the transformed input capacitance  $C_e$  and the collector to base capacitance  $C_\mu$ , makes a pole at:

$$s_1 = -1/(C_e + C_\mu) r_b \quad (3.2.65)$$

The magnitude of  $s_1$  is equal to the upper half power frequency:  $|s_1| = \omega_h$ . This pole makes the stage frequency dependent in spite of [Eq. 3.2.64](#). We have also neglected the input resistance  $\beta_0 R_e$ , but, since it is much larger than  $r_b$ , we shall not consider its influence (with it, the bandwidth would increase slightly). By introducing the pole  $s_1$  back into [Eq. 3.2.64](#), we obtain a more accurate expression for the transadmittance:

$$\boxed{\frac{i_o}{v_i} = \frac{1}{R_e} \cdot \frac{-\frac{1}{(C_e + C_\mu) r_b}}{s - \left[ -\frac{1}{(C_e + C_\mu) r_b} \right]}} \quad (3.2.66)$$



### 3.3 Common-Base Amplifier

In the previous sections we have realized that the collector to base capacitance  $C_\mu$  has a very undesirable effect on the stage bandwidth (Miller effect). But in the common base configuration the base is effectively grounded and any current through  $C_\mu$  is fed to the ground, not affecting the base current (actually, owing to the physical construction of the CB junction  $C_\mu$  is spread across the whole base resistance  $r_b$ , so part of that current would nevertheless reach the base, which we shall analyze later).

The common base circuit is drawn in [Fig. 3.3.1a](#) and its small signal equivalent circuit in [Fig. 3.3.1b](#). In wideband amplifiers the loading resistor  $R_L$  is much smaller than the collector to base resistance  $r_\mu$ , so we shall neglect the later. In order to make the expressions still simpler, at the beginning of our analysis we shall also not take into account the base resistance  $r_b$ . However, we shall have to include  $r_b$  later, when we shall discuss the input impedance.

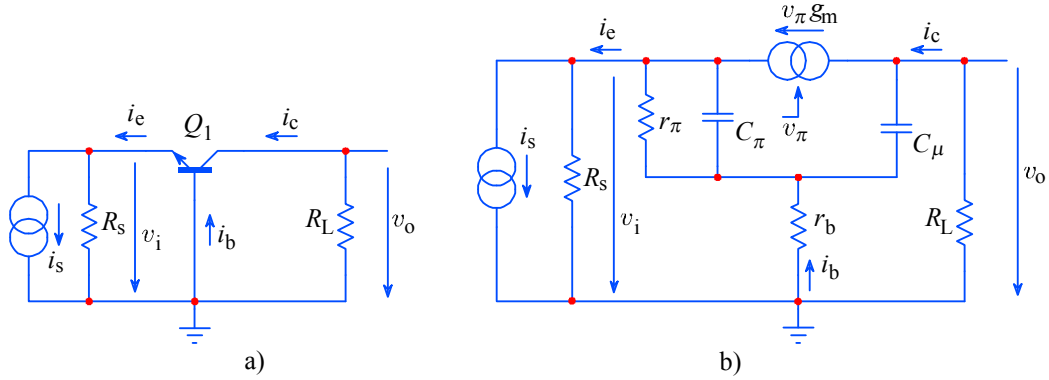


**Fig. 3.3.1:** Common base amplifier: a) schematic; b) equivalent small signal model.

The main characteristics of the common base stage are a very low input impedance, a very high output impedance, the current amplification factor  $\alpha_0 \approx 1$ , and, with the correct value of the loading resistor  $R_L$ , the possibility of achieving higher bandwidths. The last property is owed to a near elimination of the Miller effect, since  $C_\mu$  is now grounded and does not affect the input  $A_v$  times. Thus  $C_\mu$  is effectively in parallel with the loading resistor  $R_L$  and — because we can make the time constant  $R_L C_\mu$  relatively small — the bandwidth of the stage may be correspondingly large.

Another very useful property of the common base stage is that the collector to base breakdown voltage  $V_{cbo}$  is highest when the base is connected to ground and the higher reverse voltage reduces  $C_\mu$  further ([Eq. 3.1.2](#)). Owing to all the listed properties the common base stage is used almost exclusively for wideband amplifier stages where large output signals are expected.

Following the current directions in [Fig. 3.3.1](#), the input emitter current is:

$$i_e = \frac{v_\pi}{z_\pi} + g_m v_\pi \quad (3.3.1)$$

where:

$$z_\pi = \frac{r_\pi}{1 + s C_\pi r_\pi} \quad (3.3.2)$$

From these two equations it follows that:

$$i_e = v_\pi \left( g_m + \frac{1}{r_\pi} + s C_\pi \right) \quad (3.3.3)$$

The output collector current is:

$$i_c = g_m v_\pi \quad (3.3.4)$$

If we put [Eq. 3.3.3](#) into [Eq. 3.3.4](#) we obtain:

$$\frac{i_c}{i_e} = \frac{g_m}{g_m + \frac{1}{r_\pi} + s C_\pi} \approx \frac{g_m}{g_m + s C_\pi} = \frac{\alpha_0}{1 + s C_\pi r_e} \quad (3.3.5)$$

since  $g_m \approx 1/r_e$  and  $\alpha_0 = \beta_0/(\beta_0 + 1) \approx 1$ . This equation has the pole at  $-1/C_\pi r_e$ , which lies extremely high in frequency, because  $r_e$  is normally very low. Since the output pole  $-1/R_L C_\mu$ , which we shall consider next, becomes prevalent we can neglect  $s C_\pi r_e$  and assume that  $i_c \approx i_e$ . The output voltage is:

$$v_o = -i_c Z_L = -i_c \frac{R_L}{1 + s C_\mu R_L} \quad (3.3.6)$$

With the simplifications considered above we can write the expression for the transimpedance, which is:

$$\boxed{\frac{v_o}{i_e} \approx - \frac{R_L}{1 + s C_\mu R_L}} \quad (3.3.7)$$

Since the capacitance  $C_\mu$  is in parallel with the loading resistor  $R_L$ , we can improve the performance by applying any of the inductive peaking circuits from [Part 2](#). In practice we never consider only the ‘pure’ capacitance  $C_\mu$ , because some stray capacitances are always present and must be taken into account. Also, if the transistor  $Q_1$  is a part of an integrated circuit, we must consider the collector to substrate capacitance  $C_s$ . In such a case we use [Eq. 3.1.2](#) with the exponent  $m_c = 0.5$ .

### 3.3.1 Input Impedance

We shall calculate the input impedance of the common base stage by taking into account the base resistance  $r_b$ , which — as we shall realize very soon — represents a very nasty obstacle in achieving a wide bandwidth. We shall make our derivation on the basis of [Table 3.2.1](#), from which we have drawn [Fig. 3.3.2](#). This figure represents the equivalent small signal input circuit owed to  $r_b$ .

The input admittance of the circuit in [Fig. 3.3.2a](#) is:

$$Y_e = \frac{1}{r_b} + \frac{1}{\frac{r_b}{\beta_0} + s \tau_T r_b} \quad (3.3.8)$$

Within the frequency range of interest the value  $r_b/\beta_0$  in the second fraction is small and can be neglected. The simplified input admittance is thus:

$$Y_e \approx \frac{1}{r_b} + \frac{1}{s \tau_T r_b} \quad (3.3.9)$$

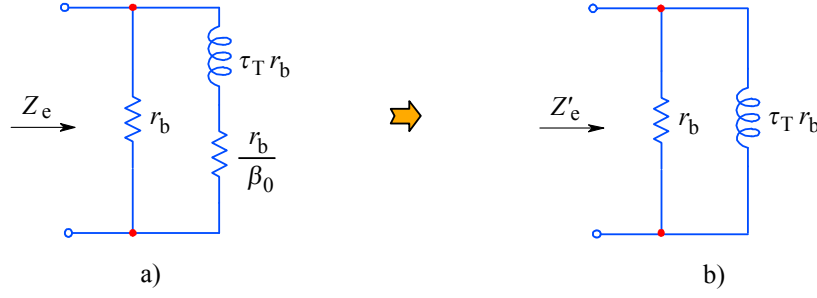


**Fig. 3.3.2:** Common base amplifier input impedance: a)  $r_b$  transformed to  $Z_e$ ; b) within the frequency range of interest,  $r_b/\beta_0$  can be neglected.

The real part represents a resistance:

$$R_e \approx r_b \quad (3.3.10)$$

and the imaginary part is an inductance:

$$L_e \approx r_b \tau_T \quad (3.3.11)$$

Normally, if the amplifier is built with discrete components, there is always some lead inductance  $L_s$  which must be added in series in order to obtain the total impedance.

In the next section, where we shall discuss the cascode amplifier, we shall find that the inductance  $L_e$ , together with the capacitance  $C_\mu$  of the common emitter current driving stage, forms a parallel resonant circuit which may cause ringing in the amplification of steep signals. In most cases the resistance  $R_e$  is too large to damp the ringing effectively enough by itself, so additional circuitry will be required.

[Eq. 3.3.10](#) and [Eq. 3.3.11](#), respectively, disclose the fact that the annoying inductance  $L_e$  and the resistance  $R_e$  are directly proportional to the base spread resistance  $r_b$ . When using this type of amplifier for the output stages, where the amplitudes are large (e.g., in oscilloscopes), we must use more powerful transistors, mostly in TO5 case type. In this case the internal transistor connections are relatively long and its total active area is large, the corresponding  $r_b$  is large as well. In order to decrease  $R_e$  and  $L_e$  we must select transistors which have low  $r_b$ . To decrease base spread resistance as much as possible and also to decrease the *transition time* (the time needed by the current carriers to pass the base width), the firm RCA has developed (already in the late 1960s) the so called *overlay transistor*. A typical overlay transistor is the 2N3866. Such transistors are essentially integrated circuits, composed of many identical small transistors connected in parallel.

(blank page)

### 3.4 Cascode Amplifier

If the common emitter amplifier of [Fig. 3.2.1a](#) is used as a driver of the common base amplifier of [Fig. 3.3.1a](#), a *cascode amplifier* [[Ref. 3.3](#), [3.7](#), [3.12](#)] is obtained. The name *cascode* springs from the times when electronic tubes were the circuit building blocks. The anode of the first tube (the equivalent of the common emitter stage) was loaded by the **cathode** input of the second tube with a grounded grid (the equivalent of the common base stage). Both electronic tubes were therefore connected in **cascade**, hence the compound word **cascode**.

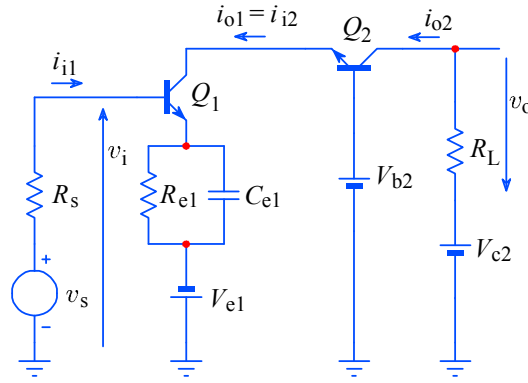


**Fig. 3.4.1:** Cascode amplifier schematic

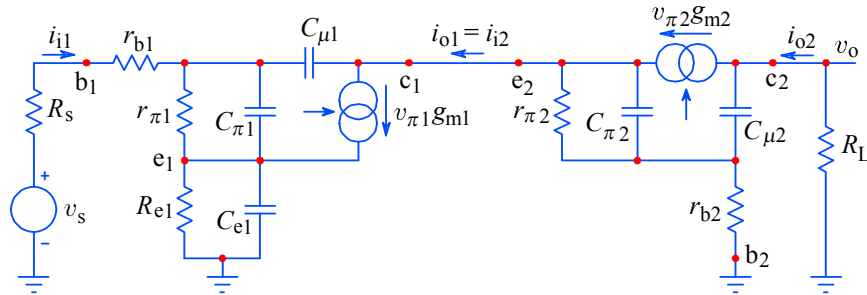


**Fig. 3.4.2:** Equivalent small signal model of a cascode amplifier. The components belonging to the common emitter circuit bear the index '1' and those of the common base circuit bear the index '2'.

#### 3.4.1 Basic Analysis

A transistor cascode amplifier is drawn in [Fig. 3.4.1](#) and [Fig. 3.4.2](#) shows its small signal equivalent circuit. All the components that belong to transistor  $Q_1$  bear the index '1' and all that belong to transistor  $Q_2$  bear the index '2'.

For the emitter network of  $Q_1$  we select the values such that  $R_{e1}C_{e1} = \tau_{T1}$ .

In order to simplify the initial analysis, we shall first neglect  $R_s$ ,  $r_{b2}$ , and  $C_{\mu1}$ . Later we shall reintroduce these elements one by one to get a closer approximation.

We have already derived the equations needed for each part of the combined circuit: for the common emitter stage we have [Eq. 3.2.66](#) and for the common base we

have [Eq. 3.3.7](#). We only need to multiply these two equations to get the voltage gain of our cascode amplifier:

$$A_v = \frac{i_{o1}}{v_i} \cdot \frac{v_o}{i_{o1}} = \frac{v_o}{v_i} \approx \frac{1}{R_{e1}} \cdot \frac{1}{1 + s C_{e1} r_{b1}} \cdot \left( - \frac{R_L}{1 + s C_{\mu2} R_L} \right) \quad (3.4.1)$$

Here we have approximated  $\alpha_{02} \approx 1$ , and therefore  $i_{o2} = i_{o1}$ . The first fraction, multiplied by  $R_L$  from the third fraction, is the DC voltage amplification and the remainder represents the frequency dependence:

$$A_v \approx - \frac{R_L}{R_{e1}} \cdot \frac{1}{(1 + s C_{e1} r_{b1})(1 + s C_{\mu2} R_L)} \quad (3.4.2)$$

Obviously, the frequency dependence is a second-order function. There are two poles: the pole at the input is  $-1/C_{e1} r_{b1} = -1/\tau_{T1}$  whilst the pole  $-1/C_{\mu2} R_L = -1/\tau_{T2}$  is on the output side. As we shall see later, it is possible to apply the peaking technique on both sides.

In an ideal case the common base stage input (emitter) impedance is very low. Because of this low load the first stage voltage gain  $A_{v1} \ll 1$ , so  $C_{\mu1}$  would not be amplified by it. And if we could neglect  $r_{b2}$  the capacitance  $C_{\mu2}$  would appear in parallel to the loading resistor  $R_L$ , and therefore it would neither be multiplied by the second stage's voltage gain  $A_{v2}$ . Both  $C_{\mu1}$  and  $C_{\mu2}$  are relatively small, so it is obvious that the cascode amplifier has, potentially, a much greater bandwidth in comparison with a simple common emitter amplifier (for the same total voltage gain). The price we pay for this improvement is the additional transistor  $Q_2$ .

Of course, in practice things are not so simple, and in addition we should not neglect the inevitable stray capacitances. Those should be added to  $C_{\mu1}$  and  $C_{\mu2}$ . Also,  $(R_s + r_{b1})$  with  $C_{\mu1}$  will affect the behavior of  $Q_1$  and  $r_{b2}$  with  $C_{\mu2}$  will affect the behavior of  $Q_2$ , as we shall see in the following analysis.

### 3.4.2 Damping of the $Q_2$ Emitter

Owing to the base spread resistance  $r_{b2}$  the  $Q_2$  input (emitter) has an inductive component with the inductance  $L_{e2} = \tau_{T2} r_{b2}$  in parallel with  $r_{b2}$ , as already shown in [Table 3.2.1](#) and also in [Fig. 3.3.2](#). The equivalent input impedance of the transistor  $Q_2$  was derived in [Eq. 3.3.9](#) to [Eq. 3.3.11](#).

As shown in the simplified circuit in [Fig. 3.4.3](#), the inductance  $L_{e2}$  and the collector to base capacitance  $C_{\mu1}$  of  $Q_1$  form a series resonant circuit, damped by  $r_{b2}$  in parallel with  $L_{e2}$  (and a series emitter resistance  $r_{b2}/\beta_2$ , which is very small, so it was neglected). The other end of  $C_{\mu1}$  is connected to the base of  $Q_1$ , where we must consider the following two effects:

- at very high frequencies the input signal goes directly through  $r_{b1}$  and  $C_{\mu1}$ ;
- at lower frequencies, the signal is inverted and amplified by  $Q_1$  and the internal base junction can then be treated as the virtual ground.

In an actual cascode amplifier  $Q_2$  operates at a much higher collector voltage than  $Q_1$ , and since the collector currents are nearly equal this means a higher power dissipation for  $Q_2$ . By using for  $Q_2$  a transistor capable of higher power dissipation, we shall probably have to accept its higher  $r_{b2}$  as well. This increases the inductance  $L_{e2}$  and lowers the damping of the series resonance formed by  $C_{\mu1}$  and  $L_{e2}$ , resulting in a large peaking near the upper cut off frequency.

To prevent this from happening, an additional impedance  $Z_d$ , consisting of a resistor  $R_d$  in parallel with a capacitor  $C_d$ , is connected between the collector of  $Q_1$  and the emitter of  $Q_2$ . If  $R_d$  is made equal to  $r_{b2}$ , then  $C_d$  can be chosen so, that it cancels  $L_{e2}$ ; the result is a resistive input impedance of the  $Q_2$  emitter:  $Z_{e2} \approx r_{b2}$ .

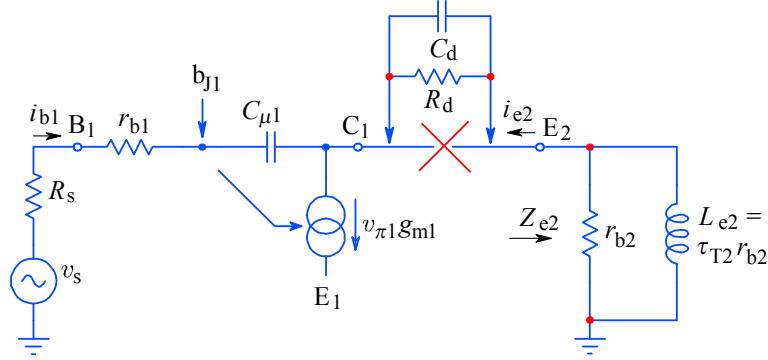


**Fig. 3.4.3:** Parasitic resonance damping of the cascode amplifier. Two current paths must be considered: at highest frequencies, for  $i_{b1}$ ,  $C_{\mu1}$  represents a non-inverting cross-talk path; at lower frequencies, for  $i_{c1}$ ,  $C_{\mu1}$  provides a negative feedback loop, thus it can be viewed as if being connected to a virtual ground ( $Q_1$  base junction  $b_{j1}$ ). The parasitic resonance, formed by  $C_{\mu1}$  and  $L_{e2}$  is only partially damped by  $r_{b2}$ ; the required additional damping is provided by inserting  $R_d$  and  $C_d$  between  $Q_1$  collector and  $Q_2$  emitter.

So let us put:

$$R_d = r_{b2} = \sqrt{\frac{L_{e2}}{C_d}} \quad (3.4.3)$$

The value of  $C_d$  is then:

$$C_d = \frac{\tau_{T2}}{r_{b2}} = \frac{1}{2\pi f_{T2} r_{b2}} \quad (3.4.4)$$

To get a feeling for actual values let us have two equal transistors with parameters such as in the examples in [Sec. 3.2.4](#) ( $f_T = 600$  MHz,  $r_{b2} = 47 \Omega$ ):

$$R_d = r_{b2} = 47 \Omega \quad C_d = \frac{1}{2\pi \cdot 600 \cdot 10^6 \cdot 47} = 5.6 \text{ pF} \quad (3.4.5)$$

The input impedance of the emitter circuit of transistor  $Q_2$  now becomes:

$$Z_{e2} \approx r_{b2} \quad (3.4.6)$$

which is resistive at all frequencies (approximately so, because we have allowed ourselves a simplification). The corresponding equivalent circuit is shown in [Fig. 3.4.4](#). The task of the impedance  $Z_d$  is actually twofold: it must damp the inductive input circuit of transistor  $Q_2$ , and as we shall see later, it can be a good choice for providing the thermal stabilization of the cascode stage.

Since we have introduced  $Z_d$  into the collector circuit of  $Q_1$  we must now account for the  $Q_1$  Miller capacitance:

$$C_{M1} \approx C_{\mu1} \left( 1 + \frac{Z_{e2}}{Z_{e1}} \right) = C_{\mu1} \left( 1 + \frac{r_{b2}}{R_{e1}} \right) \quad (3.4.7)$$

where  $Z_{e2}$  is the  $Q_2$  compensated emitter input impedance and  $Z_{e1}$  is the impedance of the emitter circuit of  $Q_1$ . With this consideration the gain, [Eq. 3.4.2](#), becomes:

$$A_v \approx - \frac{R_L}{R_{e1}} \cdot \frac{1}{[1 + s(C_{e1} + C_{M1})r_{b1}](1 + sC_{\mu2}R_L)} \quad (3.4.8)$$

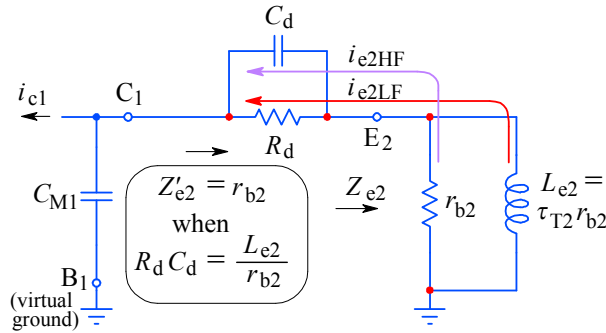


**Fig. 3.4.4:** With damping the simplified  $Q_2$  input impedance becomes (approximately) resistive. Note the high and low frequency paths.

The collector to base capacitance of the transistor  $Q_1$  allows very high frequency signals from the input bypassing this transistor and directly flowing into the emitter of transistor  $Q_2$ . Transistor  $Q_1$  amplifies, inverts, and delays the low frequency signals. In contrast, all of what comes through  $C_{\mu1}$  is *non-delayed*, *non-amplified*, and *non-inverted*, causing a pre-shoot [\[Ref. 3.1\]](#) in the step response, as shown in [Fig. 3.4.5](#). The  $Q_1$  collector current,  $i_{c1}$ , is the sum of  $i_{\mu1}$  and  $v_{\pi1}g_{m1}$ . Note that both the pre-shoot owed to  $i_{\mu1}$  and the overshoot of  $v_{\pi1}g_{m1}$  are reduced in  $v_{c2}$  by the  $Q_2$  pole ( $1/C_{\mu2}R_L$ ).

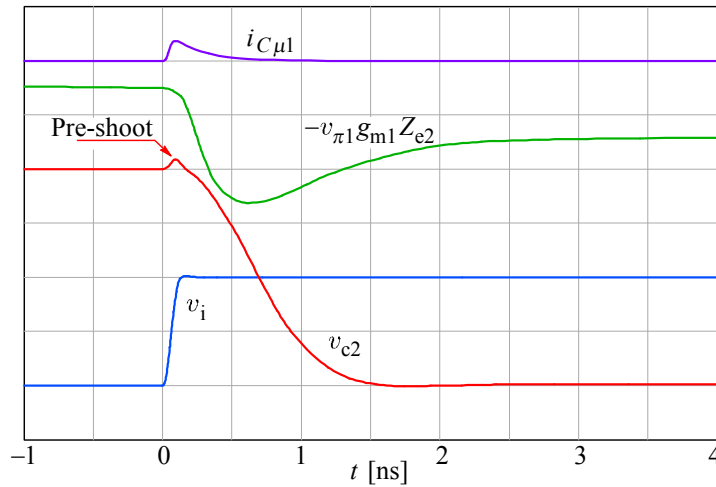


**Fig. 3.4.5:** The step response  $v_{c2}$  has a pre-shoot owed to the signal cross-talk through  $C_{\mu1}$  (arbitrary vertical units, but corresponding to  $A_v = -2$ ).



So far we have excluded  $C_{\mu 2}$  from our analysis. When included, its effect on bandwidth is severe, owing to the non-zero  $r_{b2}$  and the Miller effect. But it also affects the emitter input impedance of  $Q_2$  since  $C_{M2} = C_{\mu 2}(1 + A_v)$  appears in parallel to  $r_{b2}$  and is consequently transformed into the emitter in accordance with [Table 3.2.1](#), in the same way as in [Fig. 3.2.7](#). If  $A_v$  is relatively high the pronounced resonance owed to  $C_{\mu 2}$  can cause long ringing, even if the bandwidth is lower than the resonant frequency.

The damping by  $C_d R_d$  works only up to a certain frequency, because they add their own parasitic  $L$  and  $C$ , which we were trying to avoid in the first place, and which also reduce the bandwidth. Instead, *John Addis* [[Ref. 3.26](#)] suggests an alternative approach by modifying the base impedance: the  $Q_2$  base is connected to the bias voltage through a resistor  $R_A$  of up to a  $100\ \Omega$  and grounded by a small capacitor  $C_A \approx C_{\mu 2}$ . In [Fig. 3.4.6](#) we compare the voltage gain, the phase, and the group delay for the two cases:  $R_A = 0$  and  $R_A = 33\ \Omega$ , respectively (the value of  $33\ \Omega$  was optimized to the transistor model used in the simulation). The change in the  $Q_2$  emitter impedance (b curves) is exposed by the lower drive stage current  $i_{c1}$  near the cut off frequency.

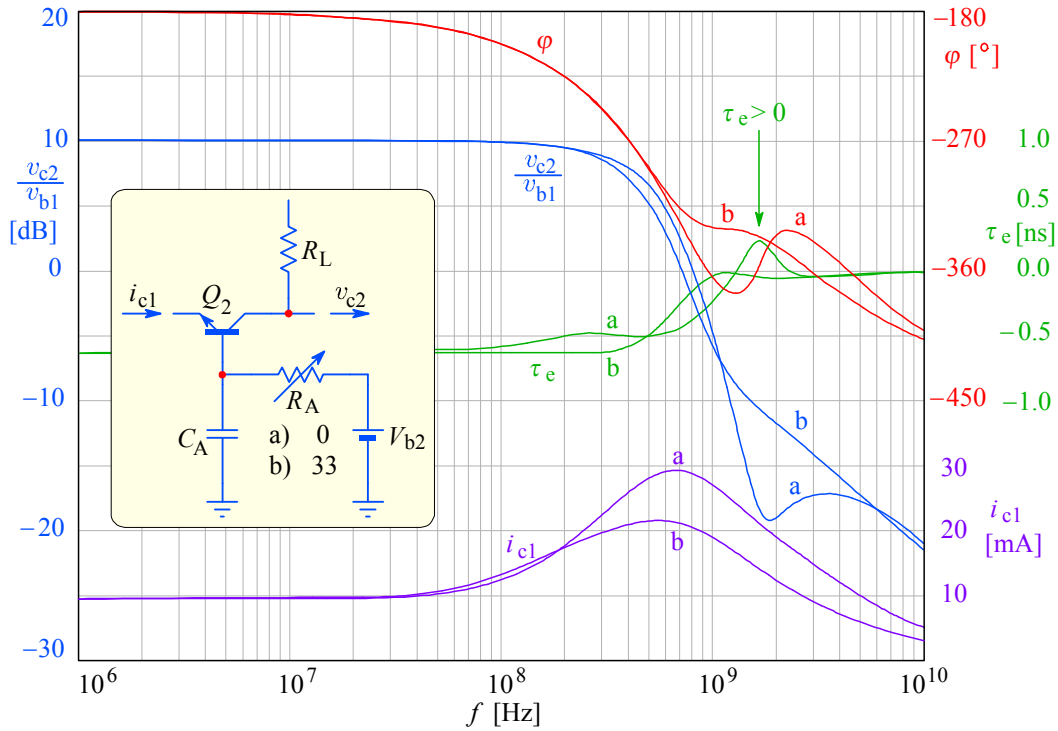


**Fig. 3.4.6:** The compensation method of  $Q_2$  as suggested by John Addis. a) With  $R_A = 0$ , the frequency response has a notch at the resonance and a phase-reversed cross-talk, which makes the group delay  $\tau_e$  positive, causing a potential instability. b) with  $R_A = 33\ \Omega$  and  $C_A = 3\ \text{pF}$  (the values suit the particular transistor model used for simulation) the frequency response slope is corrected to the  $-6\ \text{dB}/2f$ , the phase is smoothed and, although the bandwidth is reduced slightly, the group delay linearity is extended and the undesirable positive region is reduced to negative. The  $Q_2$  emitter impedance is increased near cut off, as can be deduced from the lower  $i_{c1}$  peak.

To analyze this type of compensation of the  $Q_2$  emitter impedance we must consider the equivalent circuit in [Fig. 3.4.7](#). Here the capacitance  $C_{\mu 2}$  is seen by the base as the Miller capacitance  $C_{M2}$  (remembering that  $A_v = R_L/R_{e1}$ ):

$$C_{M2} = C_{\mu 2}(1 + A_v) \quad (3.4.9)$$

which appears in parallel with the base spread resistance  $r_{b2}$ .

The external compensation network, the parallel connection of  $R_A$  and  $C_A$ , is added in series and the total can then be transformed by the same rule as in [Fig. 3.2.7](#). The base impedance is:

$$Z_{b2} = \frac{1}{\frac{1}{r_{b2}} + sC_{\mu2}} + \frac{1}{\frac{1}{R_A} + sC_A} \quad (3.4.10)$$

If  $R_A \approx r_{b2}$  and  $C_A \approx C_{\mu2}$  then  $Z_{b2}$  becomes:

$$Z_{b2} = \frac{2R_A}{1 + sC_A R_A} = \frac{R_s}{1 + sC_s R_s} \quad (3.4.11)$$

which appears at the  $Q_2$  emitter as a parallel connection of  $R_s = 2R_A$  and  $C_s = C_A/2$ .

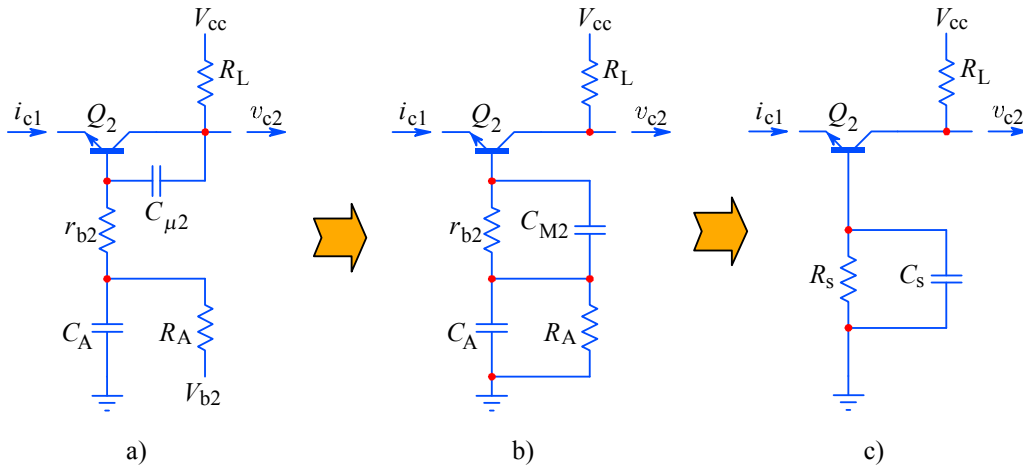


**Fig. 3.4.7:** The  $Q_2$  emitter input impedance compensation by the added base network  $R_A$  and  $C_A$  (see also [Fig. 3.2.7](#)), making it capacitive at high frequencies. By altering the value slightly it can also be used to compensate the stray base inductance.

### 3.4.3 Thermal Compensation

Amplifier's thermal stability is preferably solved by using a differential configuration. However, in order to illustrate the potential problems, we discuss a single transistor stage. The well known relation for the transistor's base-emitter voltage is:

$$V_{be} = \frac{k_B T_j}{q_e} \ln \left( \frac{I_e}{I_s} + 1 \right) \quad (3.4.12)$$

where  $T_j$  is the absolute temperature of the p-n junction, which causes the increase of  $V_{be}$  in a linear proportion. Unfortunately, the situation is complicated by the 'saturation current'  $I_s \approx 10^{-14}$  A (for a typical silicon transistor at room temperature), which approximately doubles for every 8 K increase in temperature. The combined influence results in a  $V_{be}$  temperature coefficient of  $\approx -2$  mV/K (see [Appendix 3.1](#) on the disk). All other terms are constants (as *James M. Bryant* of Analog Devices likes to joke, we can not change the Boltzmann constant  $k_B$  because *Ludwig Boltzmann* is already dead, and neither can we change the electron charge  $q_e$  because both *Charles Augustine de Coulomb* and *Joseph John Thompson* are dead, too!).

When we apply the bias and the supply voltage to a transistor, the power dissipated by the transistor depends on the collector current  $I_c$  and the voltage  $V_{ce}$  across the transistor:

$$P_D = I_c V_{ce} \quad (3.4.13)$$

If we know the ambient temperature  $T_a$  and the thermal resistance from junction to ambient  $R_{\theta ja}$  [K/W] (*kelvin per watt*), we can calculate the junction temperature  $T_j$ :

$$T_j = T_a + R_{\theta ja} P_D \quad (3.4.14)$$

In a properly designed amplifier, a certain time after power-up an equilibrium is reached: all the heat generated by the transistor dissipates into the ambient and the transistor obtains a stable, but higher temperature.

If we now apply a voltage step to the base the collector current  $I_c$  increases, changing the power dissipation (depending on the chosen DC bias it can either increase or decrease). A little later, depending on the thermal capacitance of the transistor's case  $C_{\theta c}$  and the thermal resistance  $R_{\theta ja}$ , a new temperature equilibrium is reached. As shown in [Fig. 3.4.8](#), the change occurs gradually, depending on the transistor thermal time constant. But the supply voltage is shared between the transistor and the loading resistance, whilst the same current flows through both of them, therefore the choice of the DC bias point governs whether the transistor power dissipation will increase or decrease with the signal. This is known as the 'thermal distortion'.

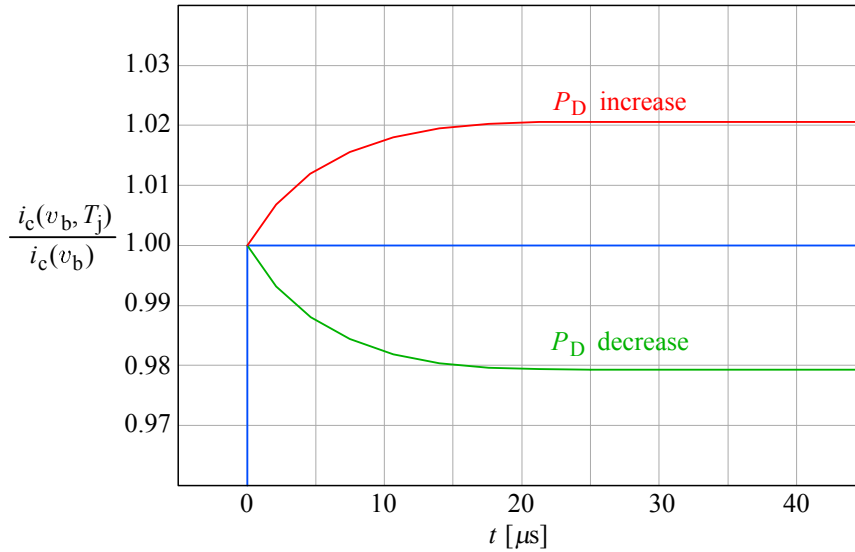


**Fig. 3.4.8:** The collector current step response is distorted by a long term thermal drift following the transient. Depending on the chosen DC bias point, the output can either increase or decrease relative to the ideal response. In addition to the junction thermal time constant, there can also be a slower one, owed to the transistor case temperature change.

Although the dynamic emitter resistance  $r_e$  is also temperature dependent (see [Eq. 3.1.1](#)), which affects the gain (see [Eq. 3.2.61](#)), in all wideband circuits we put (for bandwidth reasons!) a much larger external degeneration resistance  $R_e$  in series, reducing the gain temperature dependence. So in practice all thermal changes occur because of  $V_{be}$  and  $I_s$ .

In a multi-stage amplifier different transistors will have different operating points, thus different temperatures and temperature dependence. Also, they have different time constants, which cause longer and shorter drifts, and we can not expect all effects to cancel. Consequently even long oscillations in the step response can occur.

Before we look for the remedy for the problem of how to cancel, or at least how to substantially reduce the thermal distortion, let us take a look at [Fig. 3.4.9](#), which shows a simple common emitter stage, and the way in which the power dissipation is shared between the load and the transistor as a function of the collector current. As usual, we use capital letters for the applied DC voltages, loading resistor, etc., and small letters for the instantaneous signal voltages and currents. The transistor's power dissipation is:

$$P_D = v_{ce} i_c = v_{ce} \frac{v_L}{R_L} = v_{ce} \frac{V_{cc} - v_{ce}}{R_L} = v_{ce} \frac{V_{cc}}{R_L} - \frac{v_{ce}^2}{R_L} \quad (3.4.15)$$

Since  $v_{ce}$  cannot exceed  $V_{cc}$  if the collector load is purely resistive, the right-hand vertical axis is normalized to  $V_{cc}$ . The left-hand vertical axis is normalized to the maximum load power, which is simply  $P_{Lmax} = V_{cc}^2/R_L$  (corresponding to  $v_{ce} = 0$  and thus  $P_D = 0$ ). The transistor's power dissipation, however, follows an inverse parabolic function with a maximum at  $v_{ce} = V_{cc}/2$ :

$$P_{Dmax} = \left( \frac{V_{cc}}{2} \right)^2 \frac{1}{R_L} = \frac{V_{cc}^2}{4R_L} \quad (3.4.16)$$

This middle point is the optimum DC bias point for a transistor stage. If excited by small signals, the transistor power dissipation follows the parabola close to its broad and relatively flat top and thus it does not change very much. This means that the transistor's temperature does not change very much either.

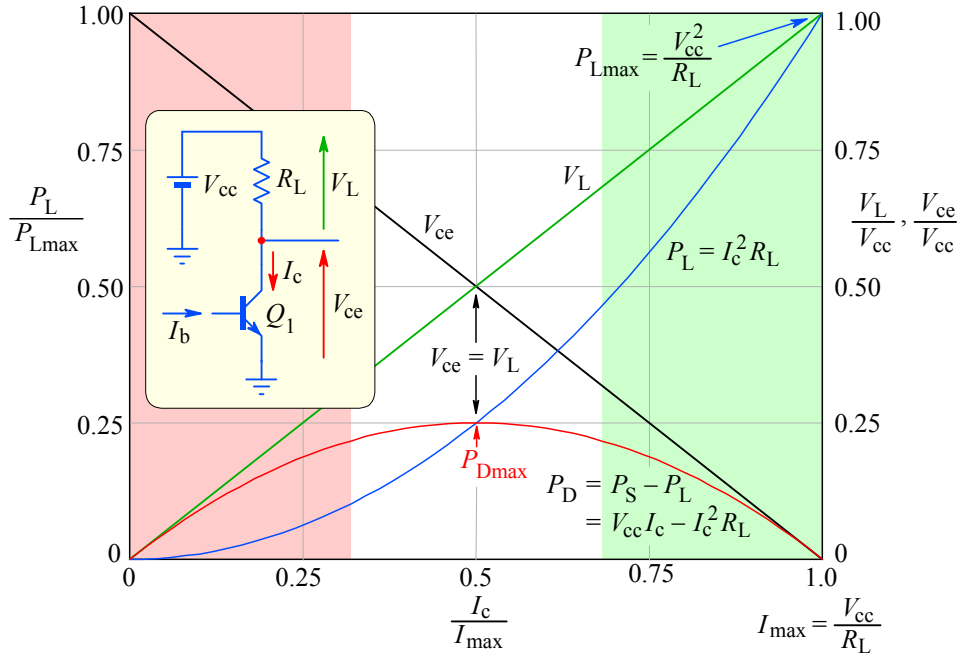


**Fig. 3.4.9:** The optimum bias point is when the voltage across the load is equal to the voltage across the transistor. This is optimal both in the sense of thermal stability, as well as in the available signal range sense.

If other design requirements force us to move the bias point far from the top of the parabola, the bias with  $V_{ce} < V_{cc}/2$  (or  $I_c > I_{max}/2$ ) is preferred, in contrast to the range  $V_{ce} > V_{cc}/2$ , because the latter situation is unstable. However, in wideband amplifiers we can hardly avoid it, because we want to have a low  $R_L$ , a high  $I_c$  and a high  $V_{cb}$  (to reduce  $C_\mu$ ) and all three conditions are required for high bandwidth.

The typical temperature coefficient of a base–emitter p–n junction voltage ( $\approx 0.6$  V) is approximately  $-2$  mV/K for silicon transistors, so we can explain the instability in the following way:

When the circuit is powered up the transistor conducts a certain collector current, which heats the transistor, increasing the transistor base–emitter p–n junction temperature. If the base is biased from a voltage source (low impedance, which in wideband amplifiers is usually the case), the temperature increase will, owing to the negative temperature coefficient, decrease the base–emitter voltage. In turn, the base current increases and, consequently, both the emitter and the collector current increase, which further increases the dissipation and the junction temperature. The load voltage drop would also increase with current and therefore reduce the collector voltage, thus lowering the transistor power dissipation. But with a low  $R_L$ , the change in the drop of load voltage will be small, so the transistor power dissipation increase will be reduced only slightly.

The effect described is cumulative; it may even lead to a thermal runaway and the consequent destruction of the transistor if the top of the parabola exceeds the maximum permissible power dissipation of the transistor (which is often the case, since we want low  $R_L$  and high  $V_{cc}$  and  $I_e$ , as stated above). In a similar way, on the basis of the  $-2$  mV/K temperature dependence of  $V_{be}$ , the reader can understand why the bias point for  $V_{ce} < V_{cc}/2$  is thermally stable.

According to [Eq. 3.4.16](#), to have the transistor thermally stable means having resistance  $R_L$  (or  $R_L + R_e$ ) such that at the bias point the voltage drop across them is equal to  $V_{cc}/2$ . In general, this principle is successfully applied in differential amplifiers: when one transistor is excited so that its bias point is pushed to one side of the parabola the bias point of the other transistor is moved exactly to the same dissipation on the opposite side of the parabola. As a result the temperature becomes lower but equal in both transistors. Thus in the differential amplifier both transistors can always have similar temperatures, even if the temperature changes by the signal (provided that we remain within the linear range of excitation). Also, the thermal drift can be minimized by using current source biasing in the emitters of a differential amplifier, as well as using emitter degeneration resistors, which minimize variations in  $\Delta V_{be}$ , even if transistor parameters vary considerably.

In our cascode circuit of [Fig. 3.4.1](#) the transistor  $Q_1$  already has an emitter resistor  $R_{e1}$  as dictated by the required current gain, and we do not want to change it. However, we can add a resistor, which we label  $R_\theta$ , in the collector circuit of  $Q_1$  to make  $V_{ce1} \approx I_{c1} (R_{e1} + R_\theta) \approx V_{e2}/2$ , where  $V_{e2}$  is the voltage at the emitter of the transistor  $Q_2$ . Suppose now that the emitter current is  $I_{e1} \approx I_{c1} = 50$  mA and the  $Q_2$  base voltage  $V_{b2} = +15$  V. Then the emitter voltage of transistor  $Q_2$  is:

$$V_{e2} = V_{b2} - V_{be2} \approx 15 - 0.6 = 14.4 \text{ V} \quad (3.4.17)$$

where  $V_{be2}$  is the base–emitter voltage (about 0.6 V for a silicon transistor).

With  $R_{e1} = 20 \Omega$  the value of the thermal compensation resistor is:

$$R_{\theta} = \frac{V_{e2}/2 - I_{c1} R_{e1}}{I_{c1}} = \frac{14.4/2 - 0.05 \cdot 20}{0.05} = 124 \Omega \quad (3.4.18)$$

Such a resistor should be used instead of  $R_d$  as calculated before to achieve both the ringing suppression and the thermal compensation. But by inserting these  $124 \Omega$  instead of  $R_d = 47 \Omega$ , the Miller capacitance  $C_M$  would increase to  $27.8 \text{ pF}$ , decreasing the amplifier bandwidth too much. Fortunately the compensating resistor  $R_{\theta}$  needs to correct the behavior of the amplifier only at very low frequencies. So we can bridge that part of it which is not needed for the suppression of ringing by an appropriate capacitor; let us call it  $C_{\theta}$ , as shown in [Fig. 3.4.10](#). By doing so, we prevent an excessive increase of Miller capacitance.

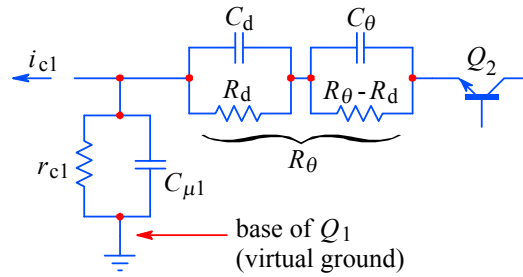


**Fig. 3.4.10:** The modified compensation network:  $R_d C_d$  provide the HF damping, whilst  $R_{\theta} C_{\theta}$  provide thermal compensation.

The question is how to calculate the proper value of  $C_{\theta}$ ? The obvious way would be to calculate the thermal capacity of the transistor's die and case mass (and an eventual heat sink) and all the thermal resistances (junction to case, case to heat sink, heat sink to air), as is usually done for high power output stages.

*Bruce Hofer* [[Ref.3.8](#)] suggests the following — more elegant — procedure, based on [Fig. 3.4.10](#). The two larger time constants in this figure must be equal:

$$(R_{\theta} - R_d) C_{\theta} = r_{c1} C_{M1} \quad (3.4.19)$$

Here  $r_{c1}$  is the dynamic collector resistance of transistor  $Q_1$ , derived from [Fig. 3.4.11](#) as  $\Delta V_{ce} / \Delta I_c$ . In this figure  $V_A$  is the *Early voltage*:

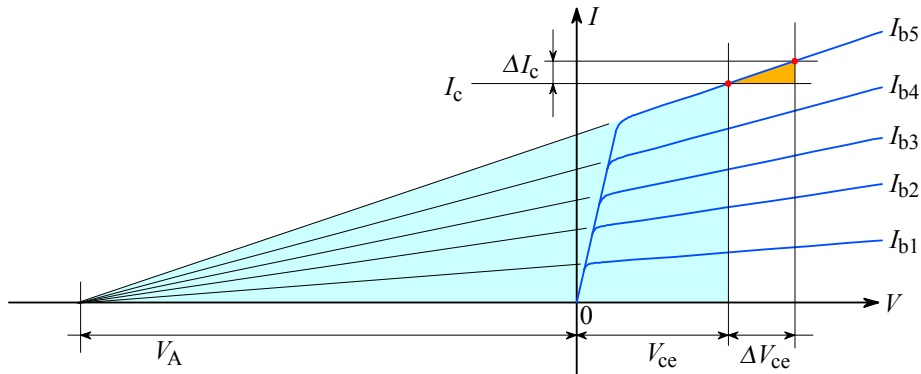


**Fig. 3.4.11:** The dynamic collector resistance  $r_{c1}$  is derived from the  $I_c(V_{ce}, I_b)$  characteristic and the Early voltage  $V_A$ .

The meaning of the Early voltage can be derived from [Fig. 3.4.11](#), where several curves of the collector current  $I_c$  vs. collector to emitter voltage  $V_{ce}$  are drawn, with base current  $I_b$  as the parameter. With increasing collector voltage the collector current increases even if the base current is kept constant. This is because the collector to base depleted area widens on the account of the (active) base width as the collector voltage increases. This in turn causes the diffusion gradient of the current carriers in the base to increase, hence the increased collector current.

By extending the lines of the collector current characteristics back, as shown in [Fig. 3.4.11](#), all the lines intersect the abscissa at the same virtual voltage point  $V_A$  (negative for NPN transistors), called the *Early voltage* (after *J.M. Early*, [[Ref. 3.11](#)]). From the similarity of triangles we can derive the collector's dynamic resistance:

$$r_{c1} = \frac{\Delta V_{ce}}{\Delta I_c} = \frac{V_c - (-V_A)}{I_c} \quad (3.4.20)$$

Since the voltage gain of the common emitter stage is low,  $C_{M1}$  will be only slightly larger than  $C_{\mu1}$ . If we now suppose that transistor  $Q_1$  has an  $r_{c1} = 0.5 \cdot 10^6 \Omega$  and  $C_{\mu1} = 3 \text{ pF}$ , the value of  $C_\theta$  should be:

$$C_\theta = \frac{r_{c1} C_{M1}}{R_\theta - R_d} = \frac{0.5 \cdot 10^6 \cdot 3 \cdot 10^{-12}}{124 - 47} = 19.5 \text{ nF} \quad (3.4.21)$$

In practice, we can take the closest standard values, e.g.,  $C_\theta = 22 \text{ nF}$  and  $R_\theta - R_d = 124 - 47 = 77 \Omega \approx 75 \Omega$ . Since, in general, a wideband amplifier has several amplifying stages, each one having its own temperature and damping problems, these values can be varied substantially in order to achieve the desired performance. Thermal problems tend to be more pronounced towards the output stages where the signal amplitudes are high. Here experimentation should have the last word. Nevertheless, the values obtained in this way represent a good starting point.

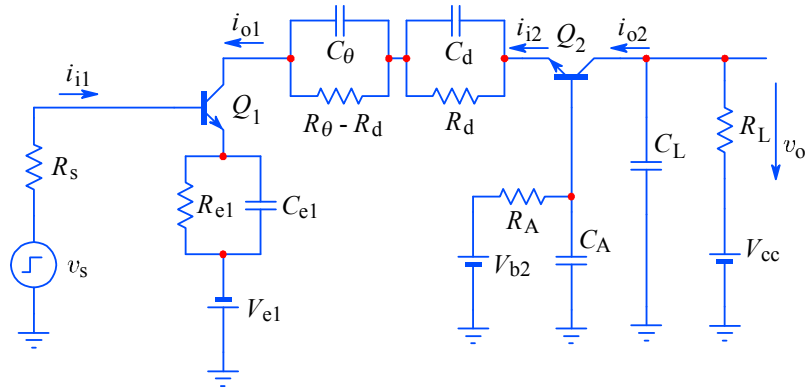


**Fig. 3.4.12:** The compensated cascode amplifier. If  $R_A C_A$  compensation is used,  $R_d C_d$  may become unnecessary. The main bandwidth limiting time-constants are now  $(R_s + r_{b1})C_{e1}$  and  $(C_{\mu2} + C_L)R_L$ .

In order to achieve a good thermal compensation, the same half-voltage principle ([Fig. 3.4.9](#)) can be applied to both  $Q_1$  and  $Q_2$ , although this will rarely be possible. On the other hand, a cascode amplifier can always be implemented as a differential amplifier, simplifying the problem of thermal compensation and, as a bonus, doubling the gain. We shall see this later in [Sec. 3.7](#). There are, as we are going to see in following sections, still some points for possible improvement of the cascode amplifier.

All the discussion on thermal compensation in this section was based on the simple single stage cascode amplifier shown in [Fig. 3.4.12](#).

It is however important to note that a multistage DC coupled amplifier must necessarily be built in a differential configuration. Then many of the effects described would be either compensated automatically or at least reduced significantly. Not all, unfortunately. Often the biggest problems will be caused by the first stage, since its output will be amplified by all the remaining gain of the chain. But the stages following it might also have their share, because of the increased signal amplitude. And the output stage is usually the one to drive the load, thus it is required to handle most of the power. It is therefore necessary to pay attention to thermals at each stage.

In addition, in an integrated circuit it is also necessary to check the adjacent circuits, such as current mirrors, constant current bias circuits and voltage references; they will all be affected by every thermal gradient across the chip. They will also tend to have their own particular thermal time constant, and changes in those can in turn affect the main signal chain. Consequently a complex system can be difficult to control and compensate properly.

Finally, in amplifiers employing DC feedback the thermal problems are usually reduced to only those of the first stage, but still the output stage could be prone to thermal runaway under heavy load.

Some of these problems will be mentioned again in discussions of differential circuit configurations in further sections and chapters.



### 3.5 Emitter Peaking in a Cascode Amplifier

Here we shall examine the possibility of improving the cascode amplifier bandwidth by applying the emitter peaking technique.

Let us return to the basic cascode amplifier of [Fig. 3.4.1](#) and [Fig. 3.4.2](#), but with a little modification: we shall assume a current signal source in parallel with the source resistance  $R_s$ . We shall also assume that there is an output capacitance in parallel with the load resistance  $R_L$  such that its value is  $C_o = C_{\mu 2} + C_L$ . To simplify the analysis we shall disregard the damping and thermal compensation described in the previous section. We shall basically follow the steps of Carl Battjes [[Ref. 3.1](#)], to show a different approach to the cascode amplifier design.

#### 3.5.1 Basic Analysis

The transimpedance of the amplifier in [Fig. 3.5.1](#) is:

$$\frac{v_o}{i_s} = \frac{i_{b1}}{i_s} \cdot \frac{i_{c1}}{i_{b1}} \cdot \frac{i_{c2}}{i_{c1}} \cdot \frac{v_o}{i_{c2}} \quad (3.5.1)$$

where:

$$\frac{i_{b1}}{i_s} = \frac{R_s}{R_s + Z_i} \quad \text{and} \quad \frac{i_{c1}}{i_{b1}} = \beta(s) = \frac{1}{\frac{1}{\beta_0} + s \tau_{T1}} \quad (3.5.2)$$

with  $Z_i$  being the input impedance looking into the base of transistor  $Q_1$  and  $R_s$  the source resistance. At higher frequencies, when the input capacitance of transistor  $Q_1$  prevails (see [Eq. 3.2.12](#) and [[Ref. 3.1](#)]), we have:

$$\frac{i_{c1}}{i_{b1}} \approx \frac{1}{s \tau_{T1}} \quad \text{and} \quad \tau_{T1} = \frac{1}{2\pi f_{T1}} \quad (3.5.3)$$

Further, for  $Q_2$  we have:

$$\frac{i_{c2}}{i_{c1}} = \alpha_2 \approx 1 \quad \text{and} \quad \frac{v_o}{i_{c2}} = \frac{R_L}{1 + s R_L C_o} = \frac{R_L}{1 + s \tau_L} \quad (3.5.4)$$

where  $\tau_L = R_L C_o$  and  $C_o = C_{\mu 2} + C_L$ .

We shall temporarily neglect the base spread resistance  $r_{b1}$  and calculate the input impedance  $Z_i$  at the base-emitter junction of  $Q_1$  by [Eq. 3.2.15](#):

$$Z_i = [\beta(s) + 1] Z_{e1} = \left( \frac{1}{s \tau_{T1}} + 1 \right) Z_{e1} = \frac{1 + s \tau_{T1}}{s \tau_{T1}} Z_{e1} \quad (3.5.5)$$

The emitter peaking technique basically involves the introduction of a zero at  $s_z = -\omega_R = -1/\tau_R$  in the emitter network of  $Q_1$  to cancel the pole of the  $Q_2$  collector load at  $s_p = -\omega_L = -1/\tau_L$ . For an efficient peaking  $\tau_R$  must be lower than  $\tau_L$ , but still above the time constant  $\tau_{T1}$  of  $Q_1$ :

$$\tau_{T1} < \tau_R < \tau_L \quad (3.5.6)$$

The complete emitter circuit should look as in [Fig. 3.5.1a](#), in which  $\tau_R = RC$  and its HF impedance is:

$$Z_{e1} = \frac{R_{e1} (1 + s \tau_R)}{(1 + s \tau_{T1}) (1 + s \tau_L)} = \frac{R_{e1} (1 + s \tau_R)}{s^2 \tau_{T1} \tau_L + s (\tau_{T1} + \tau_L) + 1} \quad (3.5.7)$$

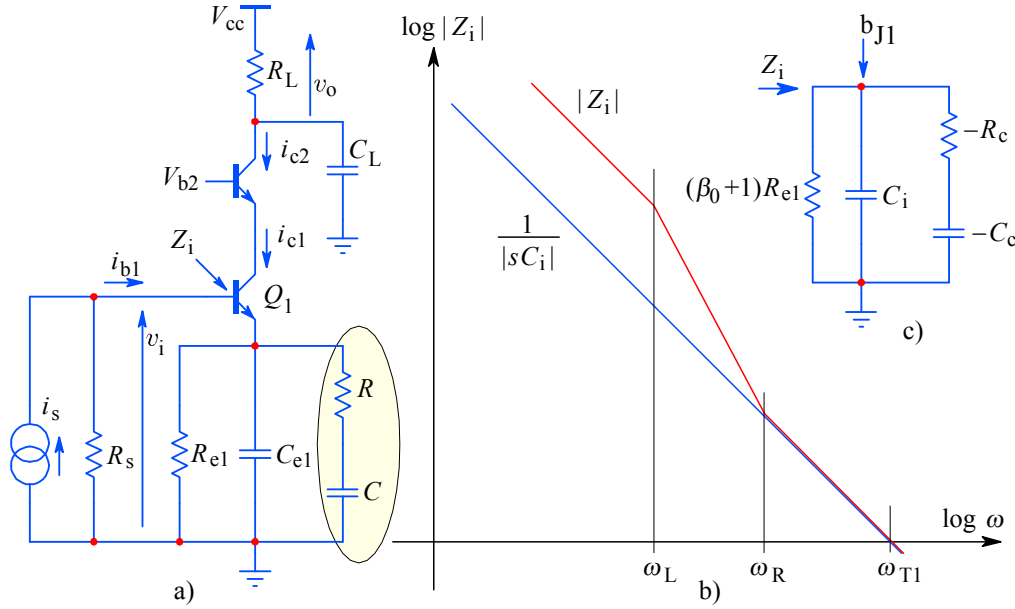


**Fig. 3.5.1:** Emitter peaking in cascode amplifiers. a) By adding a zero at  $\omega_R = 1/RC$  to the emitter network of  $Q_1$ , we modify the input impedance  $Z_i$  at the base junction of  $Q_1$ ; b) the frequency dependent asymptote plot of  $Z_i$ ; c) the equivalent schematic has negative components, too. See the explanation in [Sec. 3.5.2](#).

By introducing [Eq. 3.5.7](#) back into [Eq. 3.5.5](#) the input impedance can be expressed as:

$$Z_i = \frac{1 + s \tau_{T1}}{s \tau_{T1}} \cdot \frac{R_{e1} (1 + s \tau_R)}{(1 + s \tau_{T1}) (1 + s \tau_L)} = \frac{R_{e1} (1 + s \tau_R)}{s \tau_{T1} (1 + s \tau_L)} \quad (3.5.8)$$

Now we put [Eq. 3.5.2](#) and [Eq. 3.5.8](#) into [Eq. 3.5.1](#):

$$\begin{aligned} \frac{v_o}{i_s} &= \frac{R_s R_L}{\left[ R_s + \frac{R_{e1} (1 + s \tau_R)}{s \tau_{T1} (1 + s \tau_L)} \right] s \tau_{T1} (1 + s \tau_L)} \\ &= \frac{R_s R_L}{s^2 R_s \tau_{T1} \tau_L + s (R_s \tau_{T1} + R_{e1} \tau_R) + R_{e1}} \end{aligned} \quad (3.5.9)$$

Next we put the denominator into the canonical form and equate it to zero:

$$s^2 + s \frac{R_s \tau_{T1} + R_{e1} \tau_R}{R_s \tau_{T1} \tau_L} + \frac{R_{e1}}{R_s \tau_{T1} \tau_L} = s^2 + a s + b = 0 \quad (3.5.10)$$

where we set the coefficients:

$$a = \frac{R_s \tau_{T1} + R_{e1} \tau_R}{R_s \tau_{T1} \tau_L} \quad \text{and} \quad b = \frac{R_{e1}}{R_s \tau_{T1} \tau_L} \quad (3.5.11)$$

The general solution of [Eq. 3.5.10](#) is:

$$s_{1,2} = -\frac{a}{2} \pm \sqrt{\frac{a^2}{4} - b} \quad (3.5.12)$$

An efficient peaking must have complex poles, so the expression under the square root must be negative, therefore:  $b > a^2/4$ . We can then extract the negative sign as the imaginary unit and write [Eq. 3.5.12](#) in the form:

$$s_{1,2} = -\frac{a}{2} \pm j\sqrt{b - \frac{a^2}{4}} \quad (3.5.13)$$

From [Eq. 3.5.13](#) we can calculate the tangent section of the pole angle  $\theta$ :

$$\tan \theta = \frac{\Im\{s_1\}}{\Re\{s_1\}} = \frac{\sqrt{b - \frac{a^2}{4}}}{\frac{a}{2}} = \sqrt{\frac{4b}{a^2} - 1} \quad (3.5.14)$$

It follows that:

$$1 + \tan^2 \theta = \frac{4b}{a^2} \quad (3.5.15)$$

Now we insert the expressions from [Eq. 3.5.11](#) for  $a$  and  $b$  and obtain:

$$1 + \tan^2 \theta = \frac{4 \frac{R_{e1}}{R_s \tau_{T1} \tau_L}}{\left( \frac{R_s \tau_{T1} + R_{e1} \tau_R}{R_s \tau_{T1} \tau_L} \right)^2} = \frac{4 R_{e1} R_s \tau_{T1} \tau_L}{(R_s \tau_{T1} + R_{e1} \tau_R)^2} \quad (3.5.16)$$

By taking the square root the result is:

$$\sqrt{1 + \tan^2 \theta} = \frac{2 \sqrt{R_{e1} R_s \tau_{T1} \tau_L}}{R_s \tau_{T1} + R_{e1} \tau_R} \quad (3.5.17)$$

Finally we solve this for  $\tau_R$  and obtain:

$$\tau_R = RC = 2 \sqrt{\frac{R_s \tau_{T1} \tau_L}{R_{e1} (1 + \tan^2 \theta)}} - \frac{R_s \tau_{T1}}{R_{e1}} \quad (3.5.18)$$

The admittance  $Y_{e1}$  of the emitter circuit in [Fig. 3.5.1](#) is:

$$\begin{aligned} Y_{e1} &= \frac{1}{R_{e1}} + sC_{e1} + \frac{1}{R + \frac{1}{sC}} \\ &= \frac{s^2 CR C_{e1} R_{e1} + s(CR + CR_{e1} + C_{e1} R_{e1}) + 1}{R_{e1}(1 + sCR)} \end{aligned} \quad (3.5.19)$$

The emitter impedance  $Z_{e1}$  is the inverse value of  $Y_{e1}$  and it must be equal to [Eq. 3.5.7](#):

$$\begin{aligned} Z_{e1} &= \frac{R_{e1}(1 + sCR)}{s^2 CR C_{e1} R_{e1} + s(CR + CR_{e1} + C_{e1} R_{e1}) + 1} \\ &= \frac{R_{e1}(1 + s\tau_R)}{s^2 \tau_{T1} \tau_L + s(\tau_{T1} + \tau_L) + 1} \end{aligned} \quad (3.5.20)$$

The coefficients of  $s^2$  and  $s$  respectively must be equal in both fractions, therefore:

$$CR C_{e1} R_{e1} = \tau_{T1} \tau_L \quad (3.5.21)$$

and:

$$CR + R_{e1}(C + C_{e1}) = \tau_{T1} + \tau_L \quad (3.5.22)$$

The value of  $R_{e1}$  is constrained by the DC current amplification  $R_L/R_{e1}$ . Thus we need the expressions for  $C$ ,  $C_{e1}$ , and  $R$ . By using [Eq. 3.5.18](#), [3.5.21](#), and [3.5.22](#) we obtain:

$$C_{e1} = \frac{\tau_{T1} \tau_L}{R_{e1} \tau_R} \quad (3.5.23)$$

and:

$$C = \frac{\tau_{T1} + \tau_L - \tau_R - \tau_{T1} \frac{\tau_L}{\tau_R}}{R_e} \quad (3.5.24)$$

where  $\tau_R$  should be calculated by [Eq. 3.5.18](#). Once the value of  $C$  is known we can easily calculate the value of the resistor  $R = \tau_R/C$ . Of course,  $\tau_R$  is determined by the angle  $\theta$  of the poles selected for the specified type of response.

[Fig. 3.5.2a](#) and [3.5.2b](#) show the normalized pole loci in the complex plane. As seen already in examples in [Part 1](#) and [Part 2](#), to achieve the maximally flat envelope delay response (MFED), a single stage 2<sup>nd</sup>-order function must have the pole angle  $\theta = \pm 150^\circ$ . The original circuit has two real poles  $s_{T1}$  and  $s_L$ , but when the emitter peaking zero  $s_R$  is brought close to  $s_L$  the poles form a complex conjugate pair.

The frequency response is altered as shown in [Fig. 3.5.2c](#) and the bandwidth is extended. The emitter current increase  $i_{e1}(\omega)/I_{e1}$  owing to the introduced  $RC$  network has two break points: the lower is owed to  $R_{e1}(C + C_{e1})$  and the upper is owed to  $RC$ . If the break point at  $\omega_R$  is brought exactly over  $\omega_L$  they cancel each other, and the final response is shaped by the break point  $\omega_{T1}$  of the transistor and the second break point in the emitter peaking network,  $\omega_C$ . The peaking can thus be adjusted by  $R$  and  $C$ .

Let us consider an example with these data:  $f_{T1} = 2000$  MHz,  $R_s = 60 \Omega$ ,  $R_e = 20 \Omega$ ,  $C_o = 9$  pF,  $R_L = 390 \Omega$ . We want to make the amplifier with such an emitter peaking network which will suit the Bessel pole loci (MFED), where the pole angle  $\theta = \pm 150^\circ$ . First we calculate both time constants:

$$\tau_{T1} = \frac{1}{2\pi f_{T1}} = \frac{1}{2\pi \cdot 2000 \cdot 10^6} = 79.58 \text{ ps} \quad (3.5.25)$$

and:

$$\tau_L = R_L C_o = 390 \cdot 9 \cdot 10^{-12} = 3.51 \text{ ns} \quad (3.5.26)$$

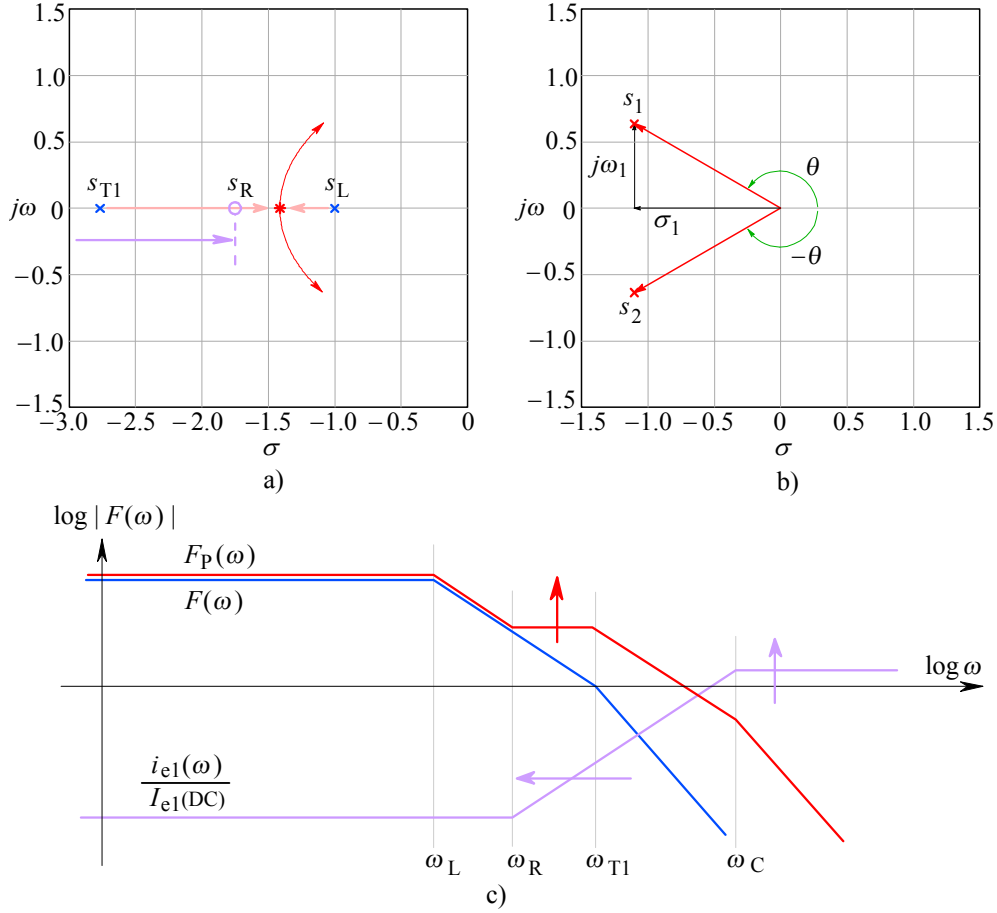


**Fig. 3.5.2:** Emitter peaking: a) two real poles travel towards each other when the emitter network zero goes from  $-\infty$  towards  $s_L$ , forming eventually a complex conjugate pair; b) poles for Eq. 3.5.14 for the 2<sup>nd</sup>-order Bessel (MFED) response. c) frequency response asymptotes — the bandwidth is extended to  $\omega_{T1}$  if  $\omega_R = \omega_L$ .

By using Eq. 3.5.18 we then calculate the third time constant:

$$\begin{aligned} \tau_R &= 2 \sqrt{\frac{R_s \tau_{T1} \tau_L}{R_{e1}(1 + \tan^2 \theta)}} - \frac{R_s \tau_{T1}}{R_{e1}} = \\ &= 2 \sqrt{\frac{60 \cdot 79.58 \cdot 10^{-12} \cdot 3.51 \cdot 10^{-9}}{20 \cdot (1 + \tan^2 30^\circ)}} - \frac{60 \cdot 79.58 \cdot 10^{-12}}{20} = 1.35 \text{ ns} \end{aligned} \quad (3.5.27)$$

Now we can calculate  $C_{e1}$  using Eq. 3.5.23:

$$C_{e1} = \frac{\tau_{T1} \tau_L}{R_{e1} \tau_R} = \frac{79.58 \cdot 10^{-12} \cdot 3.51 \cdot 10^{-9}}{20 \cdot 1.35 \cdot 10^{-9}} = 10.35 \text{ pF} \quad (3.5.28)$$

According to Eq. 3.5.24 the value of the capacitor  $C$  is:

$$C = \frac{\tau_{T1} + \tau_L - \tau_R - \tau_{T1} \frac{\tau_L}{\tau_R}}{R_e} =$$

$$\begin{aligned}
&= \frac{79.58 \cdot 10^{-12} + 3.51 \cdot 10^{-9} - 1.35 \cdot 10^{-9} - 79.58 \cdot 10^{-12} \cdot \frac{3.51 \cdot 10^{-9}}{1.35 \cdot 10^{-9}}}{20} \\
&= 101.6 \text{ pF}
\end{aligned} \tag{3.5.29}$$

Finally we calculate the value of the resistor  $R$ , from the time constant  $\tau_R$ :

$$R = \frac{\tau_R}{C} = \frac{1.35 \cdot 10^{-9}}{101.6 \cdot 10^{-12}} = 13.29 \, \Omega \tag{3.5.30}$$

### 3.5.2 Input Impedance Compensation

The introduction of the peaking elements  $R$  and  $C$  affects the HF input impedance in an unfavorable way. We have calculated the input impedance at the base emitter junction in [Eq. 3.5.8](#), which we rewrite as:

$$Z_i = \frac{R_{e1} (1 + s \tau_R)}{s \tau_{T1} (1 + s \tau_L)} = \frac{s \tau_R R_{e1} + R_{e1}}{s^2 \tau_{T1} \tau_L + s \tau_{T1}} \tag{3.5.31}$$

Here we have an additional pole at  $s_L = -\omega_L = -1/\tau_L$  and a zero at  $s_R = -\omega_R = -1/\tau_R$ , both spoiling the purely capacitive character of the input impedance, which we would like to have (frankly, we would prefer the input capacitance to be zero as well, but this is not feasible). We have seen the Bode plot of the input impedance and its configuration already in [Fig. 3.5.1b](#) and [3.5.1c](#). At very high frequencies, where  $s$  becomes dominant, the input impedance obtains a simple capacitive character:

$$Z_i = \frac{R_{e1} \tau_R}{s \tau_{T1} \tau_L} \Rightarrow C_i = \frac{\tau_{T1} \tau_L}{R_{e1} \tau_R} \tag{3.5.32}$$

Our objective is to keep such an input impedance (at the base-emitter junction of  $Q_1$ ) at lower frequencies also. In other words, at lower frequencies the plot of the input impedance should correspond to the  $|1/sC_i|$  line in [Fig. 3.5.1b](#). All other impedances that appear in the input circuit should be canceled by an appropriate compensating network. To find these impedances, we perform a ‘continued fraction expansion’ synthesis of the input admittance  $Y_i$  as derived from the right side of [Eq. 3.5.8](#). Thus:

$$Y_i = \frac{1}{Z_i} = \frac{s^2 \tau_{T1} \tau_L + s \tau_{T1}}{s \tau_R R_{e1} + R_{e1}} = s \frac{\tau_{T1} \tau_L}{R_{e1} \tau_R} + \frac{s \tau_{T1} - s \frac{\tau_{T1} \tau_L}{\tau_R}}{s \tau_R R_{e1} + R_{e1}} \tag{3.5.33}$$

The first fraction we recognize to be the input admittance  $s C_i$ . The second fraction can be inverted and, by canceling out  $s$ , we obtain the impedance:

$$\begin{aligned}
Z'_i &= \frac{s \tau_R R_{e1} + R_{e1}}{s \tau_{T1} \left(1 - \frac{\tau_L}{\tau_R}\right)} = \frac{R_{e1} \tau_R^2}{\tau_{T1} (\tau_R - \tau_L)} + \frac{R_{e1} \tau_R}{s \tau_{T1} (\tau_R - \tau_L)} \\
&= -R_c - \frac{1}{s C_c}
\end{aligned} \tag{3.5.34}$$

This means a resistor  $-R_c$  and a capacitor  $-C_c$  connected in series, and this combination is in parallel with the input capacitance  $C_i$ . The values are negative because  $\tau_R < \tau_L$  as was required in [Eq. 3.5.6](#). On the basis of these results we can draw the equivalent input impedance circuit corresponding to [Fig. 3.5.1c](#). The expression for the capacitance  $C_c$  is:

$$C_c = \frac{\tau_{T1}(\tau_L - \tau_R)}{R_{e1} \tau_R} \quad (3.5.35)$$

From [Eq. 3.5.33](#), as well as from our previous analysis, we can derive that  $R_c C_c = \tau_R$  and obtain a simpler expression for  $R_c$ :

$$R_c = \frac{\tau_R}{C_c} \quad (3.5.36)$$

Let us now continue our example of the emitter peaking cascode amplifier with the data  $R_{e1} = 20 \Omega$ ,  $\tau_{T1} = 79.58 \text{ ps}$ ,  $\tau_R = 1.51 \text{ ns}$ , and  $\tau_L = 3.51 \text{ ns}$ , and calculate the values of  $C_i$ ,  $C_c$ , and  $R_c$ . The input capacitance  $C_i$ , without  $C_M$ , is:

$$C_i = \frac{\tau_{T1} \tau_L}{R_{e1} \tau_R} = \frac{79.58 \cdot 10^{-12} \cdot 3.51 \cdot 10^{-9}}{20 \cdot 1.35 \cdot 10^{-9}} = 10.35 \text{ pF} \quad (3.5.37)$$

The value of the capacitance  $C_c$  is:

$$C_c = \frac{\tau_{T1}(\tau_L - \tau_R)}{R_{e1} \tau_R} = \frac{79.58 \cdot 10^{-12} \cdot (3.51 - 1.35) \cdot 10^{-9}}{20 \cdot 1.35 \cdot 10^{-9}} = 6.37 \text{ pF} \quad (3.5.38)$$

and the resistor  $R_c$  has a resistance of:

$$R_c = \frac{\tau_R}{C_c} = \frac{1.35 \cdot 10^{-9}}{3.51 \cdot 10^{-12}} = 385 \Omega \quad (3.5.39)$$

The next step is to compensate the series connected  $-C_c$  and  $-R_c$ . This can be done by connecting in parallel an equal combination with positive elements. The admittance of such a combination is zero and thus the impedance becomes infinity. The mathematical proof for this operation is:

$$Y'_i = \frac{1}{-R_c - \frac{1}{s C_c}} + \frac{1}{R_c + \frac{1}{s C_c}} = 0$$

and:

$$Z'_i = \frac{1}{Y'_i} \Rightarrow \infty \quad (3.5.40)$$

By doing so, only the input capacitances  $C_i + C_M$  and the input resistance  $(1 + \beta)R_{e1}$  remain effective at the (junction) input.

The impedance  $Z_i$  as given by [Eq. 3.5.8](#) is effective between the base-emitter junction and the ground. Unfortunately, no direct access is possible to the junction, because from there to the base terminal we have the base spread resistance  $r_{b1}$ . This means that  $r_{b1}$  must be subtracted from  $R_c$  to get the proper value of the compensating resistor. Supposing that  $r_{b1} = 25 \Omega$ , the proper compensating resistor is simply:

$$R'_c = R_c - r_{b1} = 385 - 25 = 360 \Omega \quad (3.5.41)$$

The complete input circuit is shown in [Fig. 3.5.3](#); the input impedance components which are reflected from the emitter to base, are shown in the shaded area.

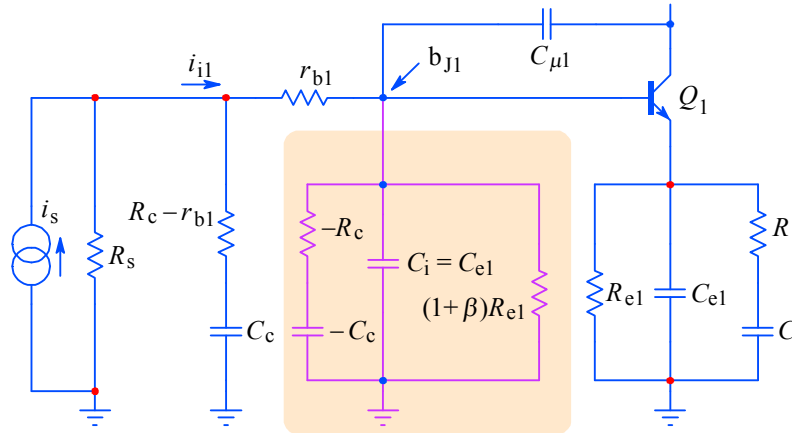


**Fig. 3.5.3:** The impedances in the emitter are reflected into the base junction of  $Q_1$ . The emitter peaking components  $R$  and  $C$  are reflected into **negative** elements  $-R_c$  and  $-C_c$ , which must be compensated by adding externally an equal and positive  $R_c$  and  $C_c$ ; for proper compensation  $r_{b1}$  must be subtracted from  $R_c$ .

The compensation of the input impedance is mandatory if we intend to apply an inductive peaking network at the input of that amplifying stage. The equivalent input capacitance, which will be seen as the load by the peaking circuit, is the capacitance from the transistor base-emitter junction to ground,  $C_i + C_M$ .

However, as mentioned before, these capacitances are seen with the base resistance  $r_{b1}$  in series. Also there is a parasitic base lead inductance, in addition to the length of PCB trace and pads having their own stray inductance and capacitance.

Therefore the inductive peaking circuit at the input of a transistor amplifying stage does not see a pure capacitance as its load. Special ‘tricks of trade’ must be applied, e.g., a modified T-coil peaking at the amplifier input, which we shall discuss in the next section.



### 3.6 Transistor Interstage T-coil Peaking

In [Part 2](#) we have shown that the greatest bandwidth extension is achieved by using T-coil peaking. The analysis was based on the assumption that the T-coil tap was loaded by a pure capacitance. Unfortunately, for a transistor amplifier this is not the case. In case of a cascode amplifier the emitter network, formed by the parallel connection of  $R_e C_e = \tau_T$ , is reflected into the base circuit as a parallel connection of  $(1 + \beta)R_e$  and  $C_e$ , paralleled also by the Miller capacitance  $C_M$ ; to this the series base spread resistance  $r_b$  must be added.

In [Fig. 3.6.1a](#) we draw such a stage [[Ref. 3.5](#)]. Since in the following analysis we do not need the transistor  $Q_2$ , we shall consider its emitter input as an ideal ground for the  $Q_1$  collector current signal (of course, the value of the Miller capacitance  $C_M$  has to be calculated by considering the actual  $Q_2$  emitter impedance). Thus we can drop the index '1', as all the parameters will belong to  $Q_1$  only. To further simplify the analysis, we shall neglect the damping and thermal compensation impedances  $Z_d$  and  $Z_\theta$ , as well as the emitter peaking. The resistor  $R_L$  is the T-coil loading resistor, which is also the load of the driving stage and we shall assume that its other end is also connected to an ideal AC ground. [Fig. 3.6.1b](#) shows the T-coil loaded by the equivalent small signal, high frequency input impedance of the transistor  $Q_1$ .

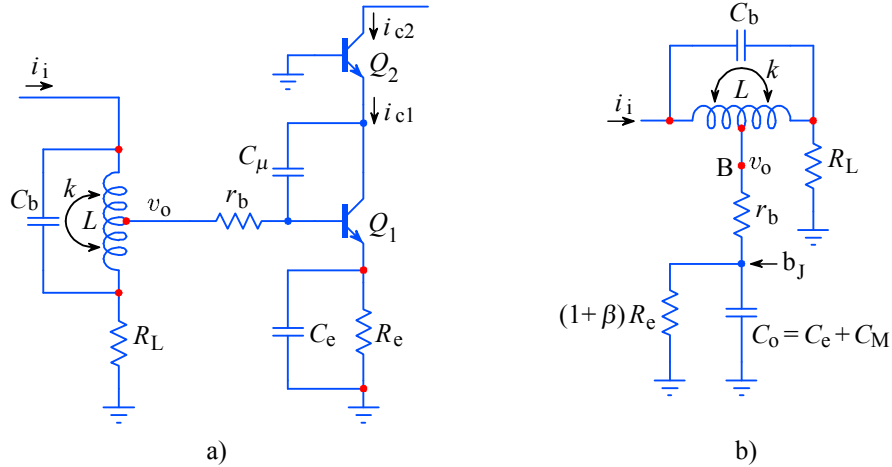


**Fig. 3.6.1:** a) The cascode amplifier with a T-coil interstage network. b) The T-coil loaded by the equivalent small signal, high frequency input impedance.

To prevent any confusion we must stress that  $C_b$  is the T-coil bridging capacitance, and not the base capacitance which is represented by  $C_o = C_e + C_M$ . As we know from the symmetrical T-coil analysis in [Part 2, Sec. 2.4](#):

$$L = L_a + L_b = R_L^2 C_o \quad (3.6.1)$$

Since the input shunt resistance  $(1 + \beta)R_e$  is usually much higher than  $r_b$ , we shall neglect it also, thus arriving at the circuit in [Fig. 3.6.2a](#). [Fig. 3.6.2b](#) shows the equivalent T-coil circuit in which we have replaced the magnetic field coupling factor  $k$  with the negative mutual inductance  $-L_M$  and the coil branches by their equivalent inductances  $L_a$  and  $L_b$ . Finally, in [Fig. 3.6.2c](#) we have replaced the branch impedances by symbols **A** to **E** to determine the three current loops  $I_1$ ,  $I_2$ ,  $I_3$ .

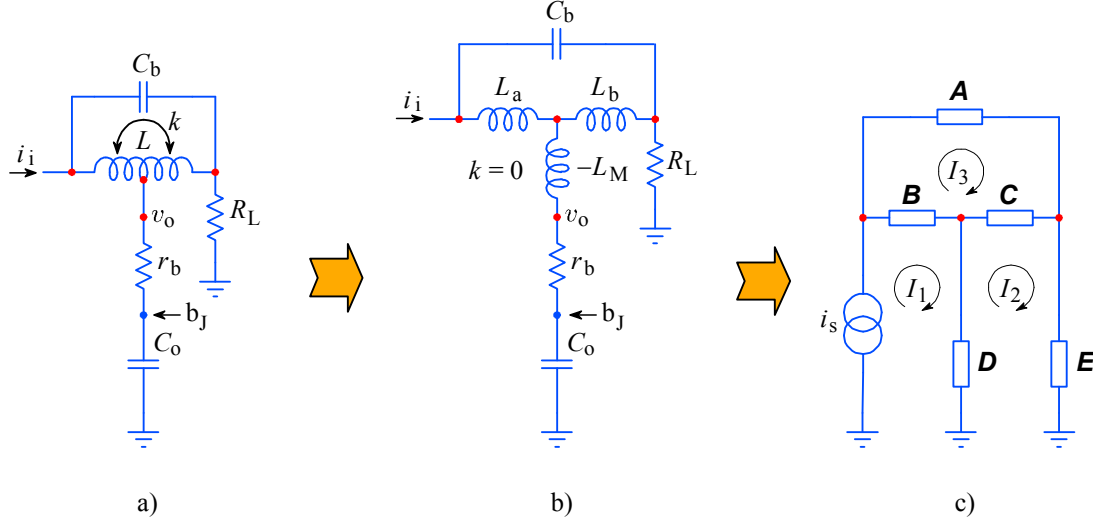


**Fig. 3.6.2:** a) The T-coil loaded by the simplified input impedance; b) the equivalent T-coil circuit in which  $k$  is substituted by  $-L_M$ ; c) the equivalent branch impedances and the three current loops.

By comparing [Fig. 2.4.1b,c, Sec. 2.4](#) with [Fig. 3.6.2b,c](#) we see that they are almost equal, except that in the branch **D**, we have the additional series resistance  $r_b$ . Let us list all these impedances again, but now including  $r_b$ :

$$\begin{aligned}
 \mathbf{A} &= \frac{1}{s C_b} \\
 \mathbf{B} &= s L_a \\
 \mathbf{C} &= s L_b \\
 \mathbf{D} &= -s L_M + r_b + \frac{1}{s C_o} \\
 \mathbf{E} &= R_L
 \end{aligned} \tag{3.6.2}$$

The general analysis of the branches, [Eq. 2.4.6–2.4.13](#), showed that the input impedance of the T-coil network is equal to its loading impedance  $Z_i = \mathbf{E} = R_L$ . As we shall soon see,  $r_b$  between the T-coil tap and  $C_o$  spoils this nice property; we shall have to compensate it. The analysis here is similar to that in [Sec. 2.4](#), so we do not have to repeat it. Here we give the final result, [Eq. 2.4.14](#), for convenience:

$$\mathbf{BCA} + \mathbf{BDA} + \mathbf{BEA} + \mathbf{DCA} - \mathbf{ECA} - \mathbf{E}^2 \mathbf{A} - \mathbf{E}^2 \mathbf{B} - \mathbf{E}^2 \mathbf{C} = 0 \tag{3.6.3}$$

By entering all substitutions from [Eq. 3.6.2](#), performing all the required multiplications and arranging the terms in the decreasing powers of  $s$ , we obtain:

$$s \left[ \left( \frac{L_a L_b}{C_b} - \frac{L L_M}{C_b} \right) - R_L^2 L \right] + \frac{L r_b}{C_b} + \frac{R_L}{C_b} (L_a - L_b) + \frac{1}{s} \left( \frac{L}{C_o C_b} - \frac{R_L^2}{C_b} \right) = 0 \tag{3.6.4}$$

or, more simply:

$$s K_1 + K_2 + s^{-1} K_3 = 0 \tag{3.6.5}$$

The difference between [Eq. 3.6.4, 3.6.5](#) and [Eq. 2.4.15, 2.4.16](#) is in the middle term. Again, if we want to have an input impedance independent of the frequency  $s$ , then each of the coefficients  $K_1$ ,  $K_2$ , and  $K_3$  must be zero [[Ref. 3.5](#)]:

$$\begin{aligned} K_1 &= \frac{-L L_M}{C_b} + \frac{L_a L_b}{C_b} - R_L^2 L = 0 \\ K_2 &= \frac{L r_b}{C_b} + \frac{R_L}{C_b} (L_a - L_b) = 0 \\ K_3 &= \frac{L}{C_o C_b} - \frac{R_L^2}{C_b} = 0 \end{aligned} \quad (3.6.6)$$

So we have the three equations from which we can calculate the parameters  $L_a$ ,  $L_b$ , and  $L_M$ . By considering [Eq. 3.6.1](#) we obtain:

$$L_a = \frac{L}{2} \left( 1 - \frac{r_b}{R_L} \right) = \frac{R_L^2 C_o}{2} \left( 1 - \frac{r_b}{R_L} \right) \quad (3.6.7)$$

$$L_b = \frac{L}{2} \left( 1 + \frac{r_b}{R_L} \right) = \frac{R_L^2 C_o}{2} \left( 1 + \frac{r_b}{R_L} \right) \quad (3.6.8)$$

$$L_M = \frac{L}{4} \left( 1 - \frac{r_b^2}{R_L^2} \right) - R_L^2 C_b = \frac{R_L^2 C_o}{4} \left( 1 - \frac{r_b^2}{R_L^2} \right) - R_L^2 C_b \quad (3.6.9)$$

Two interesting facts become evident from [Eq. 3.6.7](#) and [3.6.8](#). First,  $L_a < L_b$ , and this means that **the coil tap is not at the coil's center** any longer, but it is moved towards the coil's signal input node. Secondly,  $R_L$  must always be larger than  $r_b$ , otherwise  $L_a$  becomes negative. But we reach the limit of realizability long before that, since we know from [Part 2](#) that  $L_1 = L_a - L_M$  (and also  $L_2 = L_b - L_M$ ).

In [Eq. 3.6.9](#) we have two unknowns,  $L_M$  and  $C_b$ ; therefore we need a fourth equation to calculate them. Similarly as we did in [Part 2, Sec. 2.4](#), we shall use the transimpedance equation for this purpose. The procedure is well described from [Eq. 2.4.20](#) to [2.4.24](#) and we write the last one again:

$$\frac{V_o}{I_1} = \frac{1}{s C_o} \cdot \frac{\mathbf{CA} + \mathbf{EA} + \mathbf{EB} + \mathbf{EC}}{\mathbf{CA} + \mathbf{CB} + \mathbf{DA} + \mathbf{DB} + \mathbf{DC} + \mathbf{EA} + \mathbf{EB} + \mathbf{EC}} \quad (3.6.10)$$

If we insert the substitutions from [Eq. 3.6.2](#), we obtain the following result:

$$F(s) = \frac{V_o}{I_1} = \frac{R_L}{s^2 R_L^2 C_o C_b + s C_o \frac{R_L + r_b}{2} + 1} \quad (3.6.11)$$

In a similar way, for the transimpedance from the input to  $R_L$  we would obtain:

$$\frac{V_R}{I_i} = R_L \frac{s^2 R_L^2 C_o C_b - s C_o \frac{R_L - r_b}{2} + 1}{s^2 R_L^2 C_o C_b + s C_o \frac{R_L + r_b}{2} + 1} \quad (3.6.12)$$

Since we have the factor  $(R_L - r_b)$  in the numerator and a different factor  $(R_L + r_b)$  in the denominator, this means that **the two zeros are not symmetrically placed** in relation to the two poles in the  $s$ -plane. Therefore [Eq. 3.6.12](#) does not describe an all pass network and the input impedance is not simply  $R_L$  as before. This represents the basic obstacle to using T-coils in a transistor distributed amplifier, because the T-coil load can not be replaced by another T-coil network (for comparison see [[Ref. 2.18](#) and [2.19](#)] ).

[Eq. 3.6.11](#) has two poles, which we calculate from the canonical form of the denominator:

$$s^2 + s \frac{R_L + r_b}{2 R_L^2 C_b} + \frac{1}{R_L^2 C_o C_b} = 0 \quad (3.6.13)$$

and both poles are:

$$s_{1,2} = -\frac{R_L + r_b}{4 R_L^2 C_b} \pm \sqrt{\left(\frac{R_L + r_b}{4 R_L^2 C_b}\right)^2 - \frac{1}{R_L^2 C_o C_b}} \quad (3.6.14)$$

or, by extracting the common factor:

$$s_{1,2} = \frac{1 + r_b/R_L}{4 C_b R_L} \left( -1 \pm \sqrt{1 - \frac{16 C_b}{C_o (1 + r_b/R_L)^2}} \right) \quad (3.6.15)$$

An efficient inductive peaking must have complex poles. For Bessel poles, as was in [Fig. 3.5.2b](#), the pole angles  $\theta_{1,2} = \pm 150^\circ$  and with this pole arrangement we obtain the MFED response. If the poles are complex the tangent of the pole angle is the ratio of the imaginary to the real component of [Eq. 3.6.15](#):

$$\tan \theta = \frac{\Im\{s_1\}}{\Re\{s_1\}} = \sqrt{\frac{16 C_b}{C_o (1 + r_b/R_L)^2} - 1} \quad (3.6.16)$$

By solving this equation for  $C_b$  we obtain:

$$C_b = C_o \frac{1 + \tan^2 \theta}{16} \left( 1 + \frac{r_b}{R_L} \right)^2 \quad (3.6.17)$$

Compared to the symmetrical T-coil, here we have the additional factor  $(1 + r_b/R_L)^2$ . For Bessel poles  $\theta = 150^\circ = 5\pi/6$  and  $\tan^2 \theta = 1/3$ , thus for a single stage case:

$$C_b = \frac{C_o}{12} \left( 1 + \frac{r_b}{R_L} \right)^2 \quad (3.6.18)$$

If we replace  $C_b$  in [Eq. 3.6.9](#) with [Eq. 3.6.18](#), the mutual inductance is:

$$L_M = R_L^2 C_o \left[ \frac{1}{4} \left( 1 - \frac{r_b^2}{R_L^2} \right) - \frac{1}{12} \left( 1 + \frac{r_b}{R_L} \right)^2 \right] \quad (3.6.19)$$

With this we can calculate the coupling factor  $k$  between the coil  $L_1$  and  $L_2$  [[Ref. 3.23](#)]:

$$k = \frac{L_M}{\sqrt{L_1 L_2}} = \frac{L_M}{\sqrt{(L_a - L_M)(L_b - L_M)}} \quad (3.6.20)$$

Now we have all the equations needed for the T-coil transistor interstage coupling.

### 3.6.1 Frequency response

To calculate the frequency response we apply [Eq. 3.6.11](#), in which we shall replace the coil's bridging capacitance  $C_b$  by [Eq. 3.6.18](#), since we shall discuss only the MFED response. Then we put it into the canonical form by factoring out the common factor:

$$F(s) = \frac{R_L^2 C_o^2 \left(1 + \frac{r_b}{R_L}\right)^2}{12} \cdot \frac{R_L}{s^2 + s \frac{6}{R_L C_o} \left(1 + \frac{r_b}{R_L}\right) + \frac{12}{R_L^2 C_o^2} \left(1 + \frac{r_b}{R_L}\right)} \quad (3.6.21)$$

The denominator of the second fraction has two roots:

$$s_{1,2} = \frac{1}{R_L C_o (1 + r_b/R_L)} (-3 \pm j\sqrt{3}) = \sigma_1 \pm j\omega_1 \quad (3.6.22)$$

Sometimes we prefer the normalized form of the roots and in this case  $R_L C_o = 1/\omega_h = 1$ . To emphasize the normalization, we add the subscript 'n', so  $s_{1,2n} = \sigma_{1n} \pm j\omega_{1n}$ . By applying the normalized poles of [Eq. 3.6.22](#) to [Eq. 2.2.27](#), which is a generalized second-order magnitude function, we obtain:

$$|F(\omega)| = \frac{\sigma_{1n}^2 + \omega_{1n}^2}{\sqrt{\left[\sigma_{1n}^2 + \left(\frac{\omega}{\omega_h} + \omega_{1n}\right)^2\right] \left[\sigma_{1n}^2 + \left(\frac{\omega}{\omega_h} - \omega_{1n}\right)^2\right]}} \quad (3.6.23)$$

By comparing the Bessel poles for a simple T-coil ([Eq. 2.4.42](#)) with [Eq. 3.6.22](#), we notice that in the denominator we have an additional factor  $(1 + r_b/R_L)$ . Therefore it would be interesting to make several frequency responses with different ratios  $r_b/R_L$ , as listed in [Table 3.6.1](#):

**Table 3.6.1**

$r_b/R_L$	$\sigma_{1n}$	$\omega_{1n}$	Note
0.00	- 3.0	- 1.732	symmetrical T-coil
0.25	- 2.4	- 1.386	-
0.50	- 2.0	- 1.155	-

The corresponding frequency-response plots are drawn in [Fig. 3.6.3](#), together with the three non-peaking responses ( $L = 0$ ) as references. The bandwidth improvement factor for all three cases is  $\eta_b = 2.72$ . That is because the base resistance  $r_b$  decreases the bandwidth also for the non-peaking stage, where  $L = 0$ . We can prove this if we multiply the denominator of [Eq. 3.6.22](#) by  $R_L$ :

$$s_{1,2} = \frac{1}{C_o (R_L + r_b)} (-3 \pm j\sqrt{3}) = \omega_h (-3 \pm j\sqrt{3}) \quad (3.6.24)$$

where  $\omega_h = 1/C_o(R_L + r_b)$  is the non-peaking bandwidth considering  $r_b$ . So we shall obtain three different curves for three different ratios  $r_b/R_L$ , also for  $L = 0$ .

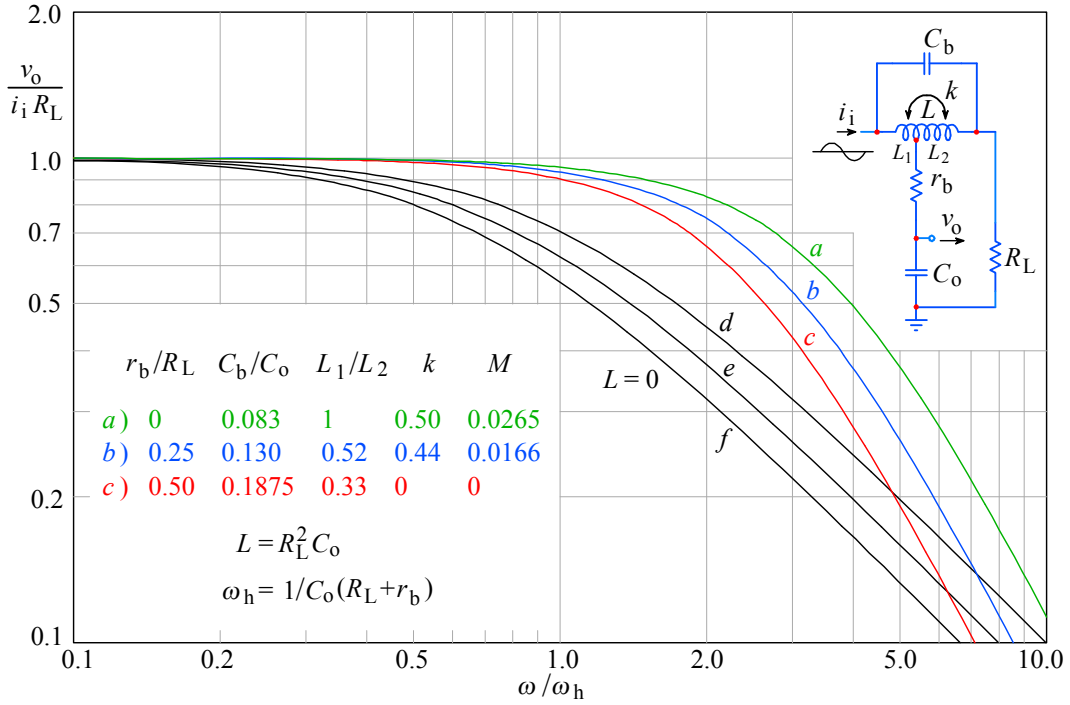


**Fig. 3.6.3:** MFED frequency response of the T-Coil transistor interstage coupling circuit for three different values of  $r_b$ : a)  $r_b = 0$ ; b)  $r_b = 0.25 R_L$ ; c)  $r_b = 0.5 R_L$ . For comparison the three reference cases ( $L = 0$ ): d), e), and f), which correspond to the same three  $r_b/R_L$  ratios, are drawn. The bandwidth improvement factor of the peaking system remains 2.72 times over the non-peaking reference for each value of  $r_b$ .

From the analysis above, we can draw an important result:

The upper half-power frequency of a non-peaking transistor amplifier must be calculated by taking into account the sum  $R_L + r_b$  (and not just  $R_L$ ).

### 3.6.2 Phase Response

To calculate the phase response we insert our poles into [Eq. 2.2.31](#):

$$\varphi = \arctan \frac{\omega/\omega_h + \omega_{1n}}{\sigma_{1n}} + \arctan \frac{\omega/\omega_h - \omega_{1n}}{\sigma_{1n}} \quad (3.6.25)$$

In [Fig. 3.6.4](#) the phase plots for the same three ratios of  $r_b/R_L$  as in the frequency response are shown, along with the three references ( $L = 0$ ).

### 3.6.3 Envelope Delay

The envelope delay is calculated using [Eq. 2.2.35](#):

$$\tau_e \omega_h = \frac{\sigma_{1n}}{\sigma_{1n}^2 + (\omega/\omega_h + \omega_{1n})^2} + \frac{\sigma_{1n}}{\sigma_{1n}^2 + (\omega/\omega_h - \omega_{1n})^2} \quad (3.6.26)$$

and the responses are drawn in [Fig. 3.6.5](#), for the three different ratios  $r_b/R_L$ , in addition to the three references ( $L = 0$ ).

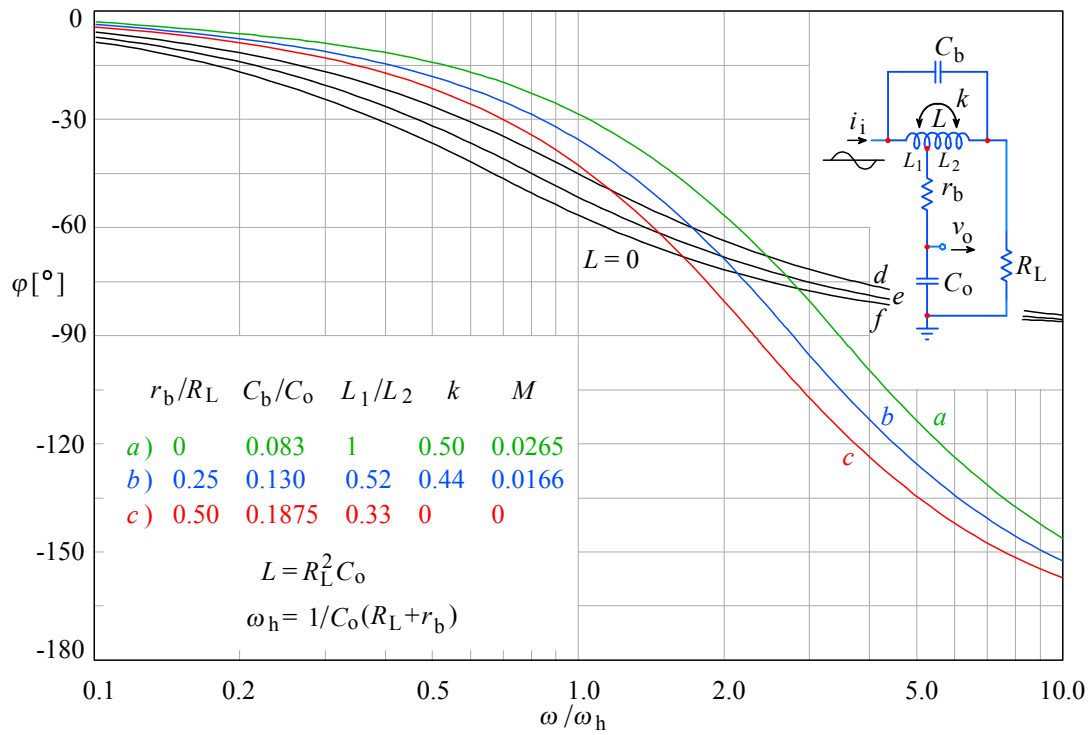


**Fig. 3.6.4:** MFED phase response of the T-Coil transistor interstage coupling circuit compared with the references ( $L = 0$ ), for the same three values of  $r_b/R_L$ .

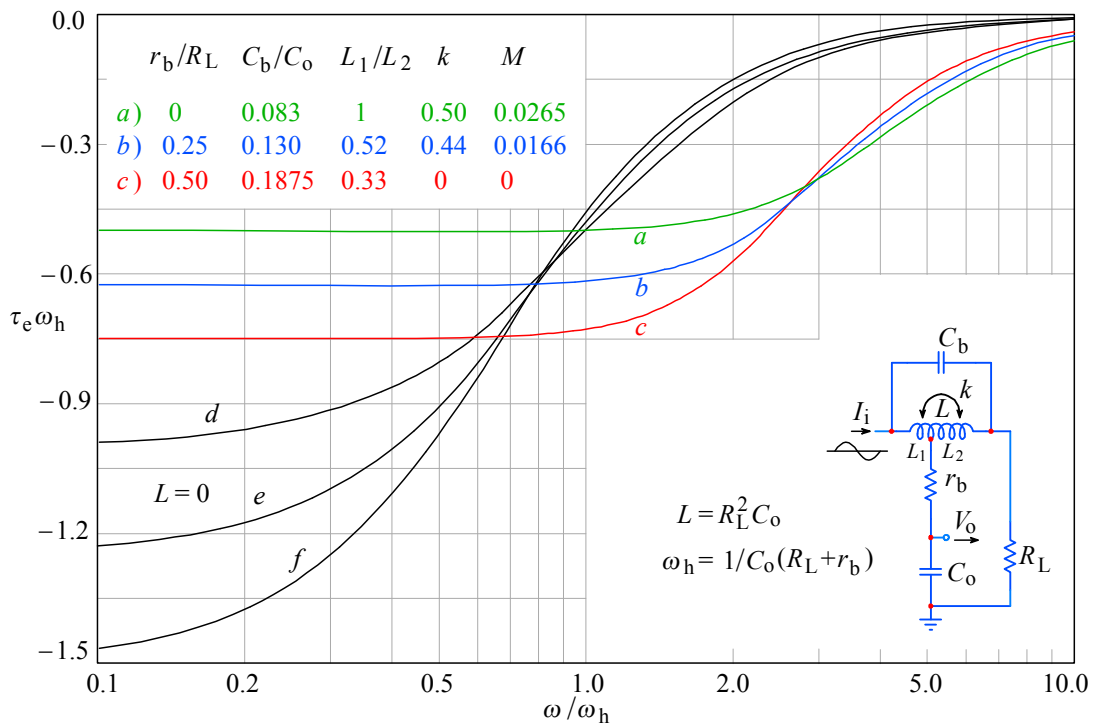


**Fig. 3.6.5:** MFED envelope delay response of the T-Coil transistor interstage coupling circuit compared with the references ( $L = 0$ ) for the same three values of  $r_b/R_L$ .

### 3.6.4 Step Response

For plotting the step response we can use [Eq. 2.4.47](#) (which was fully derived in [Part 1, Eq. 1.14.18](#)):

$$g(t) = 1 + \frac{1}{|\sin \theta|} e^{\sigma_1 t} \sin(\omega_1 t + \theta + \pi) \quad (3.6.27)$$

where  $\theta$  is the pole angle according to [Fig. 3.5.2b](#). By inserting the pole angle  $\theta = 150^\circ$  or  $5\pi/6$ , as required by the 2<sup>nd</sup>-order Bessel system, we obtain:

$$g(t) = 1 + 2 e^{-3t/T} \sin \left[ \sqrt{3} t/T + \left( 1 + \frac{5}{6} \right) \pi \right] \quad (3.6.28)$$

However, here we must use  $T = 1/\omega_h = C_o (R_L + r_b)$ , as in [Eq. 3.6.22](#) and [3.6.24](#). In [Fig. 3.6.6](#) the step-response plots are drawn for three different ratios  $r_b/R_L$  as well as the three reference cases with  $L = 0$ .

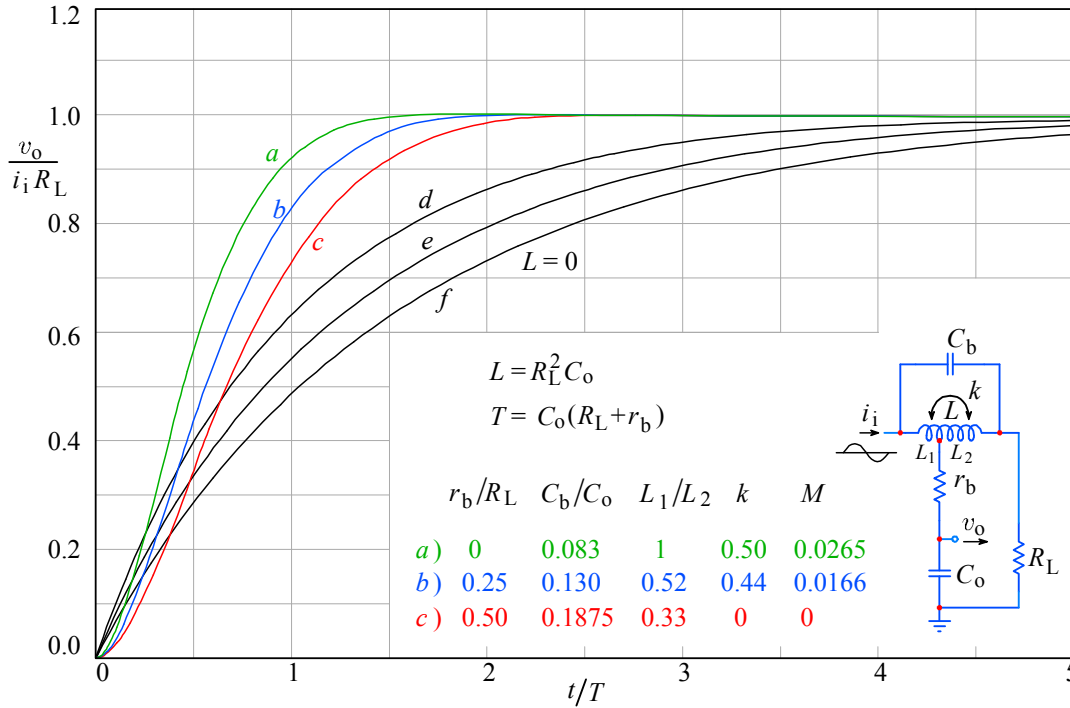


**Fig. 3.6.6:** MFED step-response of the T-coil transistor interstage coupling circuit, compared to the references ( $L = 0$ ), for the same three values of  $r_b/R_L$ .

Thus we have completed the analysis of the basic case of a transistor T-coil interstage coupling. The reader who would like to have more information should study [\[Ref. 3.5\]](#). In order to simplify the analysis, we have purposely neglected the transistor input resistance  $\beta(r_\pi + 1)$  and also stray inductance  $L_s$  of the tap to transistor base terminal. In the next steps we shall discuss both of them.



### 3.6.5 Consideration of the transistor's input resistance

[Fig. 3.6.7](#) shows the basic configuration of the transistor input circuit. We have also drawn the base-lead inductance  $L_s$  which will be discussed in the next section.

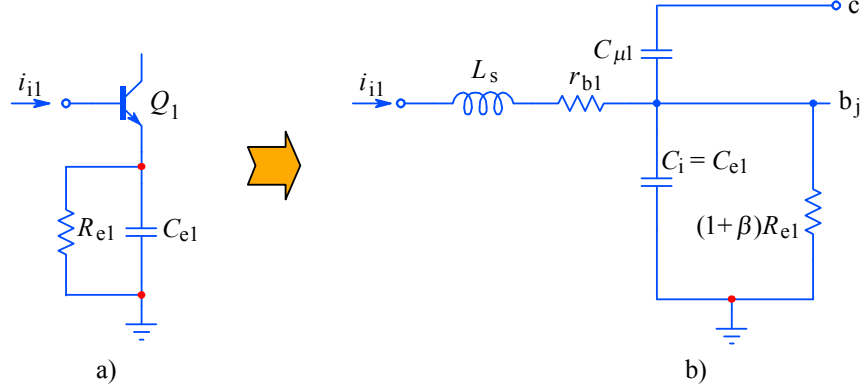


**Fig. 3.6.7:** The complete transistor input impedance: a) schematic; b) equivalent circuit, in which we include also the base lead inductance  $L_{b1}$ . The presence of the shunt resistance  $(1 + \beta) R_{e1}$  requires a modified interstage T-coil circuit.

The resistance from the base–emitter junction to ground is:

$$R_i = (1 + \beta) R_e \quad (3.6.29)$$

as we have derived in [Eq. 3.2.15](#). The effect of this resistance may be canceled if we insert an appropriate resistor  $R_s$  from the end of coil  $L_1$  to the start of coil  $L_2$ , as shown in [Fig. 3.6.8](#). It is essential that the resistor  $R_s$  is inserted on the ‘left’ side of  $L_2$  (at the T-coil tap node), because in this case the bridging capacitance of  $C_b$  (self-capacitance of the coil) and the magnetic field coupling ( $k$ ) are utilized. With the resistor placed on the ‘right’ side of  $L_2$  (at the  $R_L C_b$  node), that would not be the case.

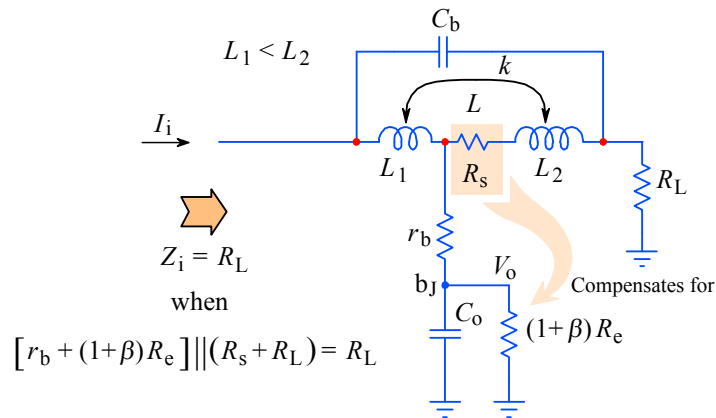


**Fig. 3.6.8:** The resistance  $R_s$  in series with  $L_2$  is inserted near the T-coil tap to compensate the error in the impedance seen by the input current at low frequencies, owed to the parallel connection of  $R_L \parallel [r_b + (1 + \beta) R_e]$ .

At very high frequencies we can replace all capacitors by short circuit and all inductors by open circuit. In this case the input resistance of the T-coil circuit is  $R_L$ . But

at very low frequencies the capacitors represent an open circuit and the inductors a short circuit. The transistor input resistance is then effectively in parallel with  $R_L$ . It is the task of the series resistor  $R_s$  to prevent this reduction of resistance. The idea is that:

$$(r_b + R_i) \parallel (R_s + R_L) = R_L \quad (3.6.30)$$

If we solve this for  $R_s$  we obtain:

$$R_s = \frac{R_L^2}{R_i + r_b - R_L} \quad (3.6.31)$$

The introduction of this resistor spoils all the expressions from our previous analysis, and, to be exact, everything we derived to determine the basic T-coil parameters should be calculated anew, considering the additional parameter  $R_s$ . Since in practice the value of this resistor is very small, no substantial changes in other circuit parameters may be expected and the additional effort, which would be required by an exact analysis, would be worthless.

A sneaky method for implementing this compensation, while at the same time decreasing the stray capacitance (and also to create difficulties to the competition to copy the circuit) is to make the coil  $L_2$  using an appropriate resistive wire.

### 3.6.6 Consideration of the base lead stray inductance

[Fig. 3.6.9a](#) shows the T-coil with the base lead stray inductance  $L_s$  at the tap. From [Fig. 3.6.9b](#) we realize that the **positive** inductance of the base lead  $L_s$  actually decreases the **negative** mutual inductance  $L_M$  of the T-coil. To retain the same conditions as in [Fig. 3.6.2c](#) at the beginning of the basic T-coil analysis, the coupling factor must be increased, thus increasing the mutual inductance to  $L_M + L_s$ .

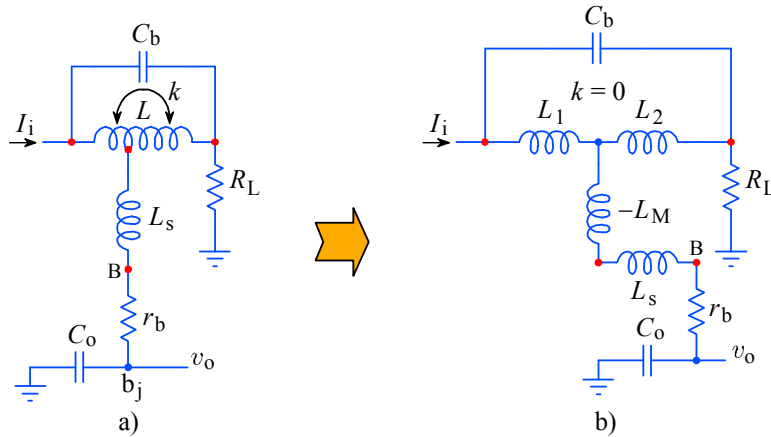


**Fig. 3.6.9:** a) The base lead inductance  $L_s$  decreases the value of mutual inductance, as indicated by the equivalent circuit in b). This can be compensated by recalculating the circuit with an increased coupling factor.

We shall mark the new T-coil circuit parameters with a prime (') to distinguish them from the original parameters of the transistor interstage T-coil:

$$L'_M = L_M + L_s \quad (3.6.32)$$

Because the inductance from  $r_b$  to either end of the coil  $L$  is now increased by  $L_s$ , both inductances  $L_a$  and  $L_b$  must be decreased by the value of  $L_s$ :

$$L'_a = L_a - L_s \quad \text{and} \quad L'_b = L_b - L_s \quad (3.6.33)$$

By considering all these changes, the new (larger) value of the coupling factor is

$$k' = \frac{L'_M}{\sqrt{(L_a - L_M - 2L_s)(L_b - L_M - 2L_s)}} \quad (3.6.34)$$

Since it is sometimes difficult to achieve the required coupling factor we must take care that the base lead stray inductance  $L_s$  is as small as possible.

### 3.6.7 Consideration of the collector to base spread capacitance

So far we have considered only the lumped collector to base capacitance  $C_\mu$ . However, in a real transistor the capacitance  $C_\mu$  is spread along the base resistance  $r_b$ , as is drawn in [Fig. 3.6.10a](#) [[Ref. 3.4](#)]. For the analysis of such a circuit we should know the actual geometry involved; unless we are designing the transistor by ourselves, this would be difficult to find out. So we shall, rather, approximate this by splitting  $C_\mu$  into three parts,  $C_{\mu1}$ ,  $C_{\mu2}$ , and  $C_{\mu3}$ , as suggested in [Fig. 3.6.10b](#), adding also a constant value  $C_s$  to account for the external leads and PCB strays.

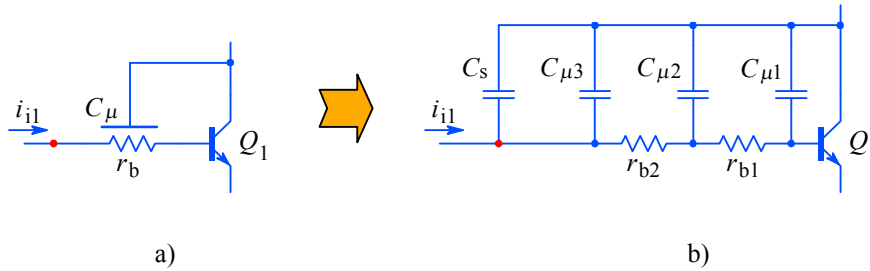


**Fig. 3.6.10:** a) The base–collector reverse capacitance  $C_\mu$  is actually spread across the base resistance  $r_b$ . b) A good approximation is achieved by splitting  $r_b$  in half and  $C_\mu$  in three parts, adding also the external stray capacitance  $C_s$ .

Those readers who are interested in the results and further suggestions, should study [[Ref. 3.20](#)].

### 3.6.8 The ‘Folded’ Cascode

While we are still speaking about cascode amplifiers, let us examine the ‘folded’ cascode circuit, [Fig. 3.6.11](#). This circuit is a handy solution in cases of a limited supply voltage, a situation commonly encountered in modern integrated circuits and battery supplied equipment.

The first thing to note is that the collector DC currents can be different, since the bias conditions for  $Q_1$  are set by the input base voltage and  $R_{e1}$ , whilst for  $Q_2$  the bias is set by  $V_{cc} - V_{b2}$  and  $R_{cc}$ .

Another interesting point is that  $R_{cc}$  (or a current source in its place) must supply the current for both transistors. Therefore when a signal is applied at the input the currents in  $Q_1$  and  $Q_2$  will be in anti-phase, i.e., when  $i_{o1}$  increases,  $i_{i2}$  decreases and vice-versa. Consequently, it is easier to achieve good thermal balance with such a circuit, than with the original cascode.

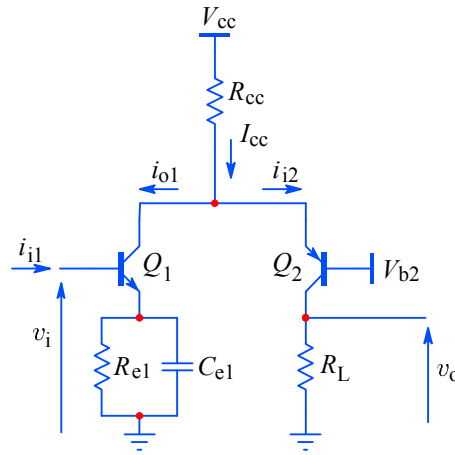


**Fig. 3.6.11:** The ‘folded’ cascode is formed by a complementary, NPN and PNP, transistor pair, connected in the otherwise usual cascode configuration. Since thermionic devices are not produced in complementary pairs, this circuit can not be realized with electronic tubes.

In an integrated circuit it is always more difficult to make fast PNP transistors, because of the lower mobility of the virtual positive charge (a vacant charge region, left behind an accelerated electron, can exist for a considerable time before another slow electron comes near enough to be trapped by it). It could then be advantageous to change the supply polarity and use a PNP type for  $Q_1$  and an NPN type for  $Q_2$ .

In all other respects, the circuit presents problems identical to those of the original cascode, so all the solutions already discussed apply here as well.

### 3.7 Differential Amplifiers

In [Sec. 3.4.2](#) we have explained that the instability of the transistor's DC bias depends on the ambient temperature and the heat generated internally, as a consequence of its power dissipation. The current amplification factor  $\beta_0$  also depends on temperature. These effects multiply in a multi-stage DC amplifier. They can be greatly reduced using a symmetrical differential amplifier.

The basic differential amplifier is shown in [Fig. 3.7.1](#). The input voltage of transistor  $Q_1$  is  $v_{i1}$  and that of  $Q_2$  is  $v_{i2} = -v_{i1}$  (we are assuming these symmetrical driving voltages in order to eliminate any common mode voltages, thus simplifying the initial analysis). The emitters of both transistors are connected together and fed via the resistor  $R_{ee}$  from the voltage  $V_{ee} < 0$ . If we assume the circuit to be entirely symmetrical, e.g.,  $Q_1 = Q_2$  and  $R_{L1} = R_{L2}$ , and if both input voltages  $v_{i1}$  and  $v_{i2}$  are zero, the DC Output voltages are also equal,  $V_{o1} = V_{o2}$ , independently of the ambient temperature.

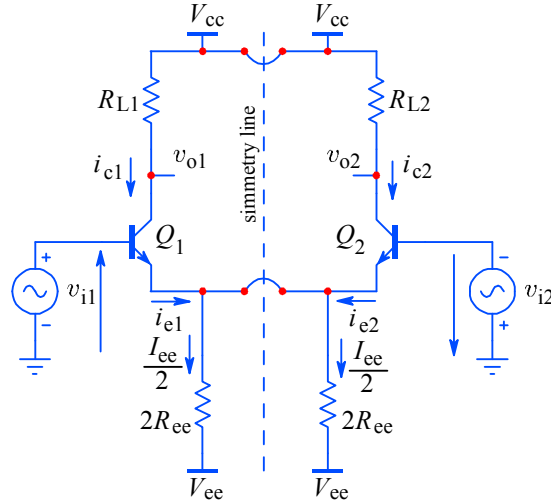


**Fig. 3.7.1:** The differential amplifier. We simplify the initial analysis by assuming  $v_{i2} = -v_{i1}$ ,  $R_{L1} = R_{L2}$  and  $Q_1 = Q_2$  (all parameters).

The name *differential amplifier* suggests that we are interested in the amplification of voltage differences. In general, if one signal input voltage, say,  $v_{i1}$ , goes positive, the other input voltage  $v_{i2}$  goes negative by the same amount (we have accounted for this by drawing the polarity of the voltage generator  $v_{i2}$  in [Fig. 3.7.1](#) opposite to  $v_{i1}$ ). This means that any increase of the emitter current in transistor  $Q_1$  is accompanied by an equal decrease in the emitter current in transistor  $Q_2$ . So the current through the resistor  $R_{ee}$  and the voltage at the emitter node are not changed. Therefore we can consider the emitter node as a virtual ground. The difference of the input voltages is:

$$v_{i1} - (-v_{i2}) = v_{i1} + v_{i2} \quad (3.7.1)$$

In a similar way as the input voltages, the signal output voltages  $v_{o1}$  and  $v_{o2}$  go up and down for an equal amount, however, we must account for the signal inversion in

the common emitter amplifier. If the voltage amplification of the input voltage difference is  $A_{vd}$  (which we can take directly from [Eq. 3.1.14](#), where we discussed a simple common-base amplifier), the output signal voltage difference is:

$$v_{o2} - (-v_{o1}) = v_{o1} + v_{o2} = -A_{vd}(v_{i1} + v_{i2}) \quad (3.7.2)$$

An attentive reader will note that we have added the subscript ‘d’ to denote the differential mode gain.

In the case of both input voltages being equal and of the same polarity, both output voltages will also be equal and of same polarity; however, the output signal’s polarity is the inverse of the input signal’s polarity (owing to the 180° phase inversion of each common emitter amplifier stage). If the symmetry of the circuit were perfect, the output voltage difference would be zero, provided that the common mode excitation at the input remains well within the linear range of the amplifier. Such operation is named *common-mode amplification*,  $A_{vc}$  (here we have added the subscript ‘c’).

For the common mode signal the excursion of both output voltages with respect to their DC value is:

$$v_{o1} = v_{o2} = -A_{vc} \frac{v_{i1} + v_{i2}}{2} \approx -\frac{R_{L1}}{2R_{ee}}(v_{i1} + v_{i2}) \quad (3.7.3)$$

A good idea to visualize the common mode operation is to ‘fold’ the circuit across the symmetry line and consider it as a ‘single ended’ amplifier with both transistors and both loading resistors in parallel.

Since we are more interested in the differential mode amplification, we have pulled the expression for the common mode amplification, so to say, ‘out of the hat’. The analysis so far is more intuitive than exact. The reason we did not bother to make a corresponding derivation of exact formulae is that the simple circuit shown in [Fig. 3.7.1](#) is almost never used as a wideband amplifier owing to its large input capacitance. A basic differential amplifier in cascode configuration, with a constant current generator instead of the resistor  $R_{ee}$ , is drawn in [Fig. 3.7.2](#). The reader who wants to study the full analysis of the basic low-frequency differential amplifier according to [Fig. 3.7.1](#) should look in [\[Ref. 3.7\]](#). We shall return briefly to the differential amplifier in [Part 5](#).

### 3.7.1 Differential cascode amplifier

The analysis of the circuit in [Fig. 3.7.2](#), a differential cascode amplifier, with the same rigor, considering all the complex impedances, would quickly run out of control owing to its complexity (remember [Table 3.2.1](#), which should be applied to each transistor). However, if we take the emitter node to be a virtual ground, each half of the differential amplifier can be analyzed separately; actually, owing to the symmetry, the analysis of only one arm is needed, which has been done already in [Sec. 3.4](#). So here we can focus on other problems which are peculiar to differential amplifiers only.

First of all, no differential amplifier is perfectly symmetrical, even if all of its transistors are on the same chip. The lack of a perfect symmetry causes the common mode input signal  $(v_{i1} + v_{i2})/2$  to appear partly as a differential output signal. For the

same reason there is still some temperature drift, although greatly reduced in comparison with the single ended amplifier. The appearance of common mode signals at the output is especially annoying in electrobiological amplifiers (electrocardiographs and electroencephalographs). In these amplifiers, very small input signal differences (of the order of several  $\mu\text{V}$ ) must be amplified in the presence of large (up to 1V) common mode signals from power lines, owing to capacitive pickup. The level of ability of the differential amplifier to reject the common mode signal is called *common mode rejection ratio*,  $\text{CMRR} = A_{\text{vc}}/A_{\text{vd}}$ , generally expressed in decibels (dB). Since this is out of scope of this book, we shall not pursue these effects in detail.

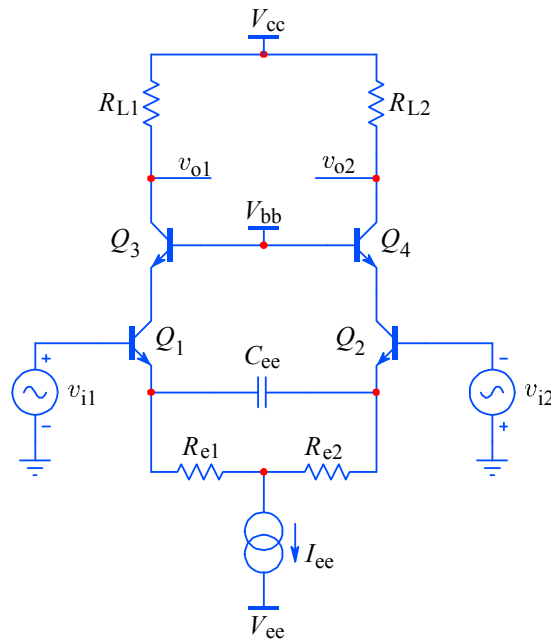


**Fig. 3.7.2:** The basic circuit of the differential cascode amplifier.

The optimum thermal stability of the differential cascode circuit could again be obtained by adjusting the quiescent currents in both halves of the differential amplifier to values such that the voltage drop on each loading resistor is equal to the voltage  $(V_{\text{cc}} - V_{\text{bb}} - V_{\text{be}})/2$ , (see [Eq. 3.4.19](#) and the corresponding explanation). However, as has been said for the simple cascode amplifier, the requirements for large bandwidth will prevent this from being realized. We would want to have low  $R_L$ , high  $V_{\text{cc}}$  and  $V_{\text{bb}}$ , and high  $I_{\text{ee}}$  to maximize the bandwidth. So the thermal stability will have to be established in a different way.

Differential amplifiers are particularly suitable for compensation of many otherwise insolvable errors. This is achieved by cross-coupling and adding anti-phase signals, so that the errors cancel. For example, the pre-shoot of the simple cascode amplifier, which is owed to capacitive feed through, can be effectively eliminated if two capacitors with the same value as  $C_{\mu 1,2}$  are connected from the  $Q_1$  emitter to the  $Q_2$  collector, and vice-versa.

Similarly, by cross-coupling diodes or transistors we can achieve nonlinearity cancellation, leakage current compensation, better gain stability, DC stability, etc. In integrated circuits, even production process variations can be compensated in this way. Some such examples are given in [Part 5](#).

### 3.7.2 Current source in the emitter circuit

To improve the common mode rejection, instead of having a large resistor  $R_{ee}$  and a correspondingly high voltage  $V_{ee}$  (resulting in an unnecessarily high power dissipation  $P \approx V_{ee}^2/R_{ee}$ ) the common practice is to use high *incremental* resistance. This is usually done by a special connection of active devices in a configuration called *current source*. Such generators can have a high incremental resistance even when working with a relatively low  $V_{ee}$ .

The ideal current generator should be independent as much as possible from the applied voltage and from ambient temperature. A simple current sink, composed of two equal transistors  $Q_5$  and  $Q_6$  is shown in Fig. 3.7.3a. (We have given them the indices ‘5’ and ‘6’ in order to avoid any confusion with the former figures). The circuit is named the *current mirror* [Ref. 3.31], because the collector current  $I_{c6}$  is in some respect a ‘mirror image’ of  $I_R$ , as shown in Fig. 3.7.3b, where the current symmetry analysis is performed by normalizing the currents to those of the base. Current mirrors are in widespread use in integrated circuits in which complex multi-stage biasing is controlled from a single point.

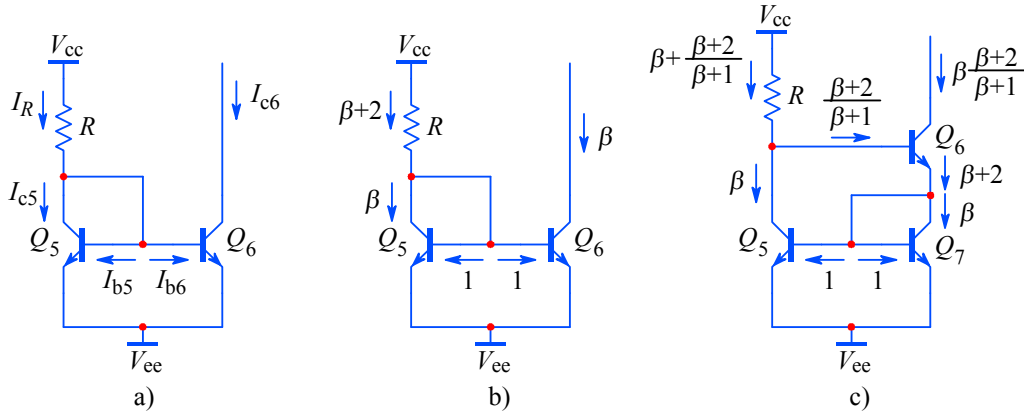


**Fig. 3.7.3:** a) The basic current mirror. b) Current symmetry analysis with the currents normalized to those of the base. c) The symmetry is improved in the Wilson mirror.

The current  $I_R$  is:

$$I_R = I_{c5} + I_{b5} + I_{b6} = I_{c5} + \frac{I_{c5}}{\beta_5} + \frac{I_{c6}}{\beta_6} \quad (3.7.4)$$

If both transistors are identical, then  $\beta_5 = \beta_6 = \beta$  and  $I_{c5} = I_{c6} = \beta I_b$ . In this case:

$$I_R = I_{c5} \left( 1 + \frac{2}{\beta} \right) \quad (3.7.5)$$

and the collector current is:

$$I_{c5} = \frac{I_R}{1 + \frac{2}{\beta}} \quad (3.7.6)$$

If  $\beta$  is very large then:

$$I_{c6} \approx I_R = \frac{V_{cc} - V_{be}}{R} \quad (3.7.7)$$



In general the collector current of a transistor is [Ref. 3.4]:

$$I_c = I_s e^{\frac{V_{be}}{V_T}} \left( 1 + \frac{V_{ce}}{V_A + V_{ce}} \right) \quad (3.7.8)$$

where:

$I_s$  = the collector saturation current (approx.  $10^{-12}$  to  $10^{-14}$  A);

$V_A$  = Early voltage (usually between 100 and 150 V, see Fig. 3.4.11);

$V_T = k_B T / q$  (as defined at the beginning of Sec. 3.1).

Eq. 3.7.8 can be written simply from the geometric relations taken from Fig. 3.4.11. For a common silicon transistor the Early voltage is at least 100 V. Suppose both silicon transistors in Fig. 3.7.3a are identical and subject to the same temperature variations (on the same chip). The collector–emitter voltage of transistor  $Q_5$  is the same as the base–emitter voltage,  $V_{ce5} = V_{be5} \approx 0.65$  V. In contrast, the collector–emitter voltage of transistor  $Q_6$  is higher, say,  $V_{ce6} = 15$  V. The ratio of both collector currents is then:

$$\frac{I_{c6}}{I_{c5}} = \frac{1 + \frac{V_{ce6}}{V_A + V_{ce6}}}{1 + \frac{V_{ce5}}{V_A + V_{ce5}}} = \frac{1 + \frac{15}{100 + 15}}{1 + \frac{0.6}{100 + 0.6}} = 1.237 \quad (3.7.9)$$

By using more sophisticated circuits it is possible to make either  $I_{c5} = I_{c6}$  or  $I_R = I_{c6}$ , or even to make any desired ratio between any of them [Ref. 3.31, 3.32, 3.33]. This is important in order to decrease the power dissipation in the resistor  $R$ . The power dissipated by  $Q_6$  will then be the product of the desired current and the collector–emitter voltage set by the desired common mode range of the differential amplifier.

Since we are interested in wideband aspects of differential amplifiers, we shall not discuss further particularities here. However, current mirrors can also be used to convert the output signal of the differential amplifier into a single ended push pull drive, as is often done in modern operational amplifiers, and we shall return to this subject later in Part 5, with a discussion of the *Wilson* mirror [Ref. 3.32], Fig. 3.7.3c.

Before closing the analysis of current sinks, let us calculate the incremental collector resistance  $r_o$  of transistor  $Q_6$ , which can be derived simply from Fig. 3.4.11:

$$r_o = \frac{\Delta V_{ce6}}{\Delta I_{c6}} = \frac{V_A + V_{ce6}}{I_{c6}} \quad (3.7.10)$$

Returning to our differential amplifier example of Fig. 3.7.2 with  $V_{ee} = -15$  V, suppose we require a differential amplifier current  $I_{ee} = I_{e1} + I_{e2} = I_{c6} = 0.03$  A. By assuming the Early voltage  $V_A = 135$  V and  $V_{ce6} \approx V_{ee}$ , the incremental collector resistance is:

$$r_o = \frac{135 + 15}{0.03} = 5 \text{ k}\Omega \quad (3.7.11)$$

If we were to replace the current generator by a simple resistor  $R_{ee} = r_o$ , the voltage  $V_{ee}$  in Fig. 3.7.2 would have to be:

$$(I_{e1} + I_{e3}) R_{ee} = 0.03 \text{ A} \cdot 5000 \Omega = 150 \text{ V} \quad (3.7.12)$$

which is 10 times more. Correspondingly, the power dissipation in the resistor  $R_{ee}$  would also be 10 times greater, or 4.5 W, compared to 0.45 W for  $Q_6$ .

A high incremental resistance  $r_o$  is also important for achieving high CMRR, because it gives the differential amplifier a higher immunity to power supply voltage variations (which is also a common mode signal).

A simple way of improving the current generator, thus achieving even greater CMRR factors, is shown in Fig. 3.7.4, where negative feedback, provided by the  $Q_5$  gain, is used to stabilize the collector current of  $Q_6$  and increase the incremental resistance, whilst a low voltage Zener diode (named after its inventor, the American physicist *Clarence M. Zener*, 1905-1993) reduces the  $V_{be}$  thermal drift of  $Q_5$ , owing to an almost equal, but opposite thermal coefficient.

In this circuit any increase in  $Q_6$  collector current  $I_{c6}$  is sensed by its voltage drop on  $R_2$ , increasing  $V_{b5}$ , which in turn increases  $I_{e5}$ , thus reducing  $I_{b6}$  and therefore also  $I_{c6}$ . The reduction feedback factor is nearly equal to the  $Q_5$  current gain  $\beta$ . Effectively, the output resistance is increased from  $r_o$  of Eq. 3.7.10 to about  $\beta r_o$ . Note that this circuit does not rely on identical transistor parameters, so it can be used in discrete circuits.

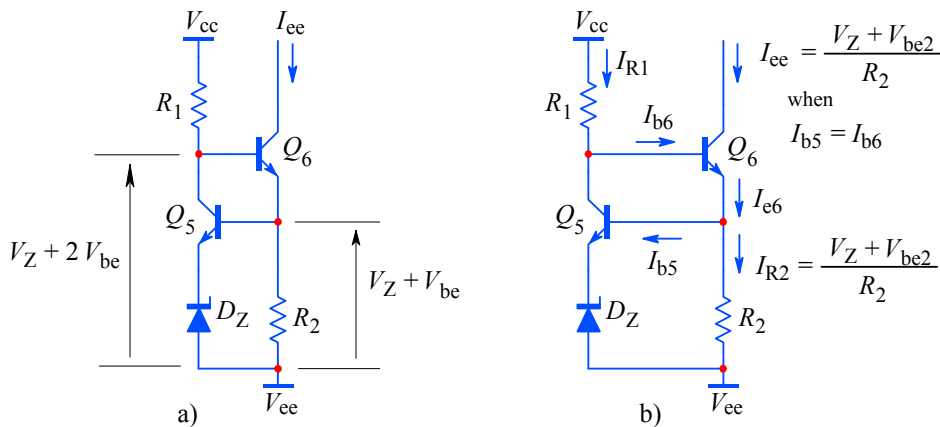


Fig. 3.7.4: Improved current generator: a) voltage drops; b) current analysis.

The circuits shown and only briefly discussed here should give the reader a starting point in current control design. Many more circuits, either simple or more elaborate, can be found in the references quoted.

### 3.8 The $f_T$ Doubler

Let us return to the differential cascode amplifier of [Fig. 3.7.2](#), where the basic analysis was done with the assumption that the inputs were driven by a differential voltage source. Here we shall analyze a current driven stage, which could suitably be used as an intermediate amplifier stage with the T-coil peaking at the input, such as the cascode of [Fig. 3.6.1](#). The T-coil peaking has already been analyzed in detail, so we shall concentrate on the active part of the circuit and see how it can be improved.

In [Fig. 3.8.1](#) we have the differential cascode circuit, driven differentially by the current source  $i_s$ . This current source is loaded by the resistance  $R_s$  which we have split in half and grounded its middle point. The output currents from the collectors of  $Q_3$  and  $Q_4$  drive the differential inputs of the next amplifying stage and we are not interested in it now. What we are interested in, is the current gain of this differential stage. The reader who has followed the previous analysis with some attention should by now be able to understand the following relation intuitively:

$$\frac{i_o}{i_s} \approx \frac{R_s}{R_e} \cdot \frac{1}{1 + s \left( R_s \frac{\tau_{T1}}{R_e} + \frac{R_s}{2} C_\mu \right)} \cdot \frac{1}{1 + s \tau_{T2}} \quad (3.8.1)$$

The last fraction is the frequency dependent part owed to  $Q_{3,4}$ .

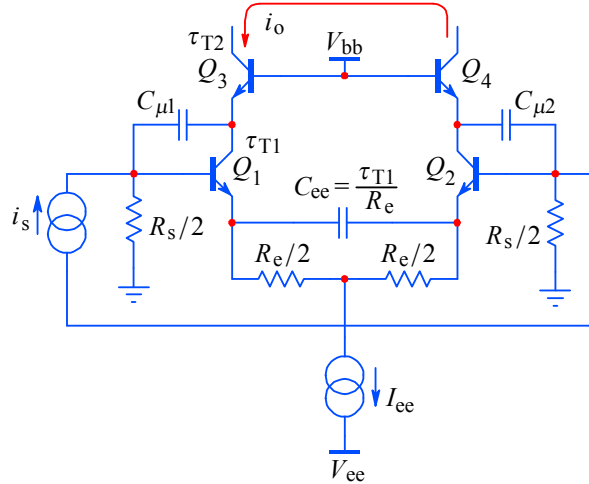


**Fig. 3.8.1:** The current driven differential cascode amplifier. We assume that the transistor pair  $Q_{1,2}$ , and the pair  $Q_{3,4}$ , respectively, have identical main parameters. The emitters of  $Q_{1,2}$  see the  $R_e C_{ee}$  network, set to equal the time constant  $\tau_{T1}$  of transistors  $Q_{1,2}$ .

The low frequency current gain is simply:

$$A_i = \frac{R_s}{R_e} \quad (3.8.2)$$

We can substitute this in [Eq. 3.8.1](#) to highlight the bandwidth dependence on gain:

$$\frac{i_o}{i_s} \approx A_i \frac{1}{1 + s \left( A_i \tau_{T1} + A_i \frac{R_e C_\mu}{2} \right)} \cdot \frac{1}{1 + s \tau_{T2}} \quad (3.8.3)$$

This means that by reducing the gain  $A_i$  we can extend the bandwidth. On the basis of this there arises the idea that we can add another differential stage to double the current (and therefore also the current gain) and then optimize the stage, choosing between the doubling of gain with the same bandwidth and the doubling of bandwidth with the same gain, or any factor in between.

The basic  $f_T$  doubler circuit, developed by *C.R. Battjes*, [Ref. 3.1], is presented in Fig. 3.8.2. Each differential pair amplifies the voltage drop on its own  $R_s/2$  and each pair sees its own  $R_e$  between the emitters, thus the current gain is simply:

$$\begin{aligned} \frac{i_o}{i_s} &\approx \frac{R_s}{R_e} \cdot \frac{1}{1 + s \left( R_s \frac{\tau_{T1}}{2 R_e} + \frac{R_s C_\mu}{2} \right)} \cdot \frac{1}{1 + s \tau_{T2}} \\ &\approx A_i \frac{1}{1 + s A_i \left( \frac{\tau_{T1}}{2} + \frac{R_e C_\mu}{2} \right)} \cdot \frac{1}{1 + s \tau_{T2}} \end{aligned} \quad (3.8.4)$$

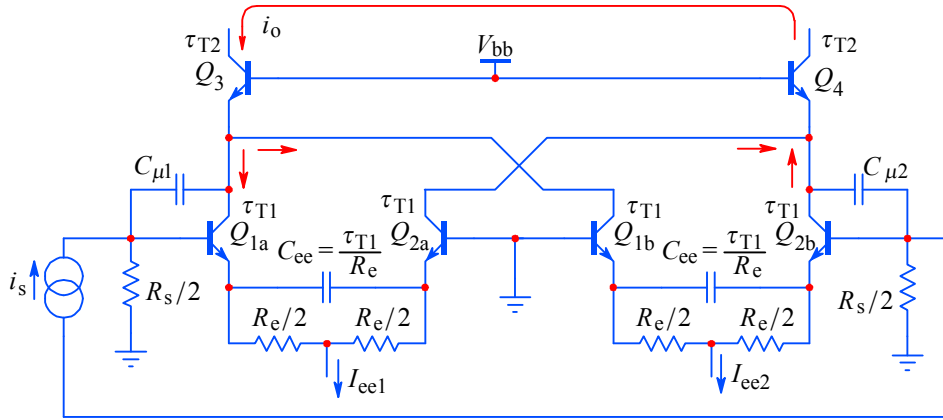


**Fig. 3.8.2:** The basic  $f_T$  doubler circuit. We assume equal transistors for  $Q_{1a,2a}$  and  $Q_{1b,2b}$ . The low input impedance of  $Q_{3,4}$  emitters allows summing the collector current of each pair, but cross-coupled for in phase signal summing.

Another advantage of this circuit is the reduced input capacitance:

$$C_i = \frac{2 \tau_{T1}}{R_e} + C_\mu \quad \text{for the circuit in Fig. 3.8.1} \quad (3.8.5)$$

$$C_i = \frac{\tau_{T1}}{R_e} + C_\mu \quad \text{for the circuit in Fig. 3.8.2} \quad (3.8.6)$$

This will ease the application of T-coil peaking at the input.

But there are also limitations. As can be deduced from Eq. 3.8.4, the ‘doubler’ term in the circuit name is misleading, because the term with  $\tau_{T2}$  is not influenced by the reduced gain. Therefore, the amount of bandwidth improvement depends on which time constant is larger. The part with  $R_e C_\mu$  can be reduced by selecting transistors with low  $C_\mu$ , but this we would do anyway. And we do not want to reduce  $R_e$ , because it would increase the gain (for same  $R_s$ ).

Another problem is that, although the transfer function is of second order, there are two real poles, so we can not ‘tune’ the system for an efficient peaking. By forcing the system to have complex conjugate poles with emitter peaking, we would increase the emitter capacitance  $C_{ee}$ , which would be reflected into the base as an increased input capacitance; this would increase exactly that term which we have just halved.

A quick estimate will give us a little more feeling of the improvement achievable. Let us have a number of transistors, with  $f_T = 3.5$  GHz,  $C_\mu = 1$  pF,  $R_s = 2 \times 50 \Omega$ ,  $Q_{3,4}$  collector load  $R_L = 2 \times 50 \Omega$ ,  $C_L = 1$  pF and the total current gain  $A_i = 3$ . Assuming that the system’s response is governed by a dominant pole, we can calculate the rise time of the conventional system as:

$$t_r = 2.2 \sqrt{A_i^2 \left( \frac{1}{2\pi f_T} + \frac{R_e C_\mu}{2} \right)^2 + \left( \frac{1}{2\pi f_T} \right)^2 + [R_L(C_L + C_\mu)]^2} \quad (3.8.7)$$

Then, for the ordinary differential cascode in [Fig. 3.8.1](#):

$$t_{r1} = 476 \text{ ps} \quad (3.8.8)$$

whilst for the  $f_T$  doubler we have:

$$t_{r2} = 355 \text{ ps} \quad (3.8.9)$$

and the improvement factor is 1.34, much less than 2. Transistors with lower  $f_T$  might give an apparently greater improvement (about 1.7 could be expected) owing to the lower contribution of the source’s impedance. However, it seems that a better idea would be to remain with the original bandwidth and use the gain doubling instead, which could lead to a system with a lower number of stages, which in turn could be optimized more easily.

On the other hand, the reduced input capacitance is really beneficial to the loading of the input T-coils. With the data from the example above, we can calculate the T-coils for the conventional and the doubler system and the resulting bandwidths. From [Eq. 3.6.21](#) we can find that:

$$\omega_H = \sqrt{\frac{12}{(R_L C_i)^2} \left( 1 + \frac{r_b}{R_L} \right)} \quad (3.8.10)$$

By assuming an  $r_b = 15 \Omega$  and  $C_i$  of 6.5 and 3.7 pF, respectively ([Eq. 3.8.5](#) and [3.8.6](#)), we can calculate an  $f_H$  of 1.9 and 3.4 GHz, a ratio of nearly 1.8, which is worth considering.

In principle one could use the same doubler implementation with 4, 6, or more transistor pairs; however, the input capacitance poses a practical limit. A system with 4 pairs is already slower than the system with two pairs.

(blank page)

### 3.9 JFET Source Follower

Wideband signals come usually from two source types: low impedance sources are usually those from the output of other wideband amplifiers, while medium and high impedance sources are usually those from sensors or other very low power sources.

In the first case, we employ standardized impedances,  $50\ \Omega$  or  $75\ \Omega$ , so that both the source and the load have the same impedance as the characteristic impedance of the cable that connects them. In this way we preserve the bandwidth and prevent reflections which would distort the signal, but we pay for this by the 50 % (–6 dB) attenuation of the signal's amplitude.

In the second case we also want a standardized value of the impedance, but this time the value is  $1\ \text{M}\Omega$ , in parallel with some (inevitable) capacitance, usually 20 pF (but values from 10 to 25 pF can also be found). The standardized capacitance is helpful not only in determining the loading of the source at high frequencies, but also to allow the use of 'probes', which are actually special HF attenuators ( $\div 10$  or  $\div 100$ ), so that the source can be loaded by a  $10\ \text{M}\Omega$  or even a  $100\ \text{M}\Omega$  resistance, while keeping the loading capacitance below some 12 pF.

With the improvement of semiconductor production processes, the so called 'active' probes have been developed, used mostly for extremely wideband signals, such as those found in modern communications and digital computers. Active probes usually have a  $10\ \text{k}\Omega \parallel 2\ \text{pF}$  input impedances, with no reduction in amplitude.

The key component of both high input impedance amplifiers and active probes is the JFET (*junction field effect transistor*) source follower [Ref. 3.16].

The basic JFET source follower circuit configuration is shown in Fig. 3.9.1. In contrast to the BJT emitter follower (with an input resistance of about  $\beta R_e$ ), the JFET source follower has a very high input resistance (between  $10^9$  and  $10^{12}\ \Omega$ ), owed to the specific construction of the JFET. Its gate (a p–n junction with the drain–source channel) is reverse biased in normal operation, modulating the channel width by the electrical field only, so the input current is mainly owed to the reverse biased p–n junction leakage and the input capacitances,  $C_{gd}$  and  $C_{gs}$ .

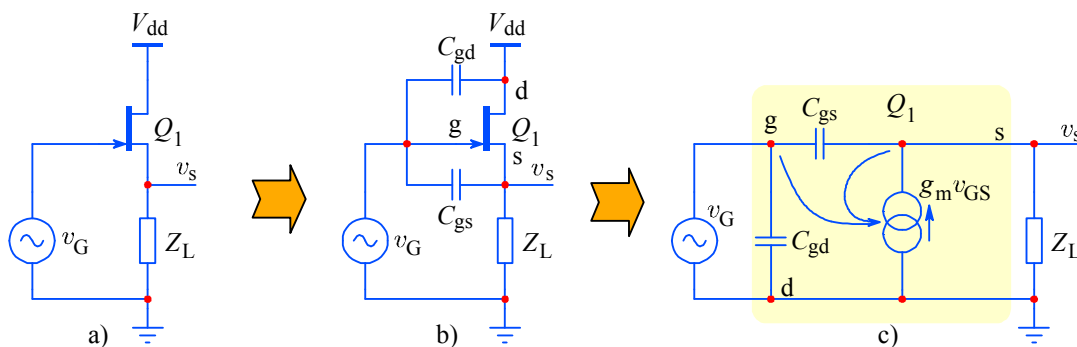


**Fig. 3.9.1:** The JFET source follower: a) circuit schematic; b) the same circuit, but with an ideal JFET and the inter-electrode capacitances drawn as external components; c) equivalent circuit.

A MOSFET (*metal oxide silicon field effect transistor*) has even greater input resistance (up to  $\sim 10^{15}\ \Omega$ ); however it also has a greater input capacitance (between 20

and 200 pF; it is also more noisy and more sensitive to damage by being overdriven), so it is not suitable for a wideband amplifier input stage.

In [Fig. 3.9.1b](#) we have drawn an ideal JFET device and its inter-electrode capacitances are modeled as external components. These capacitances determine the response at high frequencies [[Ref. 3.8](#), [3.16](#), [3.20](#), [3.35](#)]. [Fig. 3.9.1c](#) shows the equivalent circuit.

The source follower is actually the common drain circuit with a voltage gain of nearly unity, as the name ‘follower’ implies. The meaning of the circuit components is:

- $C_{gd}$  gate–drain capacitance; in most manufacturer data sheet it is labeled as  $C_{rss}$  (*common source circuit reverse capacitance*); values usually range between 1 and 5 pF;
- $C_{gs}$  gate–source capacitance; in their data sheet, manufacturers usually report the value of  $C_{iss}$ , the *common source total input capacitance*, therefore we obtain  $C_{gs} \approx C_{iss} - C_{rss}$ ; values of  $C_{gs}$  usually range from 3 to 15 pF;
- $g_m$  JFET transconductance; usual values range between 1 000 and 15 000  $\mu S$  (in some data-sheets, the symbol ‘mho’ is used to express that the unit *siemens* [S] = [1/ $\Omega$ ]);
- $Z_L$  the loading impedance of the JFET source.

The JFET drain is connected to the power supply which must be a short circuit for the drain signal current, therefore we can connect  $C_{gd}$  to ground, in parallel with the signal source. We assume the signal source impedance to be zero; so we can forget about  $C_{gd}$  for a while.

From the equivalent circuit in [Fig. 3.9.1c](#) we find the currents for the node g:

$$i_g = v_G s C_{gd} + (v_G - v_s) s C_{gs} \quad (3.9.1)$$

and the currents for the node s:

$$(v_G - v_s) s C_{gs} + (v_G - v_s) g_m = \frac{v_s}{Z_L} \quad (3.9.2)$$

which can be rewritten as:

$$v_G \left( 1 + \frac{g_m}{s C_{gs}} \right) = v_s \left( 1 + \frac{g_m}{s C_{gs}} + \frac{1}{s C_{gs} Z_L} \right) \quad (3.9.3)$$

From this we obtain the system’s voltage gain:

$$A_v = \frac{v_s}{v_G} = \frac{Z_L \left( 1 + \frac{s C_{gs}}{g_m} \right)}{Z_L \left( 1 + \frac{s C_{gs}}{g_m} \right) + \frac{1}{g_m}} \quad (3.9.4)$$

In practical follower circuits we want to make the output signal’s dynamic range as high and the voltage gain as close to 1 as possible. The simplest way to achieve this is by replacing  $Z_L$  with a constant current generator, [Fig. 3.9.2](#), much as we have done in



the differential amplifier. By doing this, we increase the real (resistive) part of the loading impedance, but we can do little to reduce the always present loading capacitance  $C_L$ .

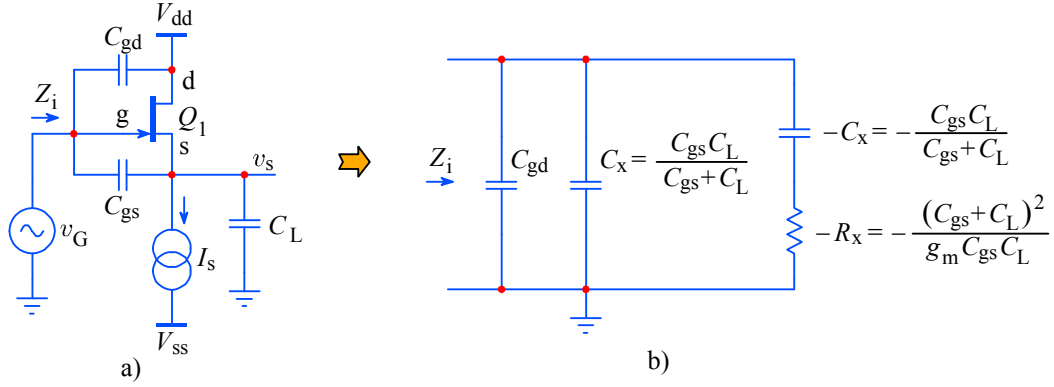


**Fig. 3.9.2:** The JFET source follower biased by a current generator and loaded only by the inevitable stray capacitance  $C_L$ : a) circuit schematic; b) the input impedance has two **negative** components, owed to  $C_{gs}$  and  $g_m$  (see [Sec. 3.9.5](#)).

In [Eq. 3.9.4](#) the term  $C_{gs}/g_m$  is obviously the characteristic JFET time constant,  $\tau_{FET}$ :

$$\frac{C_{gs}}{g_m} = \tau_{FET} = \frac{1}{\omega_{FET}} \quad (3.9.5)$$

Since we now have  $Z_L = 1/j\omega C_L$  we can rewrite [Eq. 3.9.4](#) as:

$$A_v = \frac{v_s}{v_G} = \frac{1 + \frac{j\omega}{\omega_{FET}}}{1 + j\omega \left( \frac{1}{\omega_{FET}} + \frac{C_L}{g_m} \right)} \quad (3.9.6)$$

and by replacing  $g_m$  with  $\omega_{FET} C_{gs}$  ([Eq. 3.9.5](#)) we obtain:

$$\frac{v_s}{v_G} = \frac{1 + \frac{j\omega}{\omega_{FET}}}{1 + \frac{j\omega}{\omega_{FET}} \cdot \frac{1}{D_c}} \quad (3.9.7)$$

Here  $D_c$  is the input to output capacitive divider, which would set the output voltage if only the capacitances were in place:

$$D_c = \frac{C_{gs}}{C_{gs} + C_L} \quad (3.9.8.)$$

We would like to express [Eq. 3.9.7](#) by its pole  $s_1$  and zero  $s_2$ , so we need the normalized canonical form:

$$F(s) = A_0 \frac{-s_1}{s - s_1} \cdot \frac{s - s_2}{-s_2} \quad (3.9.9)$$

Therefore we replace  $j\omega$  with  $s$ , multiply both the numerator and the denominator by  $\omega_{\text{FET}} D_c$  and obtain:

$$F(s) = D_c \frac{s - (-\omega_{\text{FET}})}{s - (-\omega_{\text{FET}} D_c)} \quad (3.9.10)$$

At zero frequency, the transfer function gain is:

$$A_0 = F(0) = D_c \frac{\omega_{\text{FET}}}{\omega_{\text{FET}} D_c} = 1 \quad (3.9.11)$$

so the zero is:

$$s_2 = -\omega_{\text{FET}} \quad (3.9.12)$$

and the pole is:

$$s_1 = -\omega_{\text{FET}} D_c \quad (3.9.13)$$

These simple relations are the basis from which we shall calculate the frequency response magnitude, the phase, the group delay and the step response of the JFET source follower (simplified at first and including the neglected components later).

### 3.9.1 Frequency response magnitude

The frequency response magnitude is the normalized absolute value of  $F(s)$  and we want to have the normalization in both gain and frequency. [Eq. 3.9.7](#) is already normalized in frequency (to  $\omega_{\text{FET}}$ ) and the gain  $A_0 = 1$ . To get the magnitude, we must multiply  $F(j\omega)$  by its complex conjugate,  $F(-j\omega)$  and take the square root:

$$|F(\omega)| = \sqrt{F(j\omega) F(-j\omega)} = \sqrt{\frac{1 + \frac{j\omega}{\omega_{\text{FET}}}}{1 + \frac{j\omega}{\omega_{\text{FET}}} \cdot \frac{1}{D_c}} \cdot \frac{1 - \frac{j\omega}{\omega_{\text{FET}}}}{1 - \frac{j\omega}{\omega_{\text{FET}}} \cdot \frac{1}{D_c}}}$$

$$|F(\omega)| = \sqrt{\frac{1 + \left(\frac{\omega}{\omega_{\text{FET}}}\right)^2}{1 + \left(\frac{\omega}{\omega_{\text{FET}} D_c}\right)^2}} \quad (3.9.14)$$

Since we want to examine the influence of loading we shall plot the transfer function for three different values of the ratio  $C_L/C_{\text{gs}}$ : 0.5, 1.0, and 2.0 (the corresponding values of  $D_c$  being 0.67, 0.5, and 0.33, respectively). The plots, shown in [Fig. 3.9.3](#), have three distinct frequency regions: in the lower one, the circuit behaves as a voltage follower, with the JFET playing an active role, so that  $v_s = v_G$ , whilst in the highest frequency region, only the capacitances are important; in between we have a transition between both operating modes.

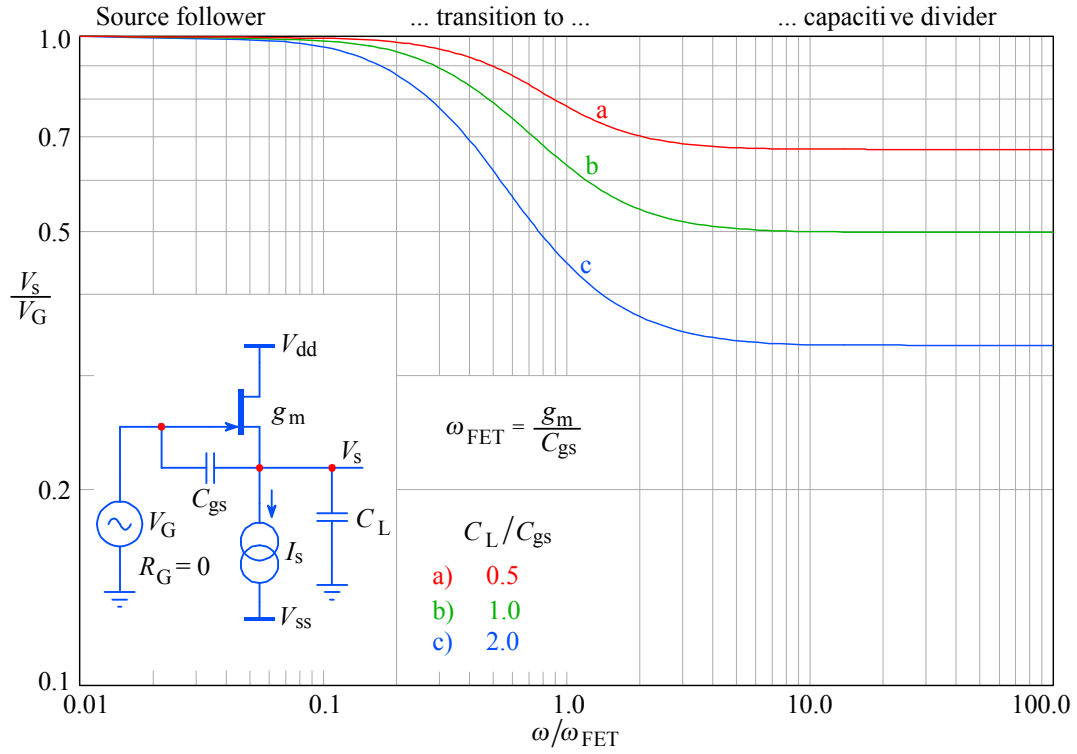


**Fig. 3.9.3:** Magnitude of the frequency response of the JFET source follower for three different capacitance ratios  $C_L/C_{gs}$ . The pole  $s_3 = -1/R_G C_i$  has not been taken into account here (see [Fig. 3.9.7](#) and [Fig. 3.9.8](#)).

The relation for the upper cutoff frequency is very interesting. If we set  $|F(\omega)|$  to be equal to:

$$\sqrt{\frac{1 + (\omega_h/\omega_{FET})^2}{1 + (\omega_h/\omega_{FET} D_c)^2}} = \frac{1}{\sqrt{2}} \quad (3.9.15)$$

it follows that:

$$\omega_h = \omega_{FET} \frac{D_c}{\sqrt{1 - 2 D_c^2}} \quad (3.9.16)$$

From [Eq. 3.9.15](#) we can conclude that by putting  $D_c = 1/\sqrt{2}$  the denominator is reduced to zero, thus  $\omega_h = \infty$ . This means that for such a capacitive ratio the magnitude never falls below  $1/\sqrt{2}$ . However attractive the possibility of achieving infinite bandwidth may seem, this can never be realized in practice, because any signal source will have some, although small, internal resistance  $R_G$ , resulting in an additional input pole  $s_3 = -1/R_G C_i$ , where  $C_i$  is the total input capacitance of the JFET. The complete transfer function will now be (see [Fig. 3.9.7](#) and [3.9.8](#)):

$$F(s) = \frac{s_1 s_3}{-s_2} \cdot \frac{s - s_2}{(s - s_1)(s - s_3)} \quad (3.9.17)$$

### 3.9.2 Phase

We obtain the phase response from [Eq. 3.9.7](#) by taking the arctangent of the ratio of the imaginary to the real part of  $F(j\omega)$ :

$$\varphi(\omega) = \arctan \frac{\Im\{F(j\omega)\}}{\Re\{F(j\omega)\}} \quad (3.9.18)$$

Since in [Eq. 3.9.7](#) we have a single real pole and a single real zero, the resulting phase angle is calculated as:

$$\varphi(\omega) = \arctan \frac{\omega}{\omega_{\text{FET}}} - \arctan \frac{\omega}{\omega_{\text{FET}} D_c} \quad (3.9.19)$$

In [Fig. 3.9.4](#) the three phase plots with same  $C_L/C_{gs}$  ratios are shown. Because of the zero, the phase returns to the initial value at high frequencies.

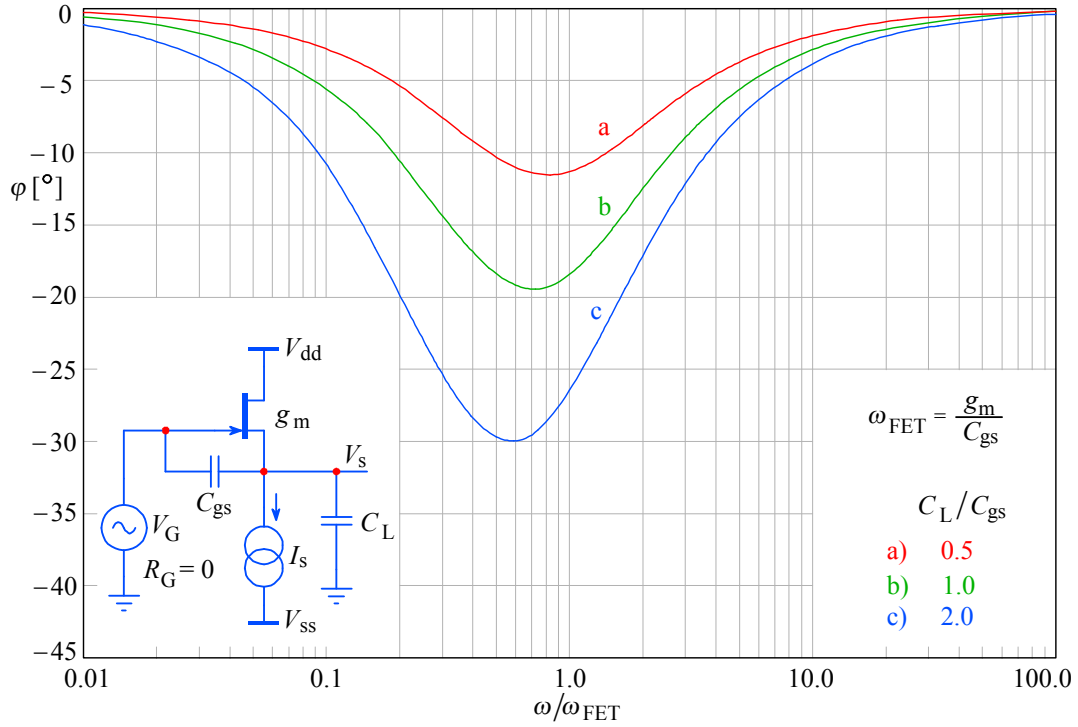


**Fig. 3.9.4:** Phase plots of the JFET source follower for the same three capacitance ratios.

### 3.9.3 Envelope delay

We obtain the envelope delay by taking the  $\omega$  derivative of the phase:

$$\tau_e = \frac{d\varphi}{d\omega} \quad (3.9.20)$$

but we usually prefer the normalized expression  $\tau_e \omega_h$ . In our case, however, the upper cut off frequency,  $\omega_h$ , is changing with the capacitance divider  $D_c$ . So instead of  $\omega_h$  we

shall, rather, normalize the envelope delay to the characteristic frequency of the JFET itself,  $\omega_{\text{FET}}$ :

$$\tau_e \omega_{\text{FET}} = \frac{1}{1 + (\omega/\omega_{\text{FET}})^2} - \frac{D_c}{D_c^2 + (\omega/\omega_{\text{FET}})^2} \quad (3.5.21)$$

The envelope delay plots for the three capacitance ratios are shown in [Fig. 3.9.5](#). Note that for all three ratios there is a frequency region in which the envelope delay becomes **positive**, implying that the output signal advance, in correlation with the phase plots, goes up with frequency. We have explained the physical background of this behavior in [Part 2, Fig. 2.2.5, 2.2.6](#). The positive envelope delay influences the input impedance in a very unfavorable way, as we shall soon see.

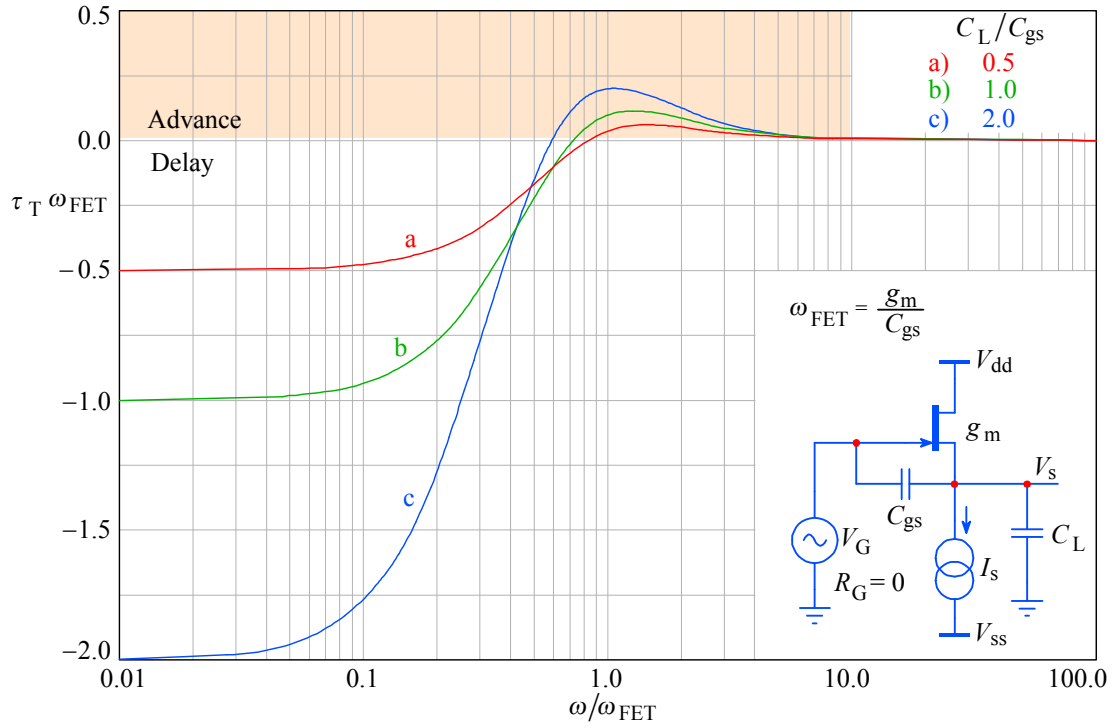


**Fig. 3.9.5:** The JFET envelope delay for the three capacitance ratios. Note the positive peak (phase advance region): trouble in sight!

### 3.9.4 Step response

We are going to use [Eq. 3.9.9](#), which we multiply by the unit step operator  $1/s$  to obtain the step response in the complex frequency domain; we then obtain the time domain response by applying the inverse Laplace transform:

$$G(s) = \frac{1}{s} F(s) = \frac{1}{s} D_c \frac{s - s_2}{s - s_1} \quad (3.9.22)$$

$$g(t) = \mathcal{L}^{-1}\{G(s)\} = D_c \sum_{s=0}^{s_1} \text{res} \frac{(s - s_2) e^{st}}{s(s - s_1)} \quad (3.9.23)$$

The residue at  $s \rightarrow 0$  is:

$$\text{res}_0 = \lim_{s \rightarrow 0} s \frac{(s - s_2) e^{st}}{s(s - s_1)} = \frac{s_2}{s_1} \quad (3.9.24)$$

and the residue at  $s \rightarrow s_1$  is:

$$\text{res}_1 = \lim_{s \rightarrow s_1} (s - s_1) \frac{(s - s_2) e^{st}}{s(s - s_1)} = \frac{s_1 - s_2}{s_1} e^{s_1 t} \quad (3.9.25)$$

By entering both residues back into [Eq. 3.9.23](#) we get:

$$g(t) = D_c \left( \frac{s_2}{s_1} + \frac{s_1 - s_2}{s_1} e^{s_1 t} \right) \quad (3.9.26)$$

and, by considering [Eq. 3.9.12](#) and [3.9.13](#), as well as that  $\omega_{\text{FET}} = 1/\tau_{\text{FET}}$  and using the normalized time  $t/\tau_{\text{FET}}$ , we end up with:

$$g(t) = 1 - (1 - D_c) e^{-D_c t / \tau_{\text{FET}}} \quad (3.9.27)$$

The plot of this relation is shown in [Fig. 3.9.6](#), again for the same three capacitance ratios. The initial output signal jump at  $t = 0$  is the input signal cross-talk (through  $C_{\text{gs}}$ ) multiplied by the  $D_c$  factor:

$$g(0) = D_c \quad (3.9.28)$$

Following the jump is the exponential relaxation towards the normal follower action at lower frequencies. If the input pole  $s_3 = -1/R_G C_i$  is taken into account, the jump would be slowed down to an exponential rise with a time constant of  $R_G C_i$ .

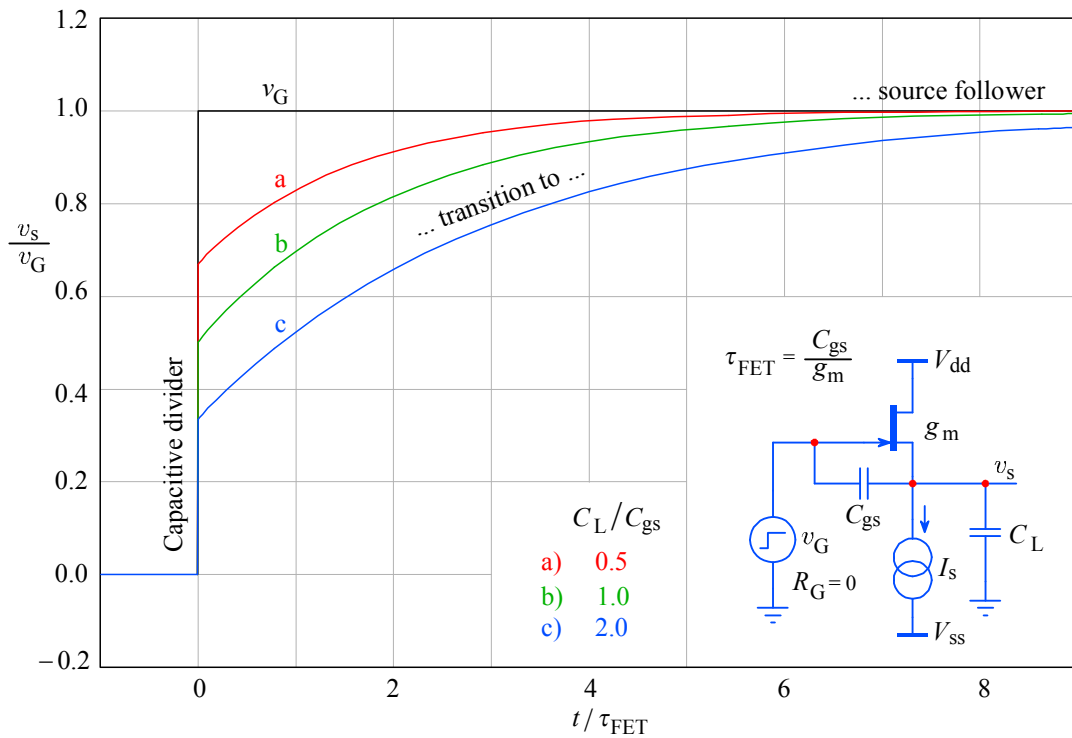


**Fig. 3.9.6:** The JFET source follower step response for the three capacitance ratios.

As mentioned earlier in connection with [Eq. 3.9.17](#), when the value of  $R_G$  is comparable to  $1/g_m$ , an additional pole has to be considered. We must derive the system transfer function again, from the following two equations:

For the currents into the node g:

$$\frac{v_G - v_g}{R_G} = \frac{v_g}{\frac{1}{s C_{gd}}} + \frac{v_g - v_s}{\frac{1}{s C_{gs}}} \quad (3.9.29)$$

and for the currents into the node s:

$$\frac{v_g - v_s}{\frac{1}{s C_{gs}}} + (v_g - v_s) g_m = \frac{v_s}{\frac{1}{s C_L}} \quad (3.9.30)$$

We first express  $v_g$  as a function of  $v_s$  from [Eq. 3.9.30](#):

$$v_g = v_s \left( 1 + \frac{s C_L}{s C_{gs} + g_m} \right) \quad (3.9.31)$$

Then we replace  $v_g$  in [Eq. 3.9.29](#) by [3.9.31](#):

$$v_G = v_s \left( 1 + \frac{s C_L}{s C_{gs} + g_m} \right) (1 + R_G s C_{gd} + R_G s C_{gs}) - v_s R_G s C_{gs} \quad (3.9.32)$$

After some further manipulation we arrive at:

$$\frac{v_s}{v_G} = \frac{1}{1 + R_G s C_{gd} + \frac{s C_L}{s C_{gs} + g_m} (1 + R_G s (C_{gd} + C_{gs}))} \quad (3.9.33)$$

Now we put this into the normalized canonical form and use [Eq. 3.9.5](#) again to replace the term  $g_m/C_{gs}$  with  $\omega_{FET}$ . Also, we express all the time constants as functions of  $\omega_{FET}$  and the appropriate capacitance ratios. Finally, we want to see how the response depends on the product  $g_m R_G$ , so we multiply all the terms containing  $R_G$  with  $g_m$  and compensate each of them accordingly. The final expression is:

$$\frac{v_s}{v_G} = \frac{(s + \omega_{FET}) \frac{1}{g_m R_G} \cdot \frac{\omega_{FET} \frac{C_{gs}}{C_{gd}}}{\left( 1 + \frac{C_L}{C_{gs}} + \frac{C_L}{C_{gd}} \right)}}{s^2 + s \frac{\omega_{FET} \left[ 1 + \frac{1}{g_m R_G} \left( \frac{C_{gs}}{C_{gd}} + \frac{C_L}{C_{gd}} \right) \right]}{\left( 1 + \frac{C_L}{C_{gs}} + \frac{C_L}{C_{gd}} \right)}} + \frac{1}{g_m R_G} \cdot \frac{\omega_{FET}^2 \frac{C_{gs}}{C_{gd}}}{\left( 1 + \frac{C_L}{C_{gs}} + \frac{C_L}{C_{gd}} \right)} \quad (3.9.34)$$

To plot the responses we shall set:

$$\frac{C_L}{C_{gs}} = 1, \quad \frac{C_{gs}}{C_{gd}} = 5, \quad \omega_{FET} = 1, \quad s = j\omega, \quad \text{and} \quad g_m R_G = [0.3, 1, 3]$$

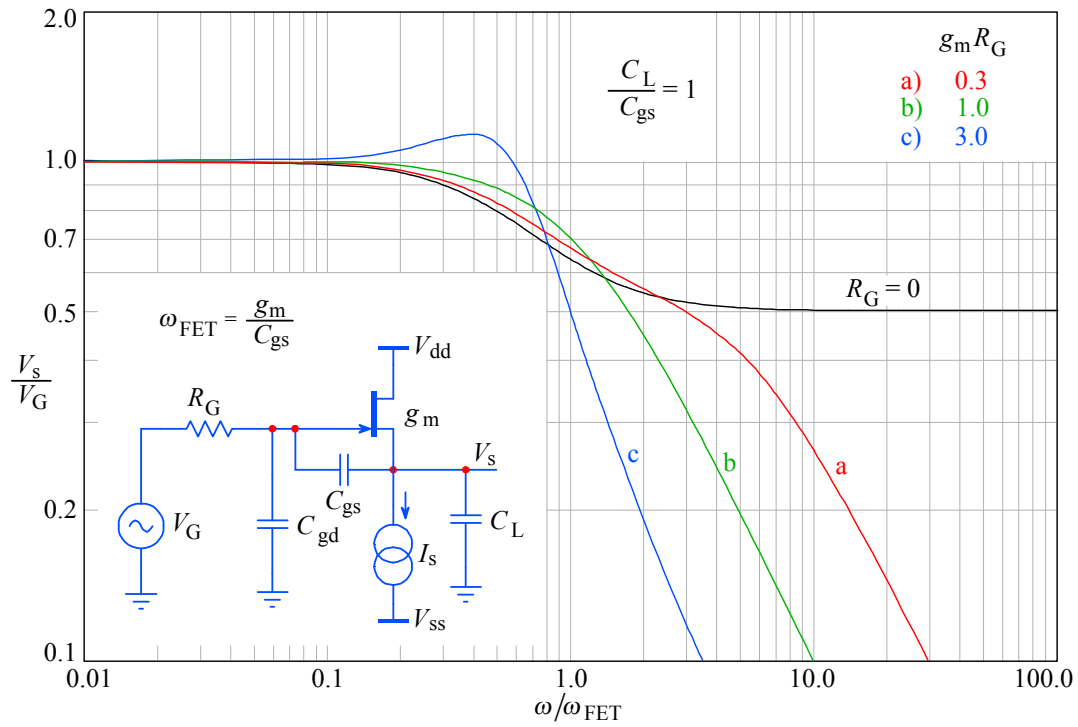


**Fig. 3.9.7:** The JFET source follower frequency response for a ratio  $C_L/C_{gs} = 1$  and a variable signal source impedance, so that  $R_G g_m$  is 0.3, 1, and 3, respectively. Note the response peaking for  $g_m R_G = 3$ .

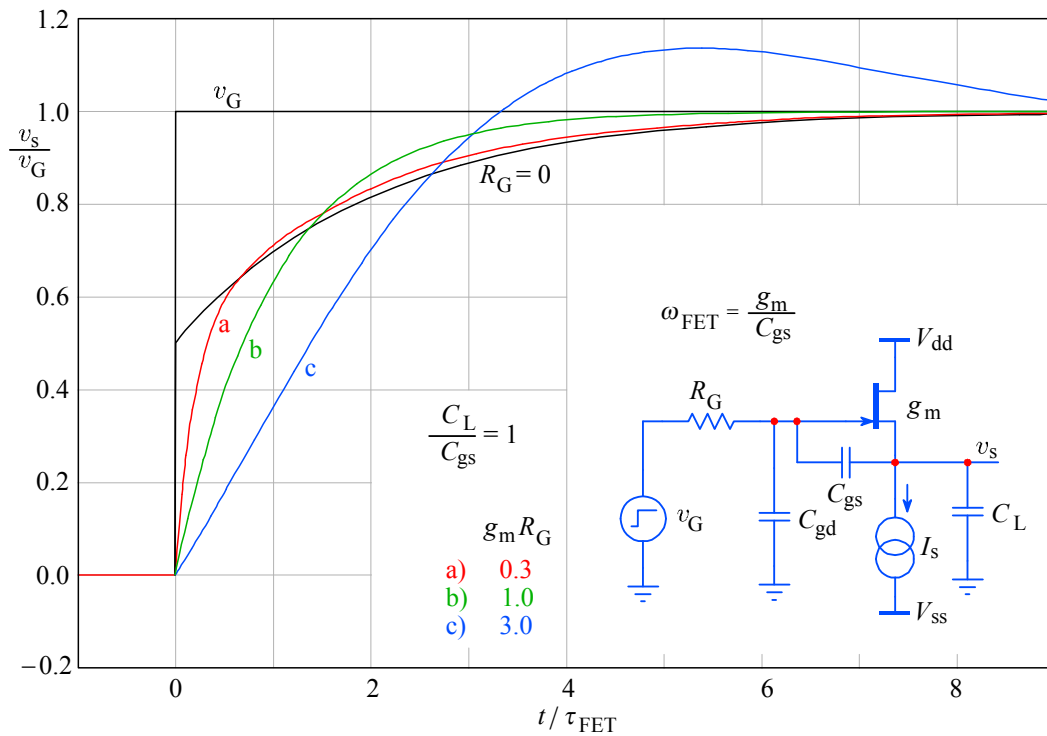


**Fig. 3.9.8:** The JFET source follower step response for the same conditions as in [Fig. 3.9.7](#).



### 3.9.5 Input impedance

In [Fig. 3.9.7](#) and [3.9.8](#) we have seen how the JFET source follower response is affected by its input impedance; this behavior becomes evident when the signal source has a non-zero resistance. Here, we are going to explore the circuit in more depth to examine the influence of a complex and, in particular, inductive signal source.

As we have done in the previous analysis, the gate–drain capacitance  $C_{gd}$  will appear in parallel with the input, so we can treat its admittance separately and concentrate on the remaining input components.

We start from [Eq. 3.9.1](#) by solving it for  $v_s$ :

$$v_s = v_G - \frac{i_i}{s C_{gs}} \quad (3.9.35)$$

This we insert into [Eq. 3.9.2](#):

$$-v_G (s C_{gs} + g_m) + \left( v_g - \frac{i_i}{s C_{gs}} \right) \left( s C_{gs} + g_m + \frac{1}{Z_L} \right) = 0 \quad (3.9.36)$$

Because the JFET source is biased from a constant current generator (whose impedance we assume to be infinite) the loading admittance is  $1/Z_L = s C_L$ . Let us put this back into [Eq. 3.3.36](#) and rearrange it a little:

$$v_G s C_L = i_i \left( 1 + \frac{g_m}{s C_{gs}} + \frac{C_L}{C_{gs}} \right) \quad (3.9.37)$$

Furthermore:

$$\begin{aligned} v_G &= i_i \left( \frac{1}{s C_L} + \frac{g_m}{s^2 C_{gs} C_L} + \frac{1}{s C_{gs}} \right) \\ &= i_i \frac{s (C_{gs} + C_L) + g_m}{s^2 C_{gs} C_L} \end{aligned} \quad (3.9.38)$$

The input impedance (without  $C_{gd}$ , hence the prime [ ' ]) is then:

$$Z'_i = \frac{v_g}{i_i} = \frac{s (C_{gs} + C_L) + g_m}{s^2 C_{gs} C_L} \quad (3.9.39)$$

To see more clearly how this impedance is comprised, we invert it to find the admittance and apply the continuous fraction synthesis in order to identify the individual components.

$$Y'_i = \frac{s^2 C_{gs} C_L}{s (C_{gs} + C_L) + g_m} = s \frac{C_{gs} C_L}{C_{gs} + C_L} - \frac{g_m s \frac{C_{gs} C_L}{C_{gs} + C_L}}{s (C_{gs} + C_L) + g_m} \quad (3.9.40)$$

The first fraction is the admittance of the capacitances  $C_{gs}$  and  $C_L$  connected in series. Let us name this combination  $C_x$ :

$$C_x = \frac{C_{gs} C_L}{C_{gs} + C_L} \quad (3.9.41)$$

The second fraction, which has a negative sign, must be further simplified. We invert it again, and after some simple rearrangement we obtain the impedance:

$$Z_x = - \frac{(C_{gs} + C_L)^2}{g_m C_{gs} C_L} - \frac{C_{gs} + C_L}{s C_{gs} C_L} \quad (3.9.42)$$

The first part is interpreted as a negative resistance, which we shall label  $-R_x$  in order to follow the negative sign in the following analysis more clearly:

$$-R_x = - \frac{(C_{gs} + C_L)^2}{g_m C_{gs} C_L} \quad (3.9.43)$$

The second part as a negative capacitance, which we label  $-C_x$  because it has the same absolute value as  $C_x$  from the [Eq. 3.9.41](#):

$$-C_x = - \frac{C_{gs} C_L}{C_{gs} + C_L} \quad (3.9.44)$$

Now that we have all the components we can reintroduce the gate–drain capacitance  $C_{gd}$ , so that the final equivalent input impedance looks like [Fig. 3.9.9](#). We can write the complete input admittance:

$$Y_i = j\omega (C_{gd} + C_x) - \frac{1}{R_x + \frac{1}{j\omega C_x}} \quad (3.9.45)$$

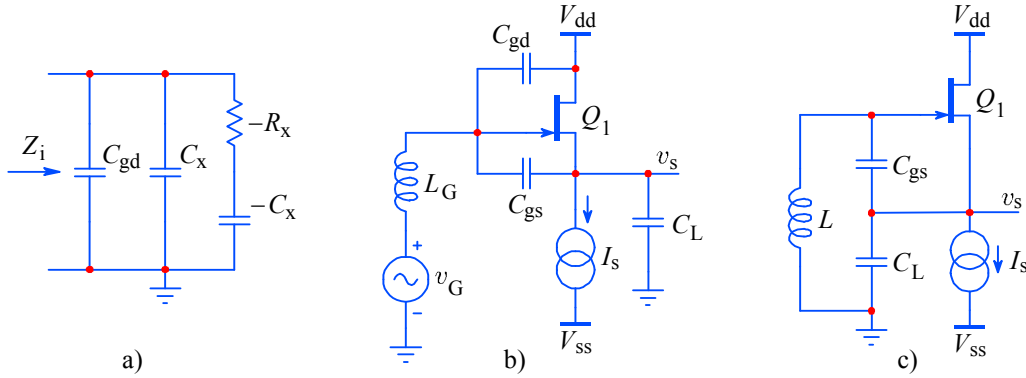


**Fig. 3.9.9:** a) The equivalent input impedance of the capacitively loaded JFET source follower has negative components which can be a nuisance if, as in b), the signal source has an inductive impedance, forming c) a familiar Colpitts oscillator. If  $C_{gd}$  is small, the circuit will oscillate for a broad range of inductance values.

We can separate the real and imaginary part of  $Y_i$  by putting [Eq. 3.9.45](#) on a common denominator:

$$\begin{aligned} Y_i &= \Re\{Y_i\} + \Im\{Y_i\} \\ &= - \frac{\omega^2 C_x^2 R_x}{1 + \omega^2 C_x^2 R_x^2} + j\omega \frac{C_{gd} + \omega^2 C_x^2 R_x^2 (C_{gd} + C_x)}{1 + \omega^2 C_x^2 R_x^2} \end{aligned} \quad (3.9.46)$$

The negative real part can cause some serious trouble [Ref. 3.24]. Suppose we are troubleshooting a circuit with a switching power supply and we suspect it to be a cause of a strong electromagnetic interference (EMI); we want to use a coil with an appropriate inductance  $L$  (which, of course, has its own real and imaginary admittance) to inspect the various parts of the circuit for EMI intensity and field direction. If we connect this coil to the source follower and if the coil resistance is low, we would have:

$$\Re\{Y_L\} + \Re\{Y_i\} \leq 0 \quad (3.9.47)$$

and the source follower becomes a familiar Colpitts oscillator, Fig. 3.9.9c [Ref. 3.25]. Indeed, some older oscilloscopes would burst into oscillation if connected to such a coil and with its input attenuator switched to maximum sensitivity (a few highly priced instruments built by respectable firms, back in early 1970's, were no exception).

By taking into account Eq. 3.9.42, 3.9.43 and 3.9.9 and substituting  $\omega_{\text{FET}} = g_m/C_{\text{gs}}$ , the real part of the input impedance can be rewritten as:

$$\Re(Y_i) = G_i = -g_m \frac{C_L}{C_{\text{gs}}} \cdot \frac{(\omega/\omega_{\text{FET}})^2}{1 + (\omega/\omega_{\text{FET}} D_c)^2} \quad (3.9.48)$$

The last fraction represents the normalized frequency dependence of this admittance:

$$G_{\text{IN}} = \frac{(\omega/\omega_{\text{FET}})^2}{1 + (\omega/\omega_{\text{FET}} D_c)^2} \quad (3.9.49)$$

Fig. 3.9.10 shows the plots of  $G_{\text{IN}}$  for the same ratios of  $C_L/C_{\text{gs}}$  as before. Note the quadratic dependence (of  $D_c$ ) at high frequencies.

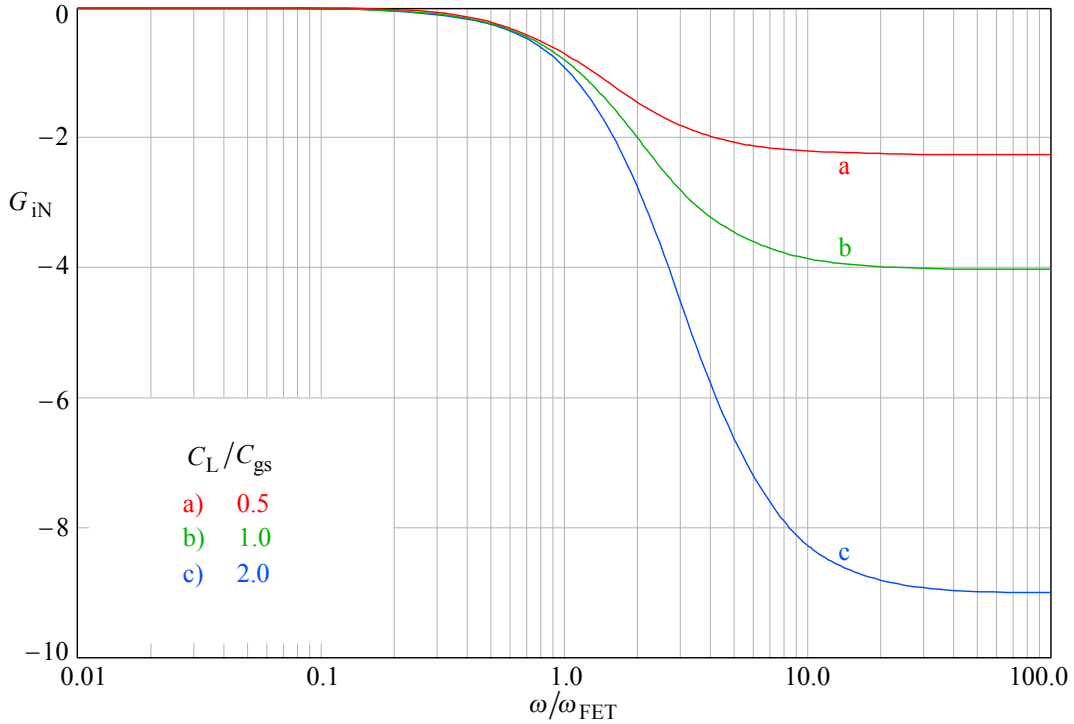


**Fig. 3.9.10:** Normalized negative input conductance  $G_{\text{IN}}$  vs. frequency.

A negative input impedance is always highly undesirable and we shall show a few possible solutions. The obvious way would be to introduce a resistor in series with

the JFET gate; since we should have some series resistance anyway in order to protect the sensitive input from static discharge or accidental overdrive, this will seem to be the preferred choice. However, after a closer look, this protection resistance is too small to prevent oscillations in case of an inductive signal source impedance. The required resistance value which will guarantee stability in all conditions will be so high that the bandwidth will be reduced by nearly an order of magnitude. Thus this method of compensation is used only if we do not care how much bandwidth we obtain.

A more elegant method of compensation is the one which we have used already in [Fig. 3.5.3](#). If we introduce a serially connected  $R_x C_x$  network in parallel with the JFET input, as shown in [Fig. 3.9.11](#), we obtain  $Y_x = 0$  and  $Z_x = \infty$ . Note the corresponding phasor diagram: we first draw the negative components,  $-R_x$  and  $-C_x$ , find the impedance vector  $-Z_x$  and invert it to find the negative admittance,  $-Y_x$ . We then compensate it by a positive admittance  $Y_x$  such that their sum  $Y_{ic} = 0$ . We finally invert  $Y_x$  to find  $Z_x$  and decompose it into its real and imaginary part,  $R_x$  and  $C_x$ :

$$Y_{ic} = \frac{1}{-R_x - \frac{1}{j\omega C_x}} + \frac{1}{R_x + \frac{1}{j\omega C_x}} = 0 \quad (3.9.50)$$

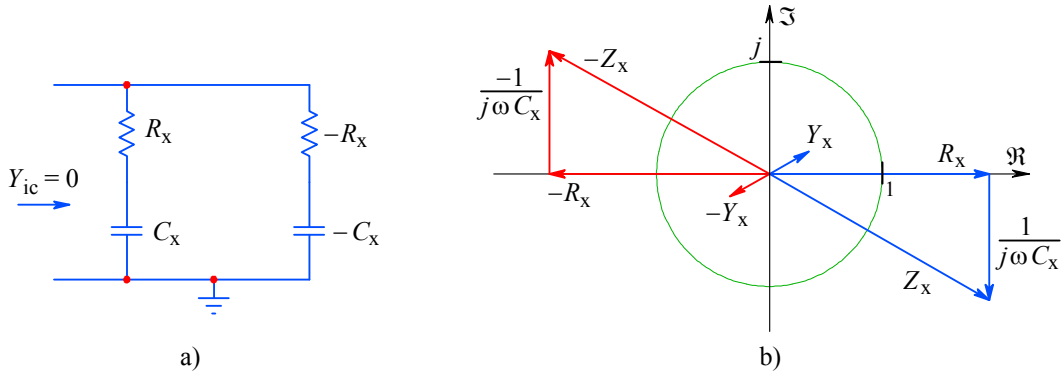


**Fig. 3.9.11:** a) The negative components of the input impedance can be compensated by an equal but positive network, connected in parallel, so that their admittances sum to zero (infinite impedance). In b) we see the corresponding phasor diagram.

With this compensation, the total input impedance is the one belonging to the parallel connection of  $C_{gd}$  with  $C_x$  and assuming a  $1 \text{ M}\Omega$  gate bias resistor  $R_{in}$ :

$$Z_i = \frac{1}{\frac{1}{R_{in}} + j\omega(C_{gd} + C_x)} = \frac{R_{in}}{1 + j\omega\left(C_{gd} + \frac{C_{gs}C_L}{C_{gs} + C_L}\right)R_{in}} \quad (3.9.51)$$

The analysis of the input impedance would be incomplete without [Fig. 3.9.12](#), where the Nyquist diagrams of the impedance are shown revealing its frequency dependence, as well as the influence of different signal source impedances.

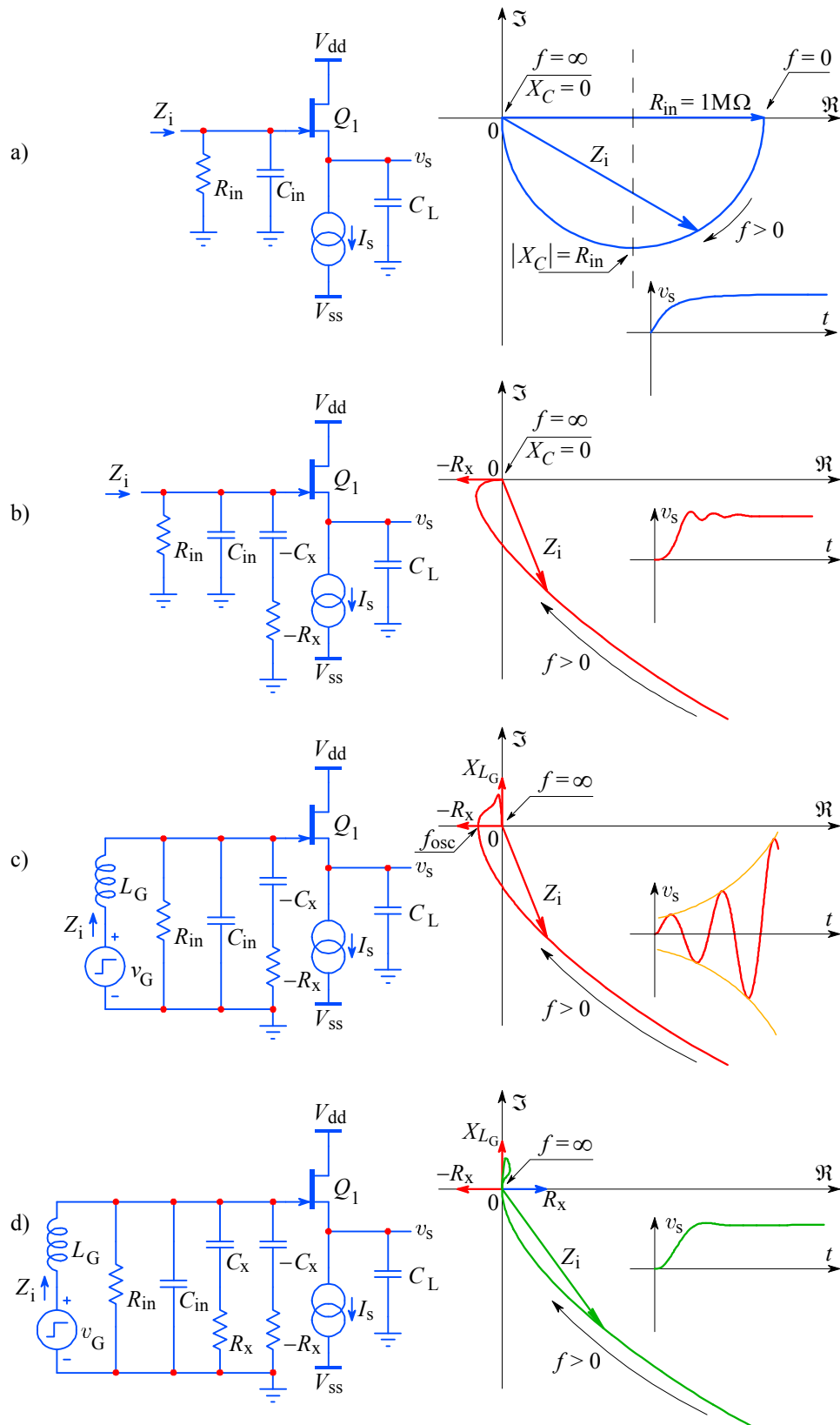


**Fig. 3.9.12:** a) The input impedance of the JFET source follower, assumed to be purely capacitive and in parallel with a  $1\text{ M}\Omega$  gate biasing resistor; thus at  $f = 0$  we see only the resistor and at  $f = \infty$  the reactance of the input capacitance is zero; b) the negative input impedance components affect the input impedance near the origin; c) with an inductive signal source, the point in which the impedance crosses the negative real axis corresponds to the system resonant frequency, provoking oscillations. d) The compensation removes the negative components.

In [Fig. 3.9.12a](#) the JFET gate is tied to ground by a  $1\text{ M}\Omega$  resistor, which, with a purely capacitive input impedance, would give a phasor diagram in the form of a half circle with frequency varying from DC to infinity.

In [Fig. 3.9.12b](#) we concentrate on the small area near the complex plane origin (high frequencies, close to  $f_{\text{FET}}$ ), where we draw the influence of the negative input impedance components, assuming a resistive signal source.

In [Fig. 3.9.12c](#) an inductive signal source (with a small resistive component) will cause the impedance crossing the real axis in the negative region, therefore the circuit would oscillate at the frequency at which this crossing occurs.

Finally, in [Fig. 3.9.12d](#) we see the same situation but with the negative components compensated as in [Fig. 3.9.11](#). Note the small loop in the first quadrant of the impedance plot — it is caused by the small resistance  $R_G$  of the coil  $L_G$ , the coil inductance, and the total input capacitance  $C_{\text{in}}$ .

In [Fig. 3.9.13](#) we see yet another way of compensating the negative input impedance. Here the compensation is achieved by inserting a small resistance  $R_d$  in the drain, thus allowing the anti-phase signal at the drain to influence the gate via  $C_{\text{gd}}$  and cancel the in-phase signal from the JFET source via  $C_{\text{gs}}$ . This method is sometimes preferred over the former method, because the PCB pads, which are needed to accommodate the additional compensation components, also create some additional parasitic capacitance from the gate to ground.

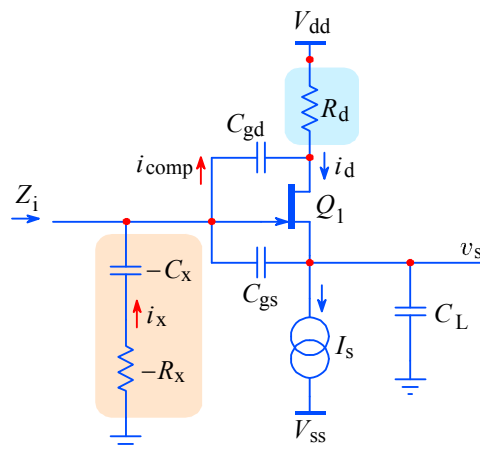


**Fig. 3.9.13:** Alternative compensation of the input impedance negative components, using negative feedback from the JFET drain.

It should be noted, however, that the negative input impedance compensation can be achieved for small signals only. Large signals vary the JFET gate's reverse bias voltage and the drain–source voltage considerably, therefore both  $C_{\text{gs}}$  and  $C_{\text{gd}}$ , as well as  $g_m$ , change with voltage. We therefore expect some nonlinear effects to appear with a large signal drive. We shall examine this and some other aspects of the source follower's performance in [Part 5](#).

### Résumé of Part 3

In this part we have analyzed some basic circuits for wideband amplification, examined their most important limitations, and explained several ways of improving their high frequency performance. The property which can cause most trouble, even for experienced designers, is the negative input impedance of some of the most useful wideband circuits, and we have shown a few possible solutions.

The reader must realize, however, that the analytical tools and solutions presented are by no means the ultimate design examples. For a final design, many other aspects of circuit performance must also be carefully considered, and, more often than not, these other factors will compromise the wideband performance severely.

As we have indicated at some points, there are ways of compensating certain unwanted circuit behavior by implementing the system in a differential configuration, but, on the negative side, this doubles the number of active components, increasing cost, power dissipation, circuit size, strays and parasitics and also the production and testing complexity. From the wideband design point of view, having many active components usually means many more poles and zeros that must be carefully analyzed and appropriately 'tuned'.

In [Part 4](#) and [Part 5](#) we shall explain some theoretical and practical techniques for an efficient design approach at the system level.

(blank page)



**References:**

- [3.1] *C.R. Battjes*, Amplifier Frequency Response and Risetime, AFTR Class Notes (Amplifier Frequency and Transient Response), Tektronix, Inc., Beaverton, 1977
- [3.2] *P. Starič*, Transistor as an Impedance Converter (in Slovenian with an English Abstract), Elektrotehniški Vestnik, 1989, pp. 17–22.
- [3.3] *D.L. Feucht*, Handbook of Analog Circuit Design, Academic Press, Inc., San Diego, 1990
- [3.4] *I.E. Getreu*, Modeling the Bipolar Transistor, Elsevier Scientific Publishing Company, Amsterdam, 1978
- [3.5] *R.I. Ross*, T-coil Transistor Interstage Coupling, AFTR Class Notes, Tektronix, Inc., Beaverton, 1968
- [3.6] *P. Starič*, Application of T-coil Transistor Interstage Coupling in Wideband Pulse Amplifiers, Elektrotehniški Vestnik, 1990, pp. 143–152.
- [3.7] *P.R. Gray & R.G. Meyer*, Analysis and Design of Analog Integrated Circuits, John Wiley, New York, 1969
- [3.8] *B.E. Hofer*, Amplifier Risetime and Frequency Response, AFTR Class Notes, Tektronix, Inc., Beaverton, Oregon, 1982
- [3.9] *J.J. Ebers & J.L. Moll*, Large-Signal Behavior of Junction Transistors, Proceedings of IRE, Vol. 42, pp. 1761–1772, December 1954
- [3.10] *H.K. Gummel & H.C. Poon*, An Integral Charge Control Model of Bipolar Transistors, Bell Systems Technical Journal, Vol. 49, pp. 827–852, May 1970
- [3.11] *J.M. Early*, Effects of Space-Charge Layer Widening in Junction Transistors, Proceedings of IRE, Vol. 40, pp. 1401–1406, November 1952
- [3.12] *P.E. Gray & C.L. Searle*, Electronic Principles, Physics, Models and Circuits, John Wiley, New York, 1969
- [3.13] *L.J. Giacoletto*, Electronics Designer's Handbook, Second Edition, McGraw-Hill, New York 1961.
- [3.14] *P.M. Chirlian*, Electronic Circuits, Physical Principles and Design, McGraw-Hill, 1971.
- [3.15] *J.E. Cathey*, Theory and Problems of Electronic Devices and Circuits, Schaum's Outline Series in Engineering, McGraw-Hill, New York, 1989
- [3.16] *A.D. Evans*, Designing with Field-Effect Transistors, (Siliconix Inc.), McGraw-Hill, New York, 1981
- [3.17] *J.M. Pettit & M. M. McWhorter*, Electronic Amplifier Circuits, Theory and Design, McGraw-Hill, New York, 1961
- [3.18] *B. Orwiller*, Vertical Amplifier Circuits, Tektronix Inc., Beaverton, Oregon, 1969
- [3.19] *C.R. Battjes*, Technical Notes on Bridged T-coil Peaking, Internal Publication, Tektronix, Inc., Beaverton, Oregon, 1969
- [3.20] *P. Antognetti & G. Massobrio*, Semiconductor Device Modeling with SPICE, McGraw-Hill, New York, 1988
- [3.21] *P. Horowitz & W. Hill*, The Art of Electronics, Cambridge University Press, Cambridge, 1987
- [3.22] *G. Bruun*, Common-Emitter Transistor Video-Amplifiers, Proceedings of the IRE, Nov. 1956, pp. 1561–1572

- [3.23] *F.W. Grover*, Inductance Calculation, (Reprint), Instrument Society of America, Research Triangle Park, N. C. 27 709, 1973.
- [3.24] *G.B. DeBella*, Stability of Capacitively-Loaded Emitter Follower, Hewlett-Packard Journal, Vol. 17, No. 8, April 1966
- [3.25] *L. Strauss*, Wave Generation and Shaping, McGraw-Hill, New York, 1960
- [3.26] *J.L. Addis*, private e-mail exchange with the authors (see [wbapdx32.PDF](#) on the disk)
- [3.27] *M.E. Van Valkenburg*, Introduction to Modern Network Synthesis, John Wiley, New York, 1960
- [3.28] SPICE - An Overview,  
<http://www.seas.upenn.edu/~jan/spice/spice.overview.html>
- [3.29] ORCAD PSpice page - Info and download of latest free evaluation version,  
<http://www.orcad.com/products/pspice/pspice.htm>
- [3.30] MicroCAP, Spectrum Software, Inc.,  
<http://www.spectrum-soft.com>
- [3.31] *R.J. Widlar*, Some Circuit Design Techniques for Linear Integrated Circuits, IEEE Transactions on Circuit Theory, Vol. CT-12, Dec. 1965, pp. 586–590
- [3.32] *G.R. Wilson*, A Monolithic Junction FET-NPN Operational Amplifier, IEEE Journal of Solid-State Circuits, Vol. SC-3, Dec. 1968, pp. 341–348
- [3.33] *A.P. Brokaw*, A Simple Three-Terminal IC Bandgap Reference, IEEE Journal of Solid-State Circuits, Vol. SC-9, Dec. 1974, pp. 388–393
- [3.34] *S. Roach*: Signal Conditioning in Oscilloscopes and the Spirit of Invention, *J. Williams* (Editor), The Art and Science of Analog Circuit Design, Ch. 7, Butterworth-Heinemann, 1995, ISBN 0-7506-9505-6
- [3.35] *P. Starič*, Wideband JFET Source Follower, Electronic Engineering, Aug. 1992, pp. 29–34
- [3.36] *J.M. Miller*, <[http://www.ieee.org/organizations/history\\_center/legacies/miller.html](http://www.ieee.org/organizations/history_center/legacies/miller.html)>